

The Biological Role of Fetuin-B:
Inhibition of Zona Pellucida Hardening and
Preservation of Female Fertility in Mice

Von der Fakultät für Mathematik, Informatik und Naturwissenschaften der RWTH
Aachen University zur Erlangung des akademischen Grades einer Doktorin der
Naturwissenschaften genehmigte Dissertation

vorgelegt von
M. Sc. Eileen Dietzel
aus Leinefelde

Berichter: Universitätsprofessor Dr. rer. nat. Wilhelm Jahnen-Dechent
Universitätsprofessor Dr. rer. nat. Marc Spehr

Tag der mündlichen Prüfung: 16.12.2014

Diese Dissertation ist auf den Internetseiten der Hochschulbibliothek online
verfügbar.

Table of Contents

Summary	4
1. Introduction	5
1.1 The Protein Fetuin-B and its Biological Function	5
1.2 Gametogenesis in Mammals	10
1.2.1 Oogenesis	10
1.2.2 Spermatogenesis in Mammals	14
1.3 The <i>Zona Pellucida</i> During Folliculogenesis, Fertilization and Embryogenesis	16
1.3.1 <i>Zona Pellucida</i> Structure	16
1.3.2 Fertilization	17
1.3.3 Embryogenesis and Implantation	20
1.3.4 Premature ZP hardening	22
1.4 The Mouse as Model Organism	24
1.5 Aim of the Study	26
2. Experimental Procedures	27
2.1 Fertility Evaluation of Fetuin-B Deficient Mice	28
2.1.1 Mouse Genotyping	28
2.1.2 Breeding Performance	28
2.1.3 Fetuin-B Western Blot (Murine and Human)	28
2.1.4 Collection of Zygotes and Oocytes	29
2.1.5 <i>In Vitro</i> Fertilization and Embryo Transfer	30
2.2 Testing for <i>Zona Pellucida</i> Hardening	32
2.2.1 Oocyte Diameter and <i>Zona Pellucida</i> Thickness	32
2.2.2 <i>Zona Pellucida</i> Digestion	32
2.2.3 Sperm Binding	32
2.2.4 ZP2 Western Blot	33
2.3 Ovastacin Inhibition by Fetuin-B	34
2.3.1 Recombinant Fetuin-A and Fetuin-B Expression	34
2.3.2 Ovastacin Expression	34
2.3.3 Inhibition Assay	34
2.4 <i>In Vitro</i> <i>Zona Pellucida</i> Hardening Under Fetuin-B Supplementation	35
2.4.1 Buffer Change for Recombinant Fetuin-B	35
2.4.2 Effects of Fetuin-B to Fertilization, Embryo Development and Hatching	35
2.4.3 <i>Zona Pellucida</i> Hardening During <i>In Vitro</i> Cultivation	36
2.4.4 Inhibition of <i>Zona pellucida</i> Hardening After one Hour of <i>In Vitro</i> Cultivation by Fetuin-B	36

-Table of Contents -

2.4.5 Effects of Fetuin-B and Cumulus Cells on <i>Zona Pellucida</i> Hardening During <i>In Vitro</i> Cultivation	37
2.5 Statistics	37
3. Results	38
3.1 Fetuin-B Deficient Female Mice are Infertile Due to an Early Block to Fertilization	38
3.2 Fetuin-B Deficient Oocytes Undergo Premature <i>Zona Pellucida</i> Hardening	46
3.3 Fetuin-B Inhibits Ovastacin and Thus <i>Zona Pellucida</i> Hardening	52
3.4 Fetuin-B Increases Fertilization Success <i>in Vitro</i>	54
4. Discussion	67
4.1 Fetuin-B Deficient Female Mice are Infertile Due to an Early Block to Fertilization	67
4.2 Fetuin-B Deficient Oocytes Undergo Premature <i>Zona Pellucida</i> Hardening	68
4.3 Fetuin-B Inhibits Ovastacin and Thus <i>Zona Pellucida</i> Hardening	70
4.4 Fetuin-B Increases Fertilization Success <i>in Vitro</i>	71
Conclusion and Future Aspects	76
References	77
Abbreviations	94
List of Figures	97
List of Tables	99
Supplement	100
Acknowledgement	106
Curriculum Vitae	107
Statutory Declaration	111

Summary

Fetuin-B is a hepatic plasma protein, well conserved in mammals. Fetuin-B associates with the extracellular matrix and was shown to surround the oocytes during development and maturation. A layer of extracellular matrix, the *Zona pellucida* (ZP), surrounds mammalian oocytes. Before fertilization sperm are able to penetrate the ZP. After fertilization proteases are released by the oocyte, leading to structural ZP modification and inhibition of further sperm binding. This process is called fertilization-triggered ZP hardening. The hardened ZP is thought to be required to block polyspermy and to support embryonic development until blastocyst hatching and implantation into the uterus wall. Premature, fertilization-independent ZP hardening is known to occur spontaneously during *in vitro* cultivation (IVC), leading to decreased fertilization success at *in vitro* fertilization (IVF).

It was shown that *Fetub*^{-/-} females are infertile due to premature ZP hardening. *Fetub*^{+/-} females only had half the serum level of fetuin-B, but were completely fertile. Infertility of *Fetub*^{-/-} females was overcome by laser-assisted IVF and subsequent embryo transfer even into fetuin-B deficient foster mothers, showing that fetuin-B is critically required before fertilization, but is dispensable during later stages of embryonic and fetal life. Recombinant murine fetuin-B was shown to inhibit the proteolytic activity of ovastacin, the oocyte specific protease that triggers definitive ZP hardening. Accordingly, recombinant murine fetuin-B inhibited ZP hardening and increased IVF success without increasing polyspermy.

In conclusion, fetuin-B inhibits spontaneously released ovastacin and thus premature ZP hardening either *in vivo* or *in vitro*, to maintain ZP permeability. After fertilization, the precipitous increase of ovastacin concentration triggered by degranulation, overwhelms the inhibition capacity of fetuin-B, resulting in fertilization-triggered ZP hardening. Fertilization-triggered ZP hardening proved less important in blocking polyspermy than thought previously. Fetuin-B deficiency either *in vivo* or *in vitro* lead to ZP hardening during oocyte maturation blocking fertilization. Thus fetuin-B represents a novel target for fertilization biology and reproductive medicine.

1. Introduction

1.1 The Protein Fetuin-B and its Biological Function

Fetuin-B is well conserved in different mammals (for comparison between murine and human fetuin-B see table 1) ¹. The murine fetuin-B gene (*Fetub*) has a size of about 21.4 kb and is located on chromosome 16. It consists of eight exons, while the coding sequence starts at the second exon, leading to a transcript of approximately 1.5 kb ². In mice, the protein fetuin-B (FetuB) is almost exclusively expressed in the liver. Low mRNA level could be detected in kidney, lung, ovary, tongue and embryo. The murine protein consists of 388 amino acids, leading to a theoretical size of 43 kDa. Due to post-translational modifications it has a molecular weight of 60 kDa under reducing conditions on SDS-PAGE. Mouse fetuin-B is secreted into the blood where it reaches serum concentrations of about $156 \pm 3 \mu\text{g/ml}$ ². Protein extraction after tissue perfusion showed that fetuin-B was present in all tested tissues with the exception of the brain. Thus it was assumed that fetuin-B either associates with the extracellular matrix or is contained within the cells.

The human fetuin-B gene (*FETUB*) has a size of about 13.0 kb and is located on chromosome 3, leading to a transcript of approximately 1.6 kb ². As in mice the protein is predominantly expressed in the liver. The fetuin-B transcript could be detected at a lower level in human placenta, which was not tested in mice. In contrast to murine data no expression was detected in human kidney and lung, while human ovary, tongue and embryo were not tested as well. The human protein consists of 382 amino acids, with a theoretical molecular weight of 43 kDa and an apparent molecular weight of 55 kDa on reducing SDS-PAGE. In humans, fetuin-B serum concentration is about $5 \pm 1 \mu\text{g/ml}$, which is more than 30 times lower than in mice ².

In both species, females show a two-times higher fetuin-B serum level with an increased variation than males, indicating sex steroid depended regulation of expression.

Table 1. Comparison of murine and human fetuin-B (modified from ²)

	Mouse	Human
Gene size (kb)	21.4	13.0
Gene location	chromosome 16 Pos. 22918382-22939768	chromosome 3 Pos. 186640360-186653008
Transcript size (kb)	1.5	1.6
Organs with transcription (lower level)	liver (kidney, lung, ovary, tongue, embryo)	liver (placenta)
Protein size (number of amino acids)	388	382
Protein size (kDa)	approx. 60	approx. 55
Serum concentration (µg/ml)	156 ± 3	5 ± 1

The fetuin protein family has a specific N-terminal DXLETXCHXL motif and comprises two members: fetuin-A (FetuA, also known as α 2-HS-glycoprotein AHSG) and fetuin-B (FetuB) ^{3,4}. Together with histidine-rich glycoprotein (HRG) and kininogen (KNG), fetuins belong to the type 3 cystatin superfamily (figure 1), comprising structurally related protease inhibitors ¹. They all show at least two aminoterminal cystatin domains and one additional ortholog-specific domain. Several disulfide bridges that link the domains form the three-dimensional protein tertiary structure.

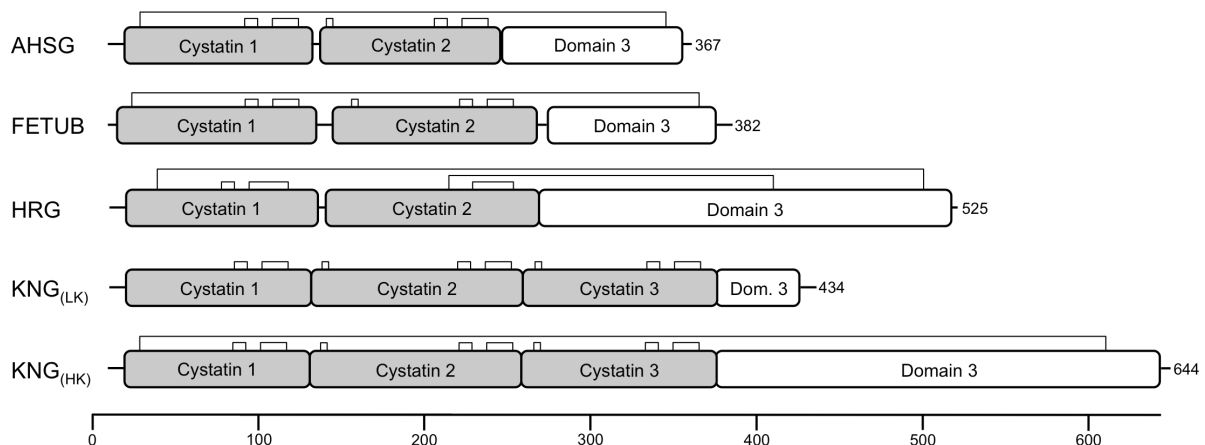


Figure 1. Schematic overview of the human type 3 cystatin superfamily that comprises fetuin-A (AHSG), fetuin-B (FETUB), histidine-rich glycoprotein (HRG) and kininogen (KNG, with two splice variants leading to high (HK) and low (LK) molecular weight). All members show at least two aminoterminal cystatin domains and one additional, more specific domain. Several disulfide bridges, indicated by rectangles, link the single domains. Numbers of amino acids are given at the right and are further indicated at the scale at the bottom (modified from ¹).

- Introduction -

The protein alignment shown in figure 2 indicates that sequence identity between fetuin-A and fetuin-B is about 26% in mice, and 28% in humans, respectively ^{5,6}. Amino acid identity of the fetuin-B coding sequences in mice and humans is 61% and sequence identity of fetuin-A in mice and humans is 59%. The fact that identity within the two fetuin-B amino acid sequences of both species is higher than the sequence identity to fetuin-A of the same species indicates that the duplication of the fetuin gene probably occurred before speciation.

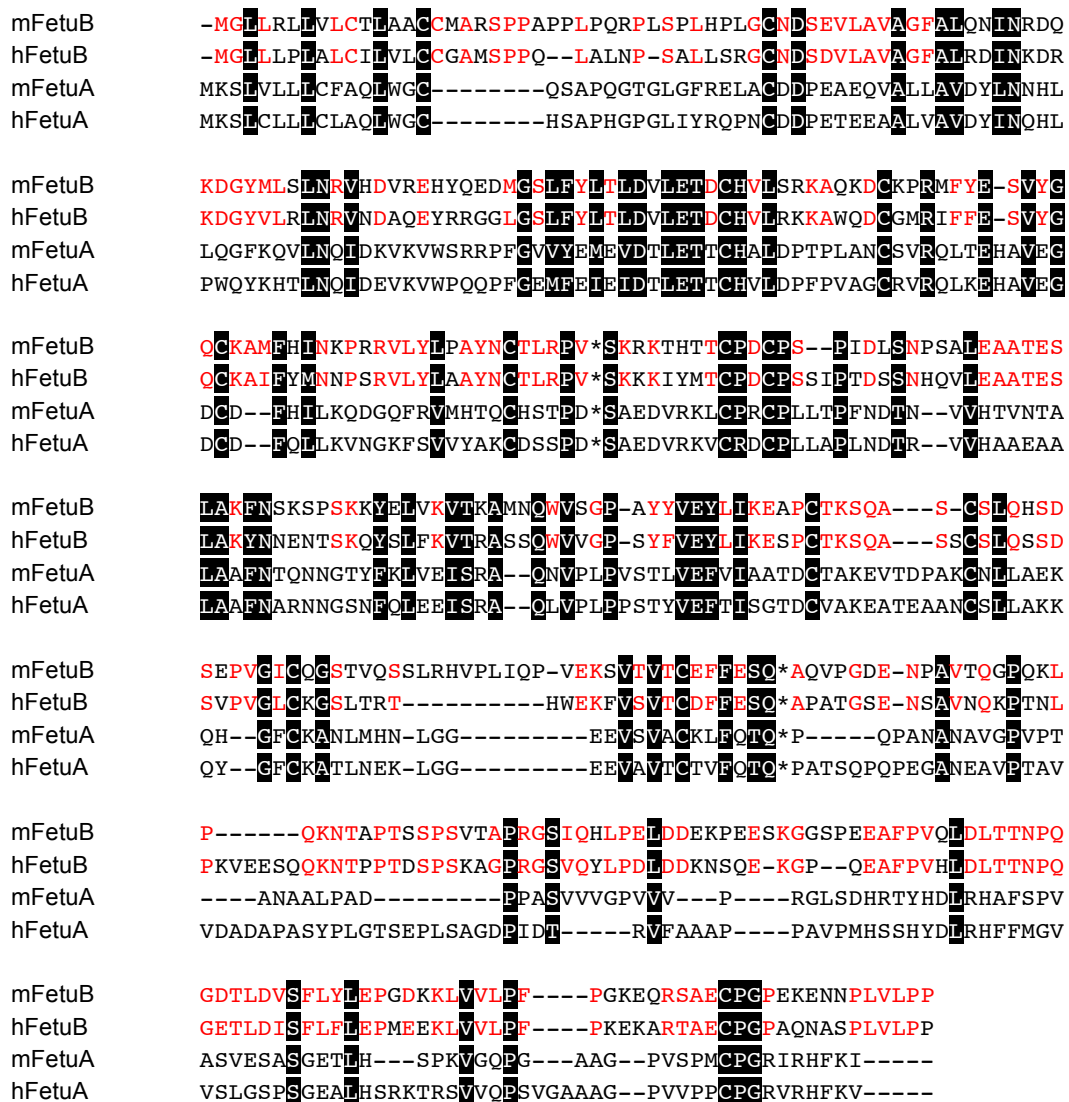


Figure 2. Multiple alignment of mouse (m) and human (h) fetuin-B (FetuB) and fetuin-A (FetuA). Species and protein are noted on the left. Identical or similar residues conserved in all four sequences are printed as white on black background. Red letters indicate similar residues only conserved in fetuin-B of both shown species. A minimum number of gaps, indicated by hyphens, has been introduced to maximize alignments. * marks the transition from one domain to the next (modified from ⁴).

Because of the structural relationship and the similar expression pattern it was first assumed that fetuin-A and fetuin-B should have similar biological roles in mice. Fetuin-A deficient mice are fertile and healthy ⁷. Depending on the genetic background fetuin-A deficient mice show mild calcification (C57BL/6 background) or severe systemic calcification of vital organs (DBA/2), indicating that the major physiological function of fetuin-A is the inhibition of unwanted calcification ^{7,8}. Bacterially expressed recombinant murine fetuin-A inhibits precipitation of calciprotein particles *in vitro* with an IC50 of approximately 2 μ M, while the IC50 of fetuin-B was three times higher ². Taking into account the different serum concentrations and molecular weights (in mice: fetuin-A, 14 μ M and 55 kDa; fetuin-B, 3 μ M and 60 kDa), fetuin-A should contribute to the overall serum inhibition precipitation 14 times more than fetuin-B in mice and even more in humans. Other studies showed no effect of recombinant murine, rat or human fetuin-B on calciprotein particle formation and structural analysis of fetuin-B revealed no functional calcium-binding domain ⁹. Fetuin-B serum concentration is twice as high in females than in males, while the amount of fetuin-A is not different, indicating different, probably sex steroid-dependent regulation of protein expression ². Thus it was concluded, that the two fetuins have similar expression patterns, but different physiological functions.

Various biological functions were proposed for fetuin-B. Genetic association studies suggested a role for fetuin-B and HRG in tumor biology ¹⁰. Overexpression of fetuin-B in skin carcinoma cells suppressed tumor growth in nude mice. Murakami et al. proposed the fetuin-B gene as a target of the farnesoid X receptor (FXR), a nuclear receptor that is involved in lipid and carbohydrate metabolism, especially in certain cancers ¹¹. Activation of the FXR increased fetuin-B expression in human hepatocytes but showed no effect in mouse hepatocytes. Together with the fact that FXR activation also induces apoptosis in human breast cancer cells these results suggested, that the FXR-fetuin-B pathway might regulate cancer cell proliferation. Choi et al. suggested a role of fetuin-B in rat fatty acid metabolism together with zinc- α 2-glycoprotein ^{12,13}. Obesity-resistant rats showed increased plasma protein levels of both proteins at high fat diet. The knockdown of both proteins in liver cells led to a significant increase in the expression of lipogenic genes, resulting in higher lipid levels. Furthermore, fetuin-B scored positive in several microarray expression and proteome studies in different animal models ¹⁴⁻¹⁶. However, the underlying molecular functions of these results have not yet been revealed.

To study the biological role of fetuin-B in detail, the gene was inactivated in mice by targeted *Fetub* gene deletion ^{17,18}. Hemizygous (*Fetub*^{+/-}) mice had half the fetuin-B serum level of wildtype (*Fetub*^{+/+}) littermates, and homozygous fetuin-B deficient (*Fetub*^{-/-}) mice had no detectable serum fetuin-B. Serum fetuin-A was not altered. There were no differences found in fetuin-B deficient mice compared to wildtype mice in body weight, systolic and diastolic

blood pressure, pulse rate and blood chemistry, arguing against a role of fetuin-B in fatty acid metabolism. Furthermore, fetuin-B deficient mice showed no pathological calcification. However, females were completely infertile. *In vivo*, fertility was restored by transplanting post-pubertal *Fetub*^{-/-} ovaries into ovariectomized isogenic wildtype recipients. Recipients became pregnant after subsequent mating with wildtype males indicating that plasma fetuin-B was necessary and sufficient to restore fertility of *Fetub*^{-/-} ovaries. Furthermore, this result excluded an early oocyte maturation defect in fetuin-B deficient females. We analyzed reproductive tract morphology, follicle development, ovulation rates, hormonal status as well as sperm motility and chemoattraction, and detected no difference between *Fetub*^{-/-} and wildtype animals¹⁹. After mating, oocytes recovered from wildtype mice were all fertilized. In contrast, the oocytes of female *Fetub*^{-/-} mice showed no signs of fertilization. Thus, a block of fertilization most likely caused the infertility in female *Fetub*^{-/-} mice. To study the fertilization block in more detail, we performed *in vitro* fertilization (IVF) with and without laser perforation of the *Zona pellucida* (ZP), a layer of extracellular matrix that surrounds mammalian oocytes^{17,19}. Conventional IVF of fetuin-B deficient oocytes using fertile sperm remained unsuccessful, whereas wildtype oocytes became fertilized. In contrast, laser beam-induced perforation of the ZP followed by IVF was met with success. Thus fetuin-B deficient oocytes could be fertilized after overcoming the ZP as a barrier and infertility of *Fetub*^{-/-} females was caused by a defect in the ZP.

1.2 Gametogenesis in Mammals

1.2.1 Oogenesis

The development of the female gamete in the ovaries until ovulation is called oogenesis. It comprises three phases: proliferation, growth and maturation (for overview see figure 3).

In humans, gamete development begins as early as the third to fourth week of embryo development²⁰. In mice, gamete development starts seven days post-fertilization²¹. The oogonia migrate to the gonadal ridge and start to proliferate (proliferation phase). In humans the proliferation period is completed after seven months, giving rise to about seven million oogonia at birth²². For several decades it was thought that the oocyte population was determined with the end of the proliferation period. Meanwhile researchers demonstrated however, the existence of post-natal oogenesis in adults. These late developing oocytes do however, not contribute to the pool of ovulated oocytes^{23,24}. The majority of the gametes already die during proliferation, the rest starts the first meiotic division²⁵. At this stage the female gametes are named primary oocytes. The gametes arrest in the first prophase of meiosis until recruitment into the growing pool throughout the reproductive years (figure 3). Together with the surrounding precursor granulosa cells primary oocytes build the primordial follicles²⁶. The exact mechanism that leads to further follicle maturation is not completely known, yet²⁷. It was shown, that the bidirectional communication between pre-granulosa cells and the oocytes as well as between the pre-granulosa cells and the surrounding tissue is very important^{28,29}. Precursor granulosa cells for example express peptide factors like stem cell factor (SCF, also known as Kit ligand) and leukemia inhibitory factor (LIF), which stimulate maturation of the primordial follicles *in vitro*^{30,31}. Members of the transforming growth factor β (TGF- β) family, like bone morphogenetic protein-4 and -7 (BMP4 and BMP7) also play an important role in primordial follicle recruitment^{32,33}. Both are secreted by follicle surrounding ovarian stroma. Other members of the TGF- β family, including growth and differentiation factor-9 (GDF9) and BMP15, are secreted by the oocytes, and support follicular maturation as well. By these mentioned factors at the age of puberty the primordial follicle starts to grow and the oocyte surrounding pre-granulosa cells develop to granulosa cells (growth phase). The diameter of murine oocytes increases from 15 μm to 80 μm ³⁴. At this stage, the follicle is called primary follicle. The follicle cells now express anti-müllerian hormone (AMH), which also belongs to the TGF- β family and inhibits further recruitment of primordial follicles³⁵. In humans, the blood AMH level signifies ovarian function and predicts ovarian response to hormonal stimulation in IVF treatment³⁶⁻³⁸.

Growing oocytes form an outer layer, the *Zona pellucida*, short ZP. The ZP is up to 7 μm thick in mice, and up to 14 μm thick in humans, but still is permeable to large molecules including proteins with a molecular weight up to 150 kDa³⁹. The ZP is perforated by cellular

protrusions from the surrounding granulosa cells to allow the exchange of nutrients and other signaling molecules⁴⁰.

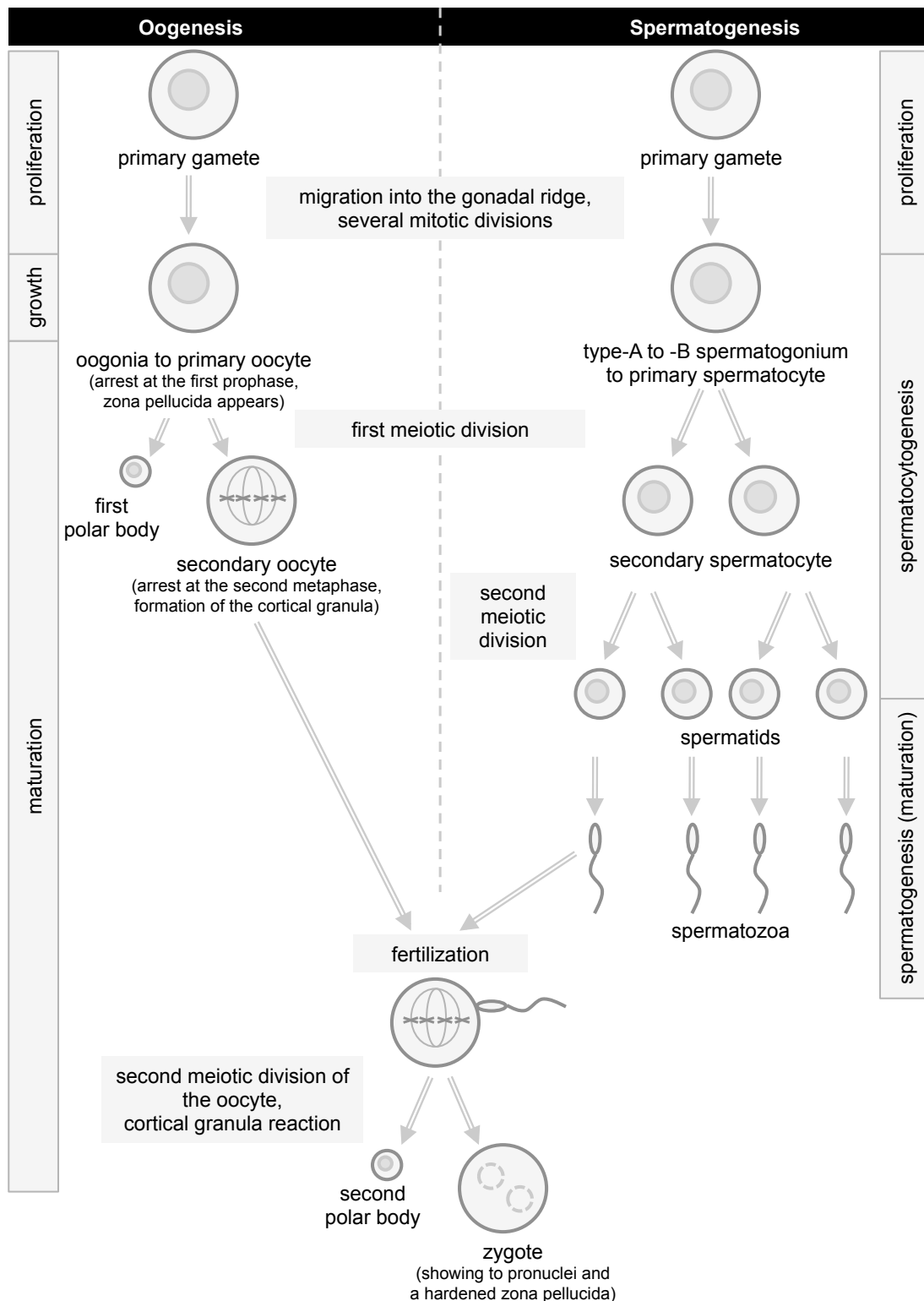


Figure 3. Schematic overview of oogenesis and spermatogenesis, from the migration of the gametes into the gonadal ridge through to meiosis, fertilization and the formation of a zygote. In oogenesis only one mature oocyte is obtained out of one primary oocyte during meiosis, while in spermatogenesis one primary spermatocyte develops into four spermatozoa. In sperm differentiation and maturation starts at the end of meiosis. Oocytes already mature during meiosis and the meiosis is not completed until after fertilization (modified from¹⁹).

With ongoing follicle maturation, the granulosa cells start dividing, and a second surrounding cell layer called the thecal cells is formed. These cells also express BMP4 and BMP7, indicating that beside primordial follicle recruitment, both factors are also important for further development³². When more than one granulosa cell layer surrounds the oocytes, the complex is called secondary follicle. Next, granulosa cells start to proliferate and express activin, another member of the TGF- β family, and its binding protein follistatin⁴¹. There are three different activin isoforms (A, AB, B), depending on the composition of the subunits. In rodents, activin-A increased the follicle growth up to the antral follicle^{42,43}. Depending on the persistence of follistatin activin-A increased granulosa cell proliferation⁴⁴. Additionally, activin induces the expression of follicle stimulating hormone (FSH) receptors in granulosa cells. A comparative function was shown for TGF- β , which is additionally expressed by thecal cells⁴⁵. In consequence the follicles get sensitive for FSH. FSH is released by the anterior lobe of the pituitary gland and is regulated by gonadotropin releasing hormone (GnRH) expression in the hypothalamus. At the beginning of each female estrus cycle FSH is secreted into the blood. In the ovaries, FSH only affects the secondary follicles by further stimulating granulosa cell proliferation. During ongoing maturation a fluid filled cavity called antrum, persists in the follicle. The follicular fluid is mainly composed of granulosa cell secretions, but also comprises components of blood plasma⁴⁶. At this stage the follicle is named antral follicle or Graafian follicle (figure 4). Granulosa cell protrusions that permeate the ZP are removed and granulosa cells differentiate into several distinct subtypes⁴⁰. The *membrana granulosa* forms the wall of the ovarian follicle interior to the basal lamina and thus to the thecal cells. The inner layer that surrounds the growing oocyte is called *corona radiata*. A structure called *cumulus oophorus* surrounds the *corona radiata* and thus connects the oocyte to the *membrana*. During the early antral stage of folliculogenesis, the level of luteinizing hormone (LH) is still very low. Under this condition thecal cells express androgens that are metabolized by the granulosa cells⁴⁷. The resulting estrogen is then secreted into the blood and initiates endometrium proliferation in the uterus. In response to increasing blood estrogen, the anterior lobe of the pituitary gland suppresses FSH expression. This triggers the release of LH and thus ovulation. The increase in LH again leads to an induction of progesterone and prostaglandins. Progesterone stimulates cell proliferation in the uterus, readying the uterus wall, which is called the

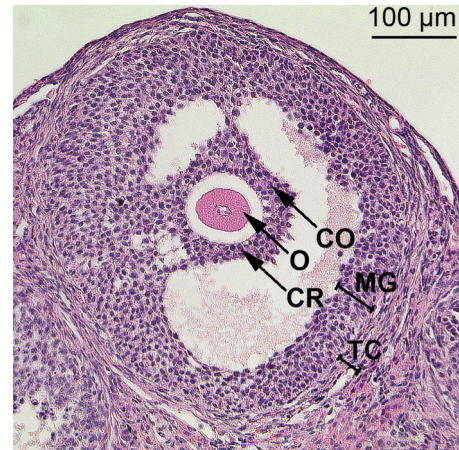


Figure 4. Microscopic picture of a murine antral follicle showing the thecal cell layer (TC), the membrana granulosa cell layer (MG), the oocyte (O) with the surrounding corona radiata (CR) and the cumulus oophorus (CO) (modified from¹⁸).

"decidua", for a potential implantation of the embryo. Together with LH, progesterone induces the oocyte to complete the first meiotic division. One of the resulting daughter cells contains almost no cytoplasm and is called first polar body. The second daughter cell is called secondary oocyte, which arrests in the second metaphase (figure 3). The golgi apparatus synthesizes small vesicles that accumulate beneath the oocyte cell membrane and form the so-called cortical granules⁴⁸. A small amount of the cortical granula content is already released during oocyte maturation, while the majority is not exocytosed until after fertilization⁴⁹. Folliculogenesis is now completed and the oocyte will be ovulated. LH induced prostaglandins induce the contraction of the ovary. In addition, increased fluid influx from the ovary capillaries into the antrum leads to an increasing antral pressure²². The LH furthermore induces the expression of plasminogen activator and collagenase. Collagenase is an enzyme that degrades collagen, the main structural protein of mammalian connective tissues. Plasminogen is mostly synthesized by the liver with a minor contribution from extrahepatic tissues⁵⁰. Plasminogen circulates in plasma and most other extracellular fluids, such as uterine fluid, ovarian follicular fluid and seminal plasma⁵¹. Trypsin-like plasminogen activators exist in oocytes and sperm converting plasminogen into plasmin. Beside a major role in fibrinolysis, plasmin can cleave a wide spectrum of proteins. Thus collagenase and plasmin lead to degradation of the follicle extracellular matrix. Due to the enzymatic cleavage and the increasing antral pressure, the follicle bursts and the oocyte is released into the oviduct. Together with the surrounding cumulus cells, the oocyte forms the so-called cumulus-oocyte complex (COC). The cells are bonded to each other by extracellular matrix comprising proteins and hyaluronic acid⁵². The residual follicle cells (*membrana granulosa*) form the *corpus luteum*, which secretes progesterone, estrogen and inhibin. Inhibin is another member of the TGF- β family and inhibits, like estrogen, the expression of FSH and thus the maturation of further follicles⁵³. Progesterone and estrogen lead to an increasing proliferation of the uterus endometrium. In rodents the post-ovulatory function of estrogen is still discussed, because the estrogen level decreases directly after ovulation. Unlike in humans the estrogen level increases with the formation of the *corpus luteum* and stays constant until its degradation at the end of the estrus cycle⁵⁴.

If fertilization fails and no embryo implantation occurs, the *corpus luteum* is degraded. Thus the plasma level of progesterone, estrogen and inhibin decrease again. The FSH expression is no longer inhibited and the estrus cycle starts again⁵⁵. In humans, the decrease of progesterone leads to a shedding of the endometrium and ensuing menstruation. In higher mammals including primates, this point in time is commonly defined as the first day of female menstrual cycle. Primitive mammals including mice have no menstruation, despite having an estrus cycle²⁰. In humans, the female cycle takes about 28.5 days to complete, and repeats until the oocytes pool is depleted²². Mice as well as some other species show a typical

phenomena: the length of the cycle varies, depending on the occurrence of a previous mating. If a female mates with a vasectomized, infertile male, the luteal phase (duration from ovulation until the beginning of a new cycle) takes about eleven to twelve days. Without mating, this phase only takes about two or three days and the *corpora lutea* synthesize less progesterone. This effect is mediated by the mechanical stimulation of the cervix during mating. Cervix stimulation further leads to a secretion of prolactin by the anterior lobe of the pituitary gland for about ten days and thus to sustained *corpora lutea* function. If this interaction fails because of lack of mating, the cycle is shorter and thus the reproductive efficiency is increased²⁰.

1.2.2 Spermatogenesis in Mammals

Spermatogenesis can be separated into three phases: proliferation, spermatocytogenesis and spermiogenesis (for general overview see figure 3). In humans the complete development of the gamete into a mature sperm takes about 65 days, in mice usually 34.5 days^{22,56}. Like in females, during embryogenesis the male gametes (spermatogonia) migrate to the genital ridge. Next, spermatogonia assemble the primitive sex cord, which persists until puberty. Prenatally and leading up to puberty the sex cords acquire cavities eventually forming the seminiferous tubules. The epithelia of these cavities differentiate into the Sertoli cells, that feed and protect the maturing sperms²². Gametes and Sertoli cells connect via N-cadherin molecules on both cell surfaces, and through galactosyltransferase molecules on the spermatogonia that bind to carbon hydrate receptors on the Sertoli cells^{57,58}. Initiation of spermatogenesis is likely mediated by BMP8b during puberty⁵⁹. At the beginning of the spermatocytogenesis, the gametes sequentially differentiate into four A-subtypes (type-A1 to A4, see figure 3, summarized as type-A-spermatogonia). These immature spermatogonia are located in close proximity to the basal membrane of the seminiferous tubules. Type-A1 spermatogonia function as stem cells²². Thus they either replicate into more type-A1 spermatogonia or they differentiate into type-A2 spermatogonia and later on into type-A3 and -A4 spermatogonia. A4 spermatogonia further develop to intermediary spermatogonia. Compared to all type-A spermatogonia, intermediary spermatogonia have smaller and more compact cell nuclei. After one mitotic division intermediary spermatogonia form two type-B spermatogonia that are no longer connected to the basal lamina of the seminiferous tubules. All types of spermatogonia undergo incomplete cell divisions, and remain connected to each other through thin cytoplasmic bridges⁶⁰. Thus the exchange of matter and signals, and thus tight coordination of cell divisions is made possible. The type-B spermatogonia perform one last mitotic division to build the primary spermatocytes. These bypass the first meiotic cell cleavage to form secondary spermatocytes (figure 3). Thereafter the secondary spermatocytes undergo meiotic division to form haploid spermatids. Thus four mature sperm

cells are formed from one spermatogonium instead of only one oocyte from a female oogonium (figure 3). Spermatids are also connected by cytoplasmic bridges so that genetic information of one cell can freely diffuse to another cell ⁶¹. Thus the spermatids have a haploid set of chromosomes, yet still can act like diploid cells. At this stage they gradually move into the lumen of the seminiferous tubules, and lose the cell contacts while differentiating into spermatozoa. The second stage of the spermatogenesis starts, the spermiogenesis. The Golgi apparatus converts into the acrosome. This vesicle contains enzymes including hyaluronidase, neuraminidase and acrosin, which are thought to be required for penetration of the cumulus cell matrix as well as the ZP ⁶². The acrosome covers the nucleus like a lid. Together they form the sperm head. During differentiation the nucleus rotates in a way that the acrosome is directed to the basal membrane of the seminiferous tubule. At the opposite side of the nucleus the flagellum is built, starting at the distal centriole. Thus the flagellum is oriented towards the lumen of the seminiferous tubule. At the end of the spermiogenesis the nucleus condenses, the remaining cytoplasm is pinched off and is phagocytized by the surrounding Sertoli cells. The mitochondria build a ring around the flagellum. After spermatogenesis, the spermatozoa must undergo further maturation steps. First, they are released by the Sertoli cells in a fluid secreted into the lumen of the seminiferous tubules ²⁰. Due to this constant fluid flow, the sperm reach the efferent ducts, where about 90% of the fluid is resorbed. In the proximate epididymis the fluid resorption is continued, so that the sperms become more concentrated. Furthermore the epididymis secretes nutrients and stimulants including fructose and glycoproteins that prepare sperm for the swimming required for oocyte fertilization ²⁰. The *cauda epididymis* can store sperm for several weeks in mice, and for several days in humans. Finally, sperm reach the seminal duct (also called *ductus deferens* or *vas deferens*), where they are stored until ejaculation. Without copulation and ejaculation, sperm are slowly released into the ureter, and then flushed out by urine.

1.3 The *Zona Pellucida* During Folliculogenesis, Fertilization and Embryogenesis

1.3.1 *Zona Pellucida* Structure

The *zona pellucida* (ZP) describes a glycoprotein matrix that surrounds human as well as other mammalian oocytes⁶³. Murine ZP is composed of three sulfated glycoproteins: ZP1 (200 kDa), ZP2 (120 kDa) and ZP3 (83 kDa)⁶⁴. Human ZP have one additional protein, ZP4⁶⁵. The ZP of one murine oocyte contains approximately 5 ng protein, with ZP1-3 comprising at least 95% of the total ZP protein amount⁶⁶. ZP proteins are exclusively expressed in the growing oocyte and are exocytosed. Several studies showed that the molecular ratio of ZP1:ZP2:ZP3 is about 1:4:4⁶⁷. In mice, ZP2 and ZP3 build filaments that are linked by homodimers of ZP1⁶⁸. How the three-dimensional meshwork of the ZP is achieved in detail is still discussed⁶⁹. The ZP first appears as individual islands of ZP material in the space between the oocyte and the surrounding granulosa cells and increases in thickness to about 7 µm in mature mouse oocytes and about 14 µm in human oocytes^{70,71}.

Genetic studies in mice revealed that a functional ZP is critical for follicular development, fertilization, and for the protection of the pre-implantation embryo. Mice that are deficient in ZP1 (*Zp1*^{-/-}) have oocytes with a thinner, more fragile ZP compared to the wildtype⁷². The filaments made of ZP2 and ZP3 are much looser, while sperm is still able to bind to and fertilize these oocytes. Lack of *Zp1*^{-/-} leads to morphologically abnormal ZP and female subfertility. Amino acid alignment indicates 68% sequence identity of murine and human ZP1, and 77% sequence similarity (supplemental figure S1). In humans one of four mutations in the *ZP1* gene was associated with decreased fertilization success *in vitro*⁷³. Compared to *Zp1* deficiency, lack of *Zp2* or *Zp3* in mice was associated with a much more drastic phenotype^{74,75}. Both transgenic mouse lines have defects in oocyte maturation and decreased numbers of ovulated oocytes, indicating the need of a ZP during follicle development. While *Zp2*^{-/-} oocytes form a thin ZP in early follicles, the ZP is completely absent in *Zp3*^{-/-} eggs. Both deficiencies lead to infertility. Oocytes could be fertilized *in vitro*, but did not lead to pregnancy after transfer into foster mothers. This finding illustrates the importance of a functioning ZP in embryo development. Multiple alignment indicates 58% sequence identity of murine and human ZP2 and 72% sequence similarity (supplemental figure S2). The alignment of murine and human *Zp3* shows 68% identical and 77% similar amino acids (supplemental figure S3). In humans four mutations are known in the *ZP2* gene and eight mutations in the *ZP3* gene⁷³. There is no known association of *ZP2* mutations and the female infertility, while two of the *ZP3* mutations are more frequent in the infertile females. *Zp4* is a pseudogene in mouse, while human *ZP4* is expressed and has four known mutations, none of which are associated with infertility (supplemental figure S4)^{65,73}. The function of the human *ZP4* is thus unknown. *ZP4* it is present in levels comparable to *ZP2*

and ZP3 (with ZP1 being a minor component in human oocytes), and therefore is assumed to have a structural role ⁷⁶.

1.3.2 Fertilization

After ovulation the cumulus-oocyte complex (COC) is transported into the oviduct by the fimbriated infundibulum ²⁰. Due to a combination of ciliary motion and oviductal muscle contraction, the COC reaches the ampulla, where the fertilization takes place ⁷⁷.

During copulation sperm are mixed with seminal fluid an alkaline fluid secreted by the seminal vesicle, the bulbourethral gland, and the prostate gland ²⁰. The seminal fluid comprises buffer substances, neutralizing the acidic milieu of the vagina, energy-rich metabolites including fructose and sorbitol, reducing agents like ascorbic acid that protect sperm from oxidation by the atmospheric oxygen, as well as prostaglandins that are thought to stimulate uterus muscle activity. During copulation, smooth muscles of prostate, seminal vesicle, seminal duct and ureter contract to ejaculate the semen. Unlike humans, male mice form a massive secretion that is released into the vulva after the seminal fluid, and hardens, preventing further copulation. This so-called "vaginal plug" is visible for 8 to 24 hours ⁷⁸.

Following copulation and ejaculation, sperm must migrate through the female genital tract to reach the oocyte. Transport through the uterus is mainly mediated by muscle contraction ⁷⁷. After entering the oviduct, sperm becomes hyperactive, an activation step mediated by sperm-specific calcium channels located in the sperm tail ⁷⁹. The movements of the flagellum intensify and become more symmetric. Furthermore, the sperm is directed by a temperature gradient (thermotaxis) between the different parts of the oviduct as well as chemical gradients (chemotaxis) released by the COC in the ampulla ^{77,80}. While the sperm migrate through the female genital tract, they undergo further modifications in preparation of fertilization proper. This process is called capacitation. It starts with a removal of steroids and non-covalently bound glycoproteins from the sperm head membrane, thought to be mediated by albumin that is present in the cervix secretion ⁸¹. These modifications lead to several effects. First, the removal of steroids increases calcium permeability. The calcium influx results in the cytoplasmatic release of cyclic adenosine monophosphate (cAMP), facilitating sperm-oocyte fusion ^{82,83}. Second, the sperm membrane becomes more fluid. Lipid rafts enriched in receptors necessary for sperm-oocyte interaction form at the anterior sperm head ⁸⁴. The removal of glycoproteins furthermore unmasks structures that are important for sperm-oocyte identification ⁸⁵. Without capacitation, sperm are incapable of chemotaxis as well as of cumulus cell matrix penetration ^{86,87}. Delayed capacitation also has positive effects. Incapacitated sperm stick to the oviductal epithelium and keep inactivated until they are

capacitated^{88,89}. This increases sperm lifespan, prevents polyspermy and allows fertilization despite possibly delayed ovulation^{77,90}.

Due to hyperactivation and membrane hyaluronidase activity, sperm penetrate the cumulus cell matrix and reach the oocyte^{91,92}. Prior to gamete fusion, sperm bind to and penetrate the ZP (figure 5)⁹³. For sperm-ZP interaction several models are discussed⁹⁴. It was long believed that sperm bind to carbohydrate chains of ZP3⁹⁵, because enzymatic deglycosylation abrogated sperm binding. Furthermore, the sperm-ZP3 binding was thought to trigger the acrosome reaction, a calcium mediated fusion of sperm membrane and outer acrosome membrane, which in turn leads to a secondary binding of the sperm to ZP2. Next, the released acrosomal enzymes locally digest the ZP and thus make it penetrable for sperm^{85,96}. Several lines of evidence however argue against the sperm-ZP3 binding model. Mutations of murine ZP3 gene glycosylation positions did not inhibit sperm-oocyte binding⁹⁷. Using transgenic mouse models and gain-of-function assays, it was instead demonstrated that ZP2 is the sperm-ZP ligand in mice and humans^{98,99}. Furthermore it was shown, that the acrosome reaction is not necessary to penetrate ZP¹⁰⁰.

After penetrating the ZP, the sperm passes the perivitelline space and binds to the plasma membrane of the oocyte, the oolemma. The detailed molecular mechanisms of sperm-oocyte binding and fusion are not completely understood, but several membrane proteins were shown to be important. The integrin CD9 is distributed almost over the entire oocyte surface^{101,102}. It is thought that CD9 binds fertilin, an ADAM (a disintegrin and a metalloprotease domain) family member at the sperm surface¹⁰³. Studies with knockout mice did not identify single, indispensable docking molecule. Sperm-oocyte interaction rather seems more to be mediated by a multi-protein complex¹⁰⁴.

Fertilization triggers the influx of calcium into the oocyte cytoplasm and several further calcium waves. In non-mammals this leads to membrane depolarization and the so-called fast membrane block to polyspermy, occurring 30-60 seconds after fertilization e.g. in sea urchin¹⁰⁵. Thus only one sperm can fuse with one oocyte and the zygote stays viable. Similar calcium induced changes in the membrane potential were not observed in mouse, hamster or rabbit oocytes, indicating that mammalian membrane block is not mediated by membrane depolarization^{106,107}. Additionally, the membrane block in mammals takes about 30-60 minutes to fully develop, and thus is much more slowly than in non-mammals. The sperm induced calcium oscillation furthermore leads to the exocytosis and degranulation of cortical granula^{108,109}, a process summarized as cortical reaction (figure 5). About 100 pg total protein containing several proteases are released into the area between the oocyte and the ZP, the perivitelline space^{69,110}. ZP2 (120 kDa) is proteolytically cleaved into ZP2f (90 kDa) and a smaller fragment (30 kDa), which remains connected via a disulfide bond¹¹¹. The ZP2 cleavage induces rapid changes in the ZP, which transforms into a physical barrier that

prevents further sperm from binding^{63,93}. This second block to polyspermy is called slow block, indicating the delay after fertilization in non-mammals¹⁰⁵. In mammals, the ZP modification is established in approximately the same time frame as the membrane block¹⁰⁷. Thus in

mammals the two blocks to polyspermy are distinguished spatially (membrane and ZP), but not temporally (fast and slow) like in sea urchin. The ZP modification in mammals is called ZP hardening, conferring resistance to proteolytic digestion, and mechanical stiffening^{112,113}. Furthermore, the permeability of the ZP decreases in that molecules from about 150 kDa can diffuse into pre- and post-ovulatory oocytes, but only molecules of around 110 kDa can diffuse into zygotes³⁹.

Several factors were thought to mediate ZP hardening. Ovoperoxidase was shown to be secreted from mouse oocytes after activation resulting in decreased ZP solubility¹¹⁴. Cortical granula located N-acetylglucosaminidase is exocytosed after fertilization, inactivates specific ZP3 oligosaccharides and thus was thought to block sperm binding¹¹⁵. In sows and heifer, the ZP hardening is also promoted by factors of the oviductal fluid. A complex of oviduct-specific glycoprotein (OGP) and heparin has been shown to increase ZP resistance to enzyme digestion¹¹⁶. In mouse however, oviduct-specific glycoprotein is not associated with ZP hardening¹¹⁷. The role of the plasminogen/plasmin system in reproduction is controversial. As already mentioned before, plasminogen activator converts blood serum plasminogen into the active enzyme plasmin that also degrades several proteins like fibrin clots. Huarte et al. showed that plasminogen is present in the fertilization environment of mice⁵¹ and this was also confirmed in pigs and cows¹¹⁸. Both murine gametes express plasminogen activators, but in the oocyte these are located close to the membrane instead of in the cortical granules, as expected. Plasmin activity was shown to increase ZP hardening in rat while the addition of plasminogen increased sperm binding in mice, pigs and cows^{51,118,119}. However, plasminogen deficiency caused no reproductive defects and mice deficient for plasminogen activators only showed slightly reduced fertility, most likely due to general thrombosis^{120,121}. Thus the role of the plasminogen / plasminogen activator / plasmin system in fertilization seems to be species specific and is still controversial. To our knowledge notably none of the above factors is reported to interact with ZP2 processing. The cleavage of ZP2 is however, regarded critical in ZP hardening.

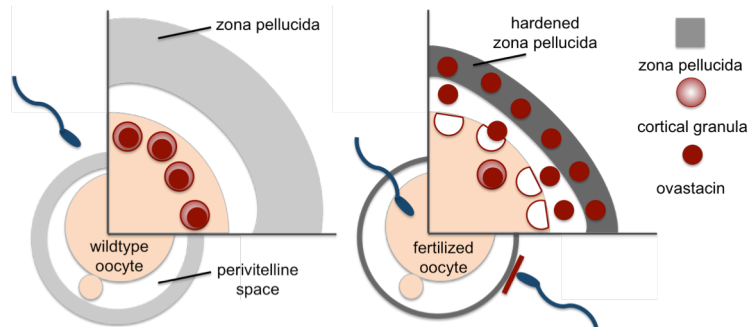


Figure 5. Illustration of the mechanism between fertilization and polyspermy block. Fertilization induces cortical granula release leading to ZP hardening and thus to a block of further sperm binding.

The metalloprotease ovastacin is the only known proteinase, which cleaves ZP2, and is expressed exclusively in the cortical granules¹²². In ovastacin deficiency (*Astf*^{-/-}), ZP2 is not cleaved after fertilization (figure 6). It was anticipated that the lack of ZP hardening should be associated with polyspermy resulting in

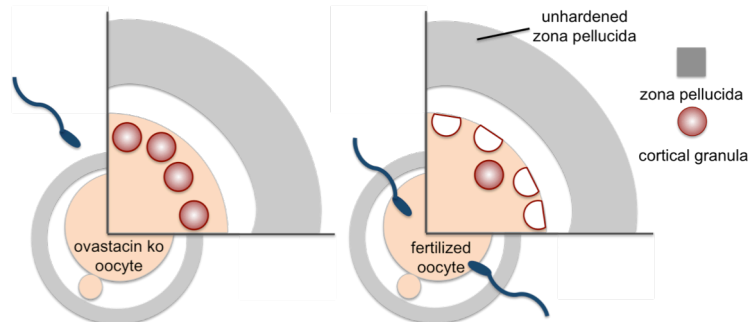


Figure 6. Illustration of the absent ZP hardening under ovastacin deficiency. Ovastacin deficient oocytes undergo fertilization and cortical granula reaction but lack ZP hardening, eventually leading to polyspermy and thus to a decreased mean litter size compared to wildtypes.

reduced zygote viability. Ovastacin deficient female mice were indeed subfertile, showing a reduced mean litter size (5.5 offspring/litter compared to 6.5 of the wildtype). In humans polyploidy has been detected in approximately 10-20% of spontaneously aborts and the majority of triploid human embryos are the result of polyspermic fertilization^{123,124}. Amino acid alignment indicates 67% sequence identity of murine and human ovastacin gene and 75% sequence similarity (supplemental figure S5). Thus the *ASTL* gene is well conserved in humans. The thousand genome project lists more than 760 variations in the human *ASTL* gene with 73 sequence variants, that change one or more bases, resulting in a different amino acid sequence but with preserved length (http://browser.1000genomes.org/Homo_sapiens/Gene/Variation_Gene/Table?db=core;g=ENSG00000188886;r=2:96789589-96804175). It is currently unknown, whether any of these variations further are associated with reduced fertility and pregnancy loss^{122,125}.

1.3.3 Embryogenesis and Implantation

Until fertilization the oocyte arrests at the second meiosis. The arrest is mediated by a complex of maturation promoting factor (MPF) and cytosolic factor (CSF)²⁰. After sperm-oocyte fusion, the calcium influx results in the breakdown of the MPF / CSF complex⁷⁷. The meiosis of the oocyte is completed and the second polar body appears. In some species including humans, the first polar body divides synchronously, giving rise to three polar bodies. The sperm including the sperm tail fuse with the oocyte and deliver two centrosomes that form the mitotic spindle for cell division. The two cell nuclei do not fuse immediately. Instead two pronuclei appear where the male and the female gamete-derived new DNA strands are synthesized. Subsequently the nuclear membranes dissolve and the chromosomes align in one metaphase plane shortly before the first mitotic division starts. Thus diploid cell nuclei first exist in the two daughter cells of the two-cell embryo. Further

segmentations lead to a progressive reduction of the cell volume and the maintenance of the embryo volume. Around the 16- to 32- cell stage, the morula with the blastocoel is formed (compaction) and afterwards the blastula forms (cavitation), separating the inner cell mass (ICM) from the trophectoderm (TE). In mice, the development from zygote to blastula takes about 3.5 - 4 days, and in humans 4 - 6 days, respectively ¹²⁶. During early development, the embryo is surrounded by the ZP and is transported from the oviduct to the uterus where it implants at the blastula stage. Premature ZP release leads to a resorption of the developing embryo by the oviductal epithelium and thus to a reduced fecundity, e.g. in the *Zp1*^{-/-} mice ⁷². These results illustrate that the ZP is required for proper oocyte development, species-specific fertilization, polyspermy block, and for the protection of the pre-implantation embryo until it reaches the uterus. The release of the blastocyst from the ZP is called ZP hatching or blastocyst hatching. ZP hatching is thought to be mediated by three different processes: 1) several autocrine and paracrine molecules, 2) dynamic cellular components and 3) hydrostatic pressure ¹²⁷. ZP hatching starts with a nick in the ZP, caused by local enzymatic digestion. Several autocrine and paracrine molecules expressed by the blastocyst or by the endometrium including growth factors, cytokines and proteases promote ZP hatching ¹²⁷. In mice the embryonic trypsin (encoded by the implantation serine proteinase 1 (*Isp1*) gene) is essential in ZP hatching ^{128,129}. ISP1 as well as the trypsin-related proteinase ISP2 are expressed in the endometrium during implantation, and are regulated by progesterone ^{130,131}. Dynamic cellular components including actin-based trophectodermal projections (TEPs) penetrate the ZP and promote ZP hatching by undulating movements ¹³². The existence of these TEPs was demonstrated for hamster, bovine, equine, monkey, human and guinea pig, but not for mice ¹³²⁻¹³⁴. ZP hatching is promoted by undulating contraction and expansion of the blastocyst. The hydrostatic (mechanical) pressure results in thinning of the ZP. Thus the blastocyst gradually escapes the ZP, which remains largely intact as a ghost ^{135,136}.

If ZP hatching fails, embryonic development stops, resulting in miscarriage. Thus several methods were developed to assist ZP hatching and improve implantation ^{137,138}. For assisted hatching the ZP is either partial dissected, locally dissolved by the use of acids or perforated by local laser exposure. Although these methods increase the incidence of implantation per embryo replaced, they are still suspected to cause damages to individual blastocyst with decreasing embryo development ^{139,140}. In addition, ZP laser perforation has been associated with an increased risk of monozygotic twinning ¹⁴¹.

After ZP hatching, the trophectoderm secretes (human) chorionic gonadotropin (hCG) to obtain the *corpus luteum*. The progesterone level stays constant and thus the shedding of the endometrium and a miscarriage is prevented. A multitude of growth factors, hormones and other substrates are expressed by the embryo and the endometrium of the uterus as the

embryo becomes competent for implantation ¹⁴². Trophoblast-derived cellular protrusions extend into the endometrium and adhere to epithelial cells by microvilli ¹²⁷. Contraction of the trophoblast microfilaments allows the blastocyst to invade between the endometrial cells. Invasion continues until the embryo finds a uterine spiral artery that will provide the embryo with nutrients during the further development ¹⁴³. After implantation, the trophectoderm sustains hCG expression ⁵⁵. HCG level reaches a peak at the end of the first trimester of the gestation period, which is exploited in the majority of pregnancy tests. Placentation occurs and is followed by further embryogenesis and fetal development until birth. In humans the development from fertilization to birth takes about 40 weeks, and in mice 18-20 days, respectively ⁷⁸.

1.3.4 Premature ZP hardening

Cortical granula release does not only occur after fertilization, but also at a low level before fertilization during meiotic maturation and ovulation ^{49,144}. In mice, germinal vesicle intact oocytes have about 5400 cortical granules, of which about 1300 are released during germinal vesicle breakdown ⁴⁹. During *in vitro* fertilization the spontaneous cortical granula release induces premature ZP hardening (figure 7) resulting in a decreased fertilization success ^{71,145}. *In vivo*, partial degranulation however, does not normally trigger ZP hardening indicating that there must be an inhibitor of ZP hardening. Cortical granule loss increases drastically *in vivo* about 30 hours after ovulation and is finished about 15 hours later ¹⁴⁶. Thus *in vivo*, spontaneous ZP hardening starts simultaneously to cortical granule loss, indicating that the inhibitor capacity is overcome. ZP hardening constantly increases for further 60 hours. Fertilization success

decreases starting directly after ovulation (from 95% to 80%). About 42 hours after ovulation the fertilization success *in vivo* drops precipitously, from 80% to 0% within two hours, indicating that partial ZP hardening is sufficient to prevent fertilization.

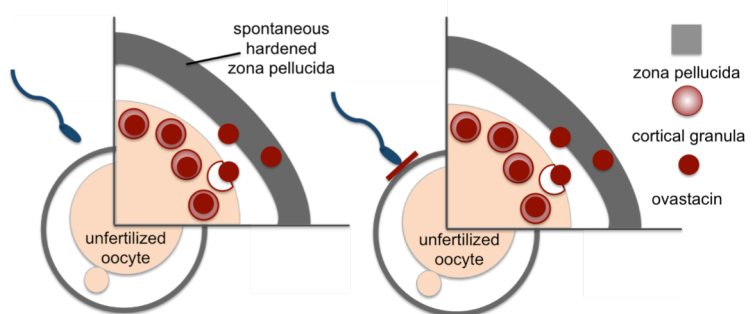


Figure 7. Illustration of the mechanism between spontaneous cortical granula reaction and premature ZP hardening. Spontaneous cortical granula release during oocyte maturation results in premature ZP hardening and thus decreases fertilization success *in vitro*.

In vitro spontaneous ZP hardening is much faster. A reduction in fertilization can already be seen after 15 minutes ¹⁴⁷. *In vitro* spontaneous ZP hardening can be prevented by adding serum, especially fetal calf serum (FCS), human serum or human follicular fluid to IVF

medium, collectively suggesting that both follicular fluid and serum contain factors that inhibit premature ZP hardening^{147,148}. One challenging task in formulating cell culture media for IVF is safety and the exclusion of protein or virus transmitted disease¹⁴⁹. In the last decades either human serum with its undefined composition or the more defined purified human serum albumin was mostly used in IVF media. Reports of notorious lot-to-lot variability in human serum and human serum albumin have been blamed for fluctuating pregnancy success in clinics. Furthermore, even after heat inactivation and filtration, human serum still carries the risk of contamination with infectious disease such as human immunodeficiency virus (HIV) or hepatitis¹⁵⁰. Pathogenic proteins like prions that may cause Creutzfeldt-Jakob Disease are likewise a serious concern¹⁵¹. Thus it was a purpose to replace serum by a defined and safe recombinant protein source. Early on, purified or recombinant human serum albumin alone were found insufficient to prevent premature ZP hardening^{149,152}. Beside FCS and human follicular fluid, the presence of an intact *cumulus oophorus* decreased premature ZP hardening and increased fertilization success, although less efficient than the addition of serum^{147,153}. These findings support the idea that the extracellular matrix of the cumulus cells stores serum-derived factors that contact the COC during folliculogenesis, especially at antrum formation. Several studies suggested that fetuin-A (originally designated fetuin) was involved in the prevention of ZP hardening^{148,152,154–156}. Kalab and colleagues showed in 1991 that the use of bovine fetuin during IVF decreased ZP hardening, and increased fertilization success¹⁵⁴. Two years later it was demonstrated that fetuin-A is present in human follicular fluid, but that the inhibitory effect of follicular fluid to ZP hardening still existed after immunodepletion by fetuin-A antibodies of the follicular fluid¹⁴⁸. The authors concluded that there should be inhibitory molecules other than fetuin present in follicular fluid that prevent premature ZP hardening. Recently it was shown that serum fetuin-A increased in patients undergoing IVF, but this increase did not correlate with fertilization success¹⁵⁷. Additionally, fetuin-A deficient mice are fully fertile, arguing against a role for fetuin-A in fertilization^{7,8,158}. Considering that fetuin-B was not known at the time of the earlier studies and that fetuin-B deficient female mice showed blocked fertilization, we hypothesized that fetuin-B could be involved in the prevention of ZP hardening¹⁷.

The fact that fetuin-B could still be extracted from most tissues even after tissue perfusion suggested, that fetuin-B tightly associates with the extracellular matrix². In addition it was shown that maintaining the cumulus mass during *in vitro* maturation decreased premature ZP hardening¹⁴⁷. Thus we hypothesized that fetuin-B diffuses from the blood into the follicular fluid, where it surrounds the oocytes during maturation (figure 8). After ovulation, the surrounding cumulus cells and their extracellular matrix could work as storage of fetuin-B until fertilization to avoid premature ZP hardening *in vivo*. After fertilization, ovastacin is released from the cortical granula, suddenly increasing the amount of ovastacin around the

oocyte. Concomitantly the amount of surrounding fetuin-B probably decreases due to sperm-mediated cumulus cell matrix degradation. Thus ovastacin concentration would exceed inhibition capacity of fetuin-B, leading to fertilization-triggered ZP hardening.

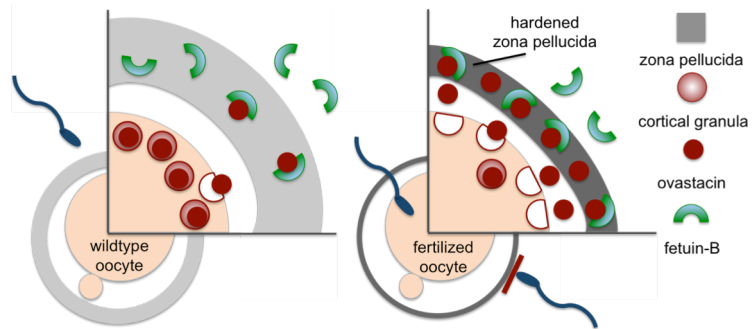


Figure 8. Illustration of the hypothesized function of fetuin-B. At spontaneous cortical granula release fetuin-B inhibits ovastacin activity and thus premature ZP hardening to maintain fertility (left). After fertilization the enhanced release of ovastacin overcomes the inhibitory capacity of fetuin-B, leading to ZP hardening and blocked polyspermy (right).

1.4 The Mouse as Model Organism

In mammalian studies the house mouse (*Mus musculus*) has often become the animal of choice. Mice in general have a small size compared to other mammals. This reduces the space necessary for animal husbandry. Mice furthermore show rapid generation times and large litter size. One mouse year equals about thirty human years, minimizing time required to perform research. In 1909 C. C. Little developed the first inbred mouse strain named DBA. One of the most popular mouse strains, C57BL/6 was likewise bred by Little in the year 1921. In the year 1982 the group of Palmiter and Brinster developed methods to insert foreign DNA into the germ line of mice. Between 1987-1989 Evans, Smithies and Capecchi created the first knockout mice, breaking new ground in genetic research.

In 2001 the first human genome was assembled and published by Venter and colleagues¹⁵⁹. The first mouse genome was published in 2002 and was reported about 14% smaller than the human genome¹⁶⁰. At the nucleotide level 40% of the human and mouse genome can be aligned. Approximately 99% of mouse genes have a homologue in the human genome, allowing the transfer of murine genetics to humans. DNA sequence comparisons between their consensus sequence and publicly funded genome data provided locations of 2.1 million single-nucleotide polymorphisms (SNPs) in the human genome and about 0.8 million in mice. Less than 1% of all SNPs resulted in variation in proteins, but the functional consequences of most of these SNPs are still unknown. To study human genomic mutations and their associated phenotypes, model organisms are required. Transgenic mice nowadays serve as

a very potent model to study the correlation between genetic defects and diseases as well as the adequate medication.

Reproductive biology, including gametogenesis, fertilization and embryogenesis is largely conserved in mammals, and most loss-of-function mutations have been determined using mice ^{161,162}. Beside small differences, for example the ZP composition (in humans ZP1-4, in mice ZP1-3), the mouse is a potential model organism to study mammalian and especially human reproduction biology.

Using mice as a model organism the choice of the strain background can have a dramatic effect on the phenotype ⁸. To avoid background specific effects, fetuin-B deficient mice were studied in two different mouse strains (C57BL/6 and DBA/2). A facts sheet of basic and reproductive parameters of C57BL/6 and DBA/2 mice is shown in table 2. DBA/2 mice show a shorter lifespan than C57BL/6. While the DBA/2 females are generally heavier than C57BL/6 females of similar age, the males show the opposite effect. Although C57BL/6 females yield lower numbers of oocytes after superovulation and have lower fertilization success after IVF they produce a higher number of pups per litter.

Table 2. Vital and reproductive statistics of C57BL/6J and DBA/2J mice. ^{163–166}

	C57BL/6J mice	DBA/2J mice
Lifespan (days) female / male	856 / 894	580 / 641
Body weight (g) female / male	2 month: 17.7 / 22.2 6 month: 23.5 / 30.7 12 month: 26.0 / 35.5 20 month: 24.1 / 32.6	2 month: 18.9 / 21.5 6 month: 29.9 / 29.5 12 month: 27.2 / 27.5 20 month: 25.7 / 21.8
Age at vaginal opening (patency) (days)	34.3	37.7
Gestation duration (days)	19.17	19.71
Number of pups / litter	7.67 ¹⁶³ 6.60 ¹⁶⁴ 5.89 ¹⁶⁵	5.73 ¹⁶³ 5.00 ¹⁶⁴ 4.85 ¹⁶⁵
Interval between litters (days)	37.3	29.1
Females responding to superovulation (%)	100	95
Oocytes per donor after superovulation / live oocytes (%)	25.2 / 98.7	34.2 / 98.5%
Fertilization success after IVF (% of 2-cell embryos)	66.2	93.5

1.5 Aim of the Study

At the beginning of this study it was known that fetuin-B deficient females are infertile because of a fertilization blockade ¹⁸. I had already demonstrated that fetuin-B deficient oocytes can be fertilized after physically overcoming the ZP by laser perforation, and that the infertility of *Fetub*^{-/-} females is caused by a defect in the ZP ¹⁹.

The aim of the dissertation was to examine if premature ZP hardening caused the female infertility of fetuin-B deficient mice. Furthermore, I investigated if fetuin-B is able to inhibit ZP hardening (by inhibiting ovastacin protease) and if the supplementation of fetuin-B during IVF can increase the fertilization success.

2. Experimental Procedures

The animal welfare committee of the Landesamt für Natur-, Umwelt- und Verbraucherschutz (LANUV) of the state of North Rhine Westfalia approved our animal study protocol. Animal maintenance, handling and anesthesia were performed according to the Federation for Laboratory Animal Science Associations FELASA recommendations in the animal facility of the University Hospital Aachen. Animals were sacrificed by isoflurane overdosing.

Laser-assisted *in vitro* fertilization (LA-IVF) and embryo transfer was performed in collaboration with Tanja Pfeffer and professor René Tolba, Institute for Laboratory Animal Science RWTH Aachen University.

The fetuin-A and fetuin-B producing adenoviruses was recombined and cells were infected by the adenovirus in the S2 laboratory of professor Ralf Weiskirchen, Institute Molecular Pathobiochemistry, Experimental Gene Therapy and Clinical Chemistry, RWTH Aachen University.

Expression of recombinant ovastacin as well as fetuin-B ovastacin inhibition assay was performed in cooperation with professor Walter Stöcker, Institute of Zoology, Cell and Matrix Biology, Johannes Gutenberg University Mainz.

2.1 Fertility Evaluation of Fetuin-B Deficient Mice

2.1.1 Mouse Genotyping

For genotyping tail biopsies of about 1-2 mm length were taken from four week old mice. The tissue was digested in 500 µl buffer (100 mM TRIS/HCl, pH 8.5, 5 mM EDTA, 0.2% SDS, 200 mM NaCl) each, containing 0.18 U/µl recombinant Proteinase K (Thermo Scientific #EO0492, PCR grade), over night at 55 °C. DNA was precipitated by isopropyl alcohol ¹⁶⁷ and again dissolved in 80 µl TE buffer (10 mM TRIS/HCl, pH 8.0, 1 mM EDTA). Genotyping was performed by multiplex-PCR, see tables 3 and 4. For amplification DreamTaq™ Green DNA Polymerase system (Thermo Scientific #EP0713) was used as well as the following primers: P4as 5'-GCT TGA ACG ATG GGA TAG GC-3', P6s 5'-CAA GTT CTA ATT CCA TCA GAA GC-3' and P8s 5'-GGG CCT GCT CAG TGT CTA CC-3'.

Table 3. Mastermix for fetuin-B genotyping.

component	end concentration
buffer (10x)	1x
dNTPs	0.2 nmol/µl
betain	1.0 µmol/µl
P4as	1.2 pmol/µl
P6s	0.8 pmol/µl
P8s	1.2 pmol/µl
Taq polymerase	0.025 U/µl
pure water	up to 23.5 µl
genomic DNA	1.5 µl

Table 4. PCR program for fetuin-B genotyping by using a T3 Thermocycler (Biometra).

temperature	time	cycles
94 °C	1 min	
94 °C	20 sec	35 x
56 °C	30 sec	
71 °C	2 min	
71 °C	7 min	
4 °C	∞	

When separated on 1% agarose gel, amplicon signifying fetuin-B deficiency showed a size of about 600 bp as expected, while the wildtype-specific amplicon showed the expected size of 1100 bp.

2.1.2 Breeding Performance

Females were mated at 10 - 25 weeks of age with 12 - 20 week old males of the identical genetic background (C57BL/6 or DBA/2). Copulation success was scored by the presence of a vaginal plug. Two weeks after copulation females were examined for pregnancy and after delivery the litter size was documented.

2.1.3 Fetuin-B Western Blot (Murine and Human)

Fetuin-B serum concentration in fetuin-B heterozygous and wildtype mice was measured by quantitative Western blot. Recombinant murine fetuin-B (Invigate, Lot. C110113-02) with a known concentration was used for calibration. Six different concentrations were loaded from 0 to 35 ng/lane. Serum samples were diluted 1:100 in sample buffer (0.125 M TRIS/HCl, pH

6.8, 5% SDS, 10% glycerol, 10% beta-mercaptoethanol, 0.01% bromophenole blue) and were heated up for five minutes at 95 °C¹⁶⁸. Fifteen µl of each sample were loaded onto a 10% polyacrylamide SDS-PAGE using the Biorad mini gel system. Proteins were “semi-dry” blotted on a nitrocellulose membrane (Whatman #10439396) with 1.5 mA/cm² for one hour. Successful protein transfer was evaluated by Ponceau-S staining (0.2% Ponceau-S red in 5% acetic acid). The blotting membrane was blocked overnight using 5% non-fat dry milk powder in PBST (phosphate buffered saline supplemented with 0.05% Tween[®]20) at 4 °C. Polyclonal rabbit anti-mouse fetuin-B (K320, bleeding 28.09.2000) was diluted 1:1000 in blocking buffer and incubated with the membrane for one hour at 37 °C in a rotating 50 ml reaction tube. Afterwards the membrane was washed three times with PBST at 37 °C for five minutes each. Polyclonal swine anti-rabbit IgG/HRP (Dako #P0217) was diluted 1:5000 in blocking solution and incubated for one hour at 37 °C. Afterwards the membrane was washed three times with PBST at 37 °C for five minutes each. Chemiluminescence signal was developed using ECL-substrate (1.25 mM 3-Aminophthalhydrazide, 0.45 mM p-Coumaric acid, 0.015% hydrogen peroxide). Luminescence was detected using a LAS4000-mini imaging system (Fuji). Quantification was performed using the software ImageJ.

The Western blot measuring human fetuin-B was done like described above for mouse. Anti-human fetuin-B antibody was used to detect bovine as well as human fetuin-B. Commercial bovine fetuin preparations (7.5 µg per lane) from various sources were separated by SDS-PAGE (10% acrylamide): Sigma-Aldrich F2379 (bov fetuin1), Sigma-Aldrich F3004 (bov fetuin2), Sigma-Aldrich F2379 (bov fetuin3) and further purified by gel filtration, AppliChem A2783 (bov fetuin4). Blocking was mediated by 1% bovine serum albumin (BSA) in PBST. Primary antiserum polyclonal rabbit anti-human fetuin-B (K316, bleeding 04.04.2001) was diluted 1:1000 and polyclonal swine anti-rabbit IgG/HRP (Dako #P0217) as secondary antibody was diluted 1:2000.

2.1.4 Collection of Zygotes and Oocytes

To confirm blocked fertilization in fetuin-B deficient oocytes potential zygotes were isolated after spontaneous mating. The zygotes and unfertilized oocytes were isolated from the ampulla and were liberated from surrounding cumulus cells by digestions in 300 µl human tubular fluid (HTF, for detailed chemical composition see table 5) medium containing 0.3 mg/ml hyaluronidase (22.5 – 45 IU/ml, Sigma) for 2-3 minutes. Afterwards oocytes and zygotes were washed five times in 50 µl HTF medium each, to get rid of the cumulus cells. A comprehensive protocol is found in “Manipulating the mouse embryo”¹⁶⁹. Subsequently potential zygotes were scored microscopically for signs of fertilization like an enlarged perivitelline space and the existence of two polar bodies.

For further oocyte analysis follicular growth of five to ten week old mice was stimulated by injection of five international units (IU) pregnant mare serum gonadotropin (PMSG, Intervet #A034A02, stock 500 IU/ml, diluted 1:10 in PBS, 100 µl/mouse injected). For the collection of pre-ovulatory oocytes, the mice were sacrificed. Using a stereo microscope and a micropipette, antral follicles were punctured to recover oocytes. For the collection of post-ovulatory oocytes, five IU human chorionic gonadotropin (hCG, Intervet #A034A01, stock 500 IU/ml, diluted 1:10 in PBS, 100 µl/mouse injected) were injected 48 hours post-PMSG to stimulate ovulation. 13 hours post-hCG the female mice were sacrificed by cervical dislocation. Oocytes were collected as described above. All incubations were done at 37 °C in gassed (5% CO₂, 5% O₂, 90% N₂) medium covered with mineral oil, pre-incubated over night.

Table 5. Chemical composition of human tubular fluid (HTF) medium

chemicals	end concentration
NaCl	5.9 g/L
KCL	350.0 mg/L
MgSO ₄ x 7 H ₂ O	49.0 mg/L
KH ₂ PO ₄	54.0 mg/L
CaCl ₂ x 2 H ₂ O	755.0 mg/L
NaHCO ₃	2.1 g/L
glucose	500.0 mg/L
Na-lactate (60% sol.)	3.4 mL/L
Na-pyruvate	37.0 mg/L
penicillin G	75.0 mg/L
streptomycin	50.0 mg/L
BSA	4.0 g/L
phenol red (0.5% sol.)	0.4 mL/L

2.1.5 *In Vitro* Fertilization and Embryo Transfer

Oocytes were collected after hormonal stimulation with PMSG and hCG (superovulation) as described in the paragraph 2.1.4 "Collection of Zygotes and Oocytes" without hyaluronidase treatment. Sperm was collected from the *cauda epididymis* and *vas deferens* of 14 - 16 week old males in TYH+MBCD medium (for chemical composition see table 6) and incubated for 60 minutes at 37 °C. Sperm was counted and a final concentration of 1 - 2.5 x 10⁶ sperm per ml was mixed with two to five COCs. Following four hours of incubation the zygotes were washed four times in 150 µl HTF medium each to remove excess sperm and any residual debris. 24 hours later the embryos were evaluated and counted. In another group of oocytes the ZP was twice perforated using a laser before the addition of sperm. All incubations were done at 37 °C in gassed (5% CO₂, 5% O₂, 90% N₂) medium covered with mineral oil, pre-incubated over

Table 6. Chemical composition of TYH + MBCD (methyl-β-cyclodextrin) medium

chemicals	end concentration
NaCl	6.98 g/L
KCL	356.0 mg/L
MgSO ₄ x 7 H ₂ O	293.0 mg/L
KH ₂ PO ₄	162.0 mg/L
CaCl ₂ x 2 H ₂ O	251.0 mg/L
NaHCO ₃	2.1 g/L
glucose	1.0 g/L
Na-pyruvate	55.0 mg/L
penicillin G	75.0 mg/L
streptomycin	50.0 mg/L
MBCD	983.0 mg/L
polyvinylalcohol	1.0 g/L

night. Laser-perforation as well as embryo transfer was performed with Tanja Pfeffer and René Tolba, Institute for Laboratory Animal Science RWTH Aachen University.

For embryo transfer, either wildtype or *Fetub*^{-/-} females eight weeks of age were mated with vasectomized males to induce pseudo pregnancy. About 36 hours post-mating the embryos derived from laser-assisted *in vitro* fertilization were transferred into the pseudo pregnant mice following established protocols¹⁶⁹. For the transfer pseudo pregnant mice were anaesthetized, the skin was disinfected and a dorsal lateral cut opened the abdomen. 15 wildtype or *Fetub*^{-/-} derived embryos were implanted each per mouse. Embryos were transferred using a micropipette directly into the infundibulum. To minimize physical strain the embryos transfer was done unilateral, meaning that only one of the two oviducts was used. After transfer the subcutis was stitched up and epidermis was closed with clips.

Fetuses were dissected at embryonic day 16 to avoid cannibalism and loss of pups. These fetuses were killed and analyzed by histology. Complete fetuses were shock-frozen using liquid nitrogen cooled iso-pentane. The tissue was cut into 10 µm sections and fixed with zinc fixative (BD Pharmingen™ #550523). Afterwards the sections were washed three times with PBS and one time with pure water for five minutes each. Basophilic cell components were stained for one minute with hematoxylin (Roth® #T865.1) and staining was differentiated under running water for ten minutes. Subsequently acidophilic cell components were stained with eosin (Roth® #X883.2) for one minute. Sections were dehydrated using a graded ethanol series (70%, 95% and 100%) and three washes with xylene for five minutes each. Sections were mounted using Roti®-Histokitt (Roth® #6640) and glass cover slips. Microphotographs were recorded using a stereomicroscope (Leica MZ6) and an attached digital camera (JVC KY-F75U).

Alternatively the transferred embryos were carried to full term to study early childhood development and maternal care. Following birth the pups were inspected for general health every other day until they reached puberty (about four weeks).

2.2 Testing for *Zona Pellucida* Hardening

2.2.1 Oocyte Diameter and *Zona Pellucida* Thickness

Oocytes were isolated after hormonal stimulation as described at paragraph 2.1.4 with removal of the cumulus cells by hyaluronidase digestion. Two-cell embryos were obtained by IVF. Oocyte diameter as well as ZP thickness was measured at three different representative positions for each oocyte or embryo using a microscope and DISKUS image acquisition and analysis software (Carl Hilgers, Königswinter). Mean values for each cell were blotted at the graph.

2.2.2 *Zona Pellucida* Digestion

Same oocytes and two-cell embryos that were used for diameter and ZP thickness measurements were also used for ZP digestion. The assay was performed like reported before using a 0.2 mg/ml chymotrypsin (10 IU/ml) solution¹⁷⁰. Oocytes and embryos were washed two times in 100 µl PBS and two times in 100 µl PBS containing 0.2 mg/ml chymotrypsin each. Oocytes and embryos were placed in a fresh 100 µl drop of chymotrypsin solution and a microscopic picture was taken every minute. The percentage of zona free oocytes was plotted against the time. Data were plotted as a sigmoidal time curve with variable slope using GraphPad Prism statistics software. T50 the time point at which 50% of oocytes had become zona free was calculated using a four parameter logistic regression.

2.2.3 Sperm Binding

Oocytes were collected as described in the paragraph 2.1.4 "Collection of Zygotes and Oocytes" with hyaluronidase treatment to remove cumulus cells. After washing the oocytes they were placed in 500 µl HTF medium. Two-cell embryos were obtained by IVF. Sperm was collected and capacitated as described in the paragraph 2.1.5 "In Vitro Fertilization and Embryo Transfer". Sperm was counted and a final concentration of 1×10^6 sperm/ml was mixed with 30-50 oocytes or 2-cell embryos, respectively. All incubations were done at 37 °C in gassed (5% CO₂, 5% O₂, 90% N₂) medium covered with mineral oil, pre-incubated over night. After one hour of incubation oocytes were washed up to ten times employing 100 µl HTF medium in each washing step to remove all but two to six sperm on normal two-cell embryos (negative control). Oocytes were fixed in 2% para-formaldehyde (PFA), and sperm binding was quantified by a microscope and DISKUS image acquisition and analysis software (Carl Hilgers, Königswinter).

2.2.4 ZP2 Western Blot

20 - 30 oocytes from wildtype and *Fetub*^{-/-} mice as well as two-cell embryos were isolated as described under 2.1.4, dissolved in sample buffer and separated by a 8% polyacrylamide SDS-PAGE to detect cleavage of ZP2 as described before ¹⁷¹. Unspecific antibody binding was blocked with 5% non-fat dry milk powder in TBST (TRIS buffered saline with 0.05% Tween20) for two hours at room temperature. Primary antibody rat anti-mouse ZP2 (M2c.2) was diluted 1:500 in blocking solution and incubated over night at 4 °C. Secondary antibody goat anti-rat IgG/HRP (Santa Cruz #SC2065) was diluted 1:5000 in blocking solution for one hour at room temperature. Chemiluminescence signal was achieved using ECL Plus substrate solution (GE Healthcare #RPN2132) and was detected by the LAS4000-mini imaging system (Fuji).

2.3 Ovastacin Inhibition by Fetuin-B

2.3.1 Recombinant Fetuin-A and Fetuin-B Expression

This work was performed by Eddy van de Leur and Ralf Weiskirchen, Institute Molecular Pathobiochemistry, Experimental Gene Therapy and Clinical Chemistry, RWTH Aachen University as well as Julia Floehr, Helmholtz-Institute for Biomedical Engineering, Biointerface Laboratory, RWTH Aachen University.

Mouse full-length fetuin-A or fetuin-B cDNA was amplified and ligated into the adenoviral shuttle vector p Δ E1sp1A and transposed into adenovirus (Ad5) as described^{17,172}. The resulting viruses were used to infect Cos-7 cells. After an overnight incubation period the media was changed to a serum-free culture and incubated for another 24 hours to obtain serum-free cell culture supernatant containing fetuin-A or fetuin-B. The cell culture supernatant was filtered through a 0.45 μ m filter and the His-tagged recombinant fetuin-A or fetuin-B was purified using HisTrap affinity columns and an ÄKTA liquid chromatography system (GE Healthcare). The fractions containing the purified proteins were pooled and dialyzed against PBS. Recombinant proteins were identified by Western blot, the purity was judged by SDS-PAGE and Coomassie Blue staining.

2.3.2 Ovastacin Expression

This work was performed by professor Walter Stöcker, Institute of Zoology, Cell and Matrix Biology, Johannes Gutenberg University Mainz and coworkers.

Mouse full-length ovastacin cDNA (Q6HA09) was amplified and transferred into pFastBac1 (Bac-to-Bac system, Life Technologies, Darmstadt) using the SphI and HindIII sites, verified by sequencing (SeqLab, Göttingen) and transposed into baculovirus¹⁷. The resulting bacmids were used to infect Sf9 insect cells for virus amplification. Cells and debris were removed by centrifugation and the proteins precipitated from the supernatant in 50 mM TRIS/HCl, pH 7.4 containing 60% (w/w) ammonium sulfate for 12 hours at 4 °C. Protein pellet was obtained by centrifugation (10.000 x g, 2 hours, 4 °C), dissolved in 1/10 volume of 50 mM TRIS/HCl, pH7.4, 150 mM NaCl, dialyzed vs. the same buffer, loaded onto a streptactin sepharose column (IBA, Göttingen) and the purified ovastacin eluted by adding 2.5 mM desthiobiotin (IBA, Göttingen).

2.3.3 Inhibition Assay

This work was performed by professor Walter Stöcker, Institute of Zoology, Cell and Matrix Biology, Johannes Gutenberg University Mainz and coworkers.

Ovastacin activity with or without added recombinant fetuin-B was monitored at 37 °C in 50 mM TRIS/HCl, pH 7.4, 150 mM NaCl using a thermostatted Varioscan fluorescence plate reader (Thermo Scientific) in FRET (fluorescence resonance energy transfer) mode, and the substrate, Ac-RE(EDANS)-DRnLVGDDPY-K(DABCYL)-NH₂ at 10 mM (Biosyntan, Berlin; nL = norleucine). IC₅₀ analysis was performed using GRAFIT (Erithacus Software, Wilmington House, UK). Initial rates were normalized to complete substrate turnover subsequently obtained by proteinase K (Sigma-Aldrich) treatment.

2.4 *In Vitro* Zona Pellucida Hardening Under Fetuin-B Supplementation

2.4.1 Buffer Change for Recombinant Fetuin-B

Recombinant murine fetuin-B (rmFetuB) was stored in PBS at concentrations of about 3.0 mg/ml. For *in vitro* experiments concentrations from 0.015 mg/ml to 1.0 mg/ml were used. PBS is thought to induce cortical granula release and thus spontaneous ZP hardening. To avoid PBS-induced ZP damages through the use of the rmFetuB a change of buffer was necessary. A 2 ml Zeba Desalt Spin Column (Thermo Scientific #89889) was rinsed with sterile ultrapure water following the instructions for use. Next, 200 - 700 µl of rmFetuB in PBS were loaded onto the column to exchange PBS for water. The flow through (rmFetuB in ultrapure water) was stored at 4 °C. The identical column was flushed with sterile HTF medium (for detailed composition see 2.1.4 “Collection of Zygotes and Oocytes”) without BSA or antibiotics. The rmFetuB in ultrapure water was loaded onto the column equilibrated with HTF medium. The flow through of this second gel filtration contained about 2 mg/ml rmFetuB in HTF medium without BSA or antibiotics. To add BSA, rmFetuB containing HTF medium without BSA and antibiotics was mixed with the same volume of HTF medium containing twice the final amount of BSA and antibiotics. The resulting HTF medium containing approximately 1 mg/ml rmFetuB, was sterilized using a 0.45 µm filter. HTF medium with 1 mg/ml rmFetuB was either used directly or was further diluted to obtain HTF medium containing 0.5 mg/ml, 0.25 mg/ml, 0.125 mg/ml, 0.063 mg/ml, 0.031 mg/ml or 0.015 mg/ml for further use.

2.4.2 Effects of Fetuin-B to Fertilization, Embryo Development and Hatching

COCs of wildtype females were isolated as described in chapter 2.1.4 without hyaluronidase treatment in either HTF medium without fetuin-B or HTF medium containing 1 mg/ml rmFetuB. All incubations were done at 37 °C in gassed (5% CO₂, 5% O₂, 90% N₂) medium

covered with mineral oil, pre-incubated over night. Collection of sperm and IVF was done as described at 2.1.5. Following four hours of incubation the zygotes were washed four times in either 100 µl HTF medium without fetuin-B or 100 µl HTF medium containing 1 mg/ml rmFetuB each, to remove excess sperm and any residual debris. 24 hours later the embryos were evaluated and counted. To test ZP hardening one half of the two-cell embryos were used for ZP digestion (see paragraph 2.2.2). For evaluation of developmental potential the other half of two-cell embryos were transferred to 100 µl drops of M2 medium (Sigma-Aldrich #M7167) covered with mineral oil, pre-incubated over night. Zygotes were evaluated 48 and 120 hours after fertilization until blastula stage and ZP hatching appeared.

2.4.3 Zona Pellucida Hardening During *In Vitro* Cultivation

COCs of three to four wildtype females were isolated in 300 µl HTF medium as described in chapter 2.1.4. All incubations were done at 37 °C in gassed (5% CO₂, 5% O₂, 90% N₂) medium covered with mineral oil, pre-incubated over night. After hyaluronidase treatment to remove cumulus cells the oocytes were washed three times in 150 µl HTF medium each. Finally oocytes from up to ten females were pooled in 400 µl HTF medium. From this oocyte stock at least 20 oocytes per condition were either directly treated with alpha-chymotrypsin as described in chapter 2.2.2 or cultured for 1, 2, 4, 6, 8, 10, 12, 16, 20, 24, 28, 32 or 36 hours before ZP digestion.

2.4.4 Inhibition of *Zona pellucida* Hardening After one Hour of *In Vitro* Cultivation by Fetuin-B

COCs of wildtype females were isolated and treated with hyaluronidase as described in chapter 2.1.4 in HTF medium without fetuin-B or HTF medium containing 1.0 mg/ml, 0.5 mg/ml, 0.25 mg/ml, 0.125 mg/ml 0.063 mg/ml, 0.031 mg/ml or 0.015 mg/ml rmFetuB. All incubations were done at 37 °C in gassed (5% CO₂, 5% O₂, 90% N₂) medium covered with mineral oil, pre-incubated over night. A minimum of 30 oocytes recovered from two to three cumulus-oocyte complexes from different females was used per condition. After one hour of *in vitro* cultivation the oocytes were fertilized as described at paragraph 2.1.5. Following four hours of incubation the zygotes were washed four times in 100 µl HTF medium without fetuin-B (because it was already known, that fetuin-B does not promote post-fertilization development and to diminish consumption of rmFetuB) to remove excess sperm and any residual debris. 24 hours later the embryos were evaluated and counted. To evaluate post-fertilization ZP hardening sperm binding was quantified using a microscope as described in paragraph 2.2.3 (fixation was not necessary, because sperm already stopped moving).

Afterwards ZP of the two-cell embryos was digested with alpha-chymotrypsin as described at paragraph 2.2.2.

2.4.5 Effects of Fetuin-B and Cumulus Cells on *Zona Pellucida* Hardening During *In Vitro* Cultivation

Ten wildtype females were used to isolate COCs as described at paragraph 2.1.4. One COC of each mouse was isolated in HTF medium without fetuin-B while the other COC was isolated in HTF medium containing 0.05 mg/ml rmFetuB. One half of the COCs that were isolated in fetuin-B free HTF medium were kept untreated, remaining the cumulus cells. For the other half as well as the COCs that were isolated in rmFetuB containing HTF medium cumulus cells were recovered by hyaluronidase treatment as described in chapter 2.1.4. After washing the oocytes of each condition were pooled in 400 µl medium. All incubations were done at 37 °C in gassed (5% CO₂, 5% O₂, 90% N₂) medium covered with mineral oil, pre-incubated over night. A minimum of 30 oocytes per condition was either fertilized directly or after 1, 3, 5, 7, 9, 13, 17 or 25 hours of *in vitro* cultivation as described at paragraph 2.1.5. For each time point sperm were freshly isolated. Following four hours of incubation the zygotes were washed four times in 100 µl HTF medium without fetuin-B to remove excess sperm and any residual debris. 24 hours later the embryos were evaluated and counted.

2.5 Statistics

Data analysis was performed using GraphPad Prism software (Macintosh version 5.0c) and the statistical testing methods detailed in the figure legends.

3. Results

3.1 Fetuin-B Deficient Female Mice are Infertile Due to an Early Block to Fertilization

Laser-assisted *in vitro* fertilization (LA-IVF) and embryo transfer was performed in collaboration with Tanja Pfeffer and Professor René Tolba, RWTH Aachen.

The female infertility of *Fetub*^{-/-} female carrying the genetic C57BL/6 background, as well as the reduced fetuin-B serum concentration in *Fetub*^{+/-} females were already known¹⁸. First results indicated that the decreased fetuin-B serum concentration in *Fetub*^{+/-} mice results in smaller litter sizes. Thus one aim of this thesis was to study the fertility of *Fetub*^{+/-} females in a larger sample size of matings.

To analyze fertility of *Fetub*^{+/-} females, serum fetuin-B was measured using Western blotting as reported¹⁸. Serum fetuin-B was measured in wildtypes as well as in fetuin-B heterozygous females (figure 9). Figure 9A shows a section of a representative Western Blot. Commercial recombinant murine fetuin-B (rmFetuB, Invigate) was used for calibration. The recombinant FetuB had a slightly higher molecular weight (approx. 65 kDa) than murine serum FetuB (60 kDa), likely due to an additional linker and His-Tag sequence added for purification of the recombinant FetuB. The size difference could be due to divergent post-translational modification, like higher glycosylation or phosphorylation in the recombinant expression system. Furthermore it is conceivable that endogenous expressed fetuin-B is modified by endogenous factors resulting in a reduced molecular weight of serum fetuin-B. Serum of *Fetub*^{+/-} females showed weaker signal intensity compared to *Fetub*^{+/+} female serum (figure 9A). Quantification of *Fetub*^{+/+} serum samples in figure 9B shows about 161.4 ± 10.5 µg/ml fetuin-B (mean ± SD, n=16). As expected, about half the normal amount of fetuin-B was present in *Fetub*^{+/-} mice (89.8 ± 2.8 µg/ml, n=29), and *Fetub*^{-/-} mice had no detectable fetuin-B.

- Results -

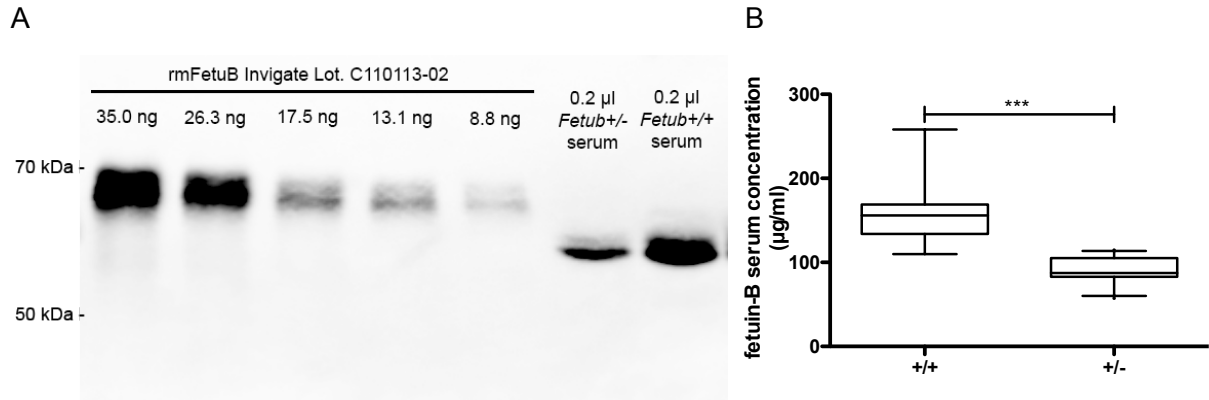


Figure 9. Heterozygous (+/-) females show half the fetuin-B serum concentration of wildtype (+/+). (A) Representative section of a murine Western blot. Molecular weight marker in kDa is indicated at the left. Commercial rmFetuB from 8.8 to 35.0 ng per lane and 0.2 µl of *Fetub*^{+/-} or *Fetub*^{+/+} serum samples were loaded each. (B) Serum fetuin-B level was significant reduced in *Fetub*^{+/-} females (89.8 ± 2.8 µg/ml, n=29) compared to wildtypes (161.4 ± 10.5 µg/ml, n=16). Boxes represents the first to the third quartile, band inside shows the median. Whiskers indicate 5-95 percentile. Pairwise two-sided t test ***p < 0.001

To explore whether the *Fetub*^{+/-} females are subfertile, all possible genotypes of females were mated with all possible genotypes of males. The results of these matings of mice carrying C57BL/6 genetic background are shown in table 7. The mean litter sizes of *Fetub*^{+/-} and *Fetub*^{+/-} females were compared with the litter size of *Fetub*^{+/+} females and the respective males. The infertility was observed exclusively in *Fetub*^{-/-} female mice (table 7). Heterozygous females remained fertile and had mean litter sizes (all three mating groups of table 7 taken together: 6.8 ± 3.4, n = 59 gestations) comparable to wildtype females (6.0 ± 1.9, n = 47 gestations) and also comparable to background specific published data (5.9 – 7.7, see table 2). Thus first results showing smaller litter sizes of *Fetub*^{+/-} females were not confirmed. Males of either genotype were fertile, too. This shows that even half the serum concentration of fetuin-B, like it was detected in *Fetub*^{+/-} females, is sufficient to maintain fertility.

- Results -

Table 7. Breeding performance of C57BL/6 mice. The mean litter sizes of *Fetub*^{-/-} and *Fetub*^{+/-} females were compared with the litter size of *Fetub*^{+/+} females and the respective males by pairwise two-sided t test, ***p < 0.001, ns = not significant (modified from ¹⁷).

C57BL/6 female (n) x male (n)	matings	gestations	pups	mean ± SD litter size	significance compared to +/+
-/- (18) x -/- (15)	26	0	0	0.0	***
-/- (8) x +/- (7)	8	0	0	0.0	***
-/- (12) x +/+ (7)	12	0	0	0.0	***
+/- (19) x -/- (11)	24	22	137	6.2 ± 3.4	ns
+/- (19) x +/- (13)	25	22	159	7.2 ± 3.9	ns
+/- (13) x +/+ (6)	16	15	103	6.9 ± 2.7	ns
+/+ (15) x -/- (8)	18	15	94	6.3 ± 1.6	-
+/+ (9) x +/- (6)	15	15	95	6.3 ± 2.0	-
+/+ (17) x +/+ (10)	24	17	91	5.4 ± 2.1	-

Because the genetic background greatly affected the calcification phenotype of fetuin-A deficient mice, we also determined the infertility phenotype of fetuin-B deficient mice against two defined genetic backgrounds ⁸. Like in C57BL/6 mice, DBA/2 heterozygous females remained fertile and had mean litter sizes (all three mating groups of table 8 taken together: 4.9 ± 2.5, n = 52 gestations) comparable to wildtype females (4.3 ± 1.9, n = 23 gestations, table 8). Mating of *Fetub*^{-/-} males with *Fetub*^{+/-} females even showed a statistically significant increased mean litter size compared to *Fetub*^{+/+} females that were mated with the identical *Fetub*^{-/-} males (5.4 ± 3.4 vs. 4.3 ± 1.8). Compared to published data on background-specific litter sizes (4.9 – 5.7, see table 2) the general mean litter size was reduced, especially when using *Fetub*^{+/+} females. This could be due to the relatively low sample number of matings. For further evaluation the number should be increased. Males of either genotype were fertile, too. In conclusion, infertility of *Fetub*^{-/-} female mice was independent of their genetic background and occurred in both C57BL/6 and DBA/2 inbred mouse strains.

- Results -

Table 8. Breeding performance of DBA/2 mice. The mean litter sizes of *Fetub*^{-/-} and *Fetub*^{+/-} females were compared with the litter size of *Fetub*^{+/+} females and the respective males by pairwise two-sided t test, *p <0.05, ***p < 0.001, ns = not significant (modified from ¹⁷).

DBA/2 female (n) x male (n)	matings	gestations	pups	mean ± SD litter size	significance compared to +/+
-/- (8) x -/- (5)	8	0	0	0.0	***
-/- (8) x +/- (4)	10	0	0	0.0	***
-/- (11) x +/+ (9)	16	0	0	0.0	*
+/- (10) x -/- (5)	18	18	97	5.4 ± 3.4	*
+/- (20) x +/- (8)	23	20	85	4.3 ± 1.8	ns
+/- (15) x +/+ (6)	16	14	71	5.1 ± 2.3	ns
+/+ (5) x -/- (4)	7	7	30	4.3 ± 1.8	-
+/+ (7) x +/- (6)	14	12	50	4.2 ± 2.0	-
+/+ (6) x +/+ (5)	6	4	18	4.5 ± 1.7	-

Earlier studies had indicated that a block of fertilization most likely caused the infertility in female *Fetub*^{-/-} mice ¹⁷⁻¹⁹. This could be confirmed for both C57BL/6 and DBA/2 mice (figure 10). About eight hours after mating, oocytes of fetuin-B deficient females were ovulated in well-organized cumulus-oocyte complexes (figure 10 A-D). After removal of the cumulus cells the oocytes of *Fetub*^{-/-} mice lacked typical signs for fertilization, like an enlarged perivitelline space (figure 10 E-H).

The total number of ovulated oocytes was comparable in *Fetub*^{-/-} and wildtype (supplemental figure 1). After mating C57BL/6 wildtypes showed about 9.0 ± 1.7 ovulated oocytes per female (n=5), while *Fetub*^{-/-} ovulated 10.2 ± 1.7 oocytes per female (n=6) and at DBA/2 background 5.5 ± 1.5 (n=2) versus 8.8 ± 0.8 (n=10) ovulated oocytes per female, respectively. The tendency of DBA/2 mice to ovulate less oocytes than C57BL/6 is also reflected in the overall smaller litter sizes shown in table 7 and 8. No data were retrievable from published literature for spontaneous ovulation, because fertility studies generally use hormonal stimulation to increase number of ovulated oocytes per donor to minimize animal number. As expected, hormonal stimulation with PMSG followed by induction of ovulation by hCG, resulted in an increase of ovulated oocytes. Wildtypes showed about 14.9 ± 1.8 ovulated oocytes per female (n=13), while *Fetub*^{-/-} mice ovulated 22.2 ± 1.9 oocytes per female (n=20) in C57BL/6 background and 33.0 ± 6.3 (n=7) versus 27.8 ± 3.3 (n=10) at DBA/2 background, respectively. Published data state that C57BL/6 mice ovulate on average 25.2 oocytes per donor after hormonal stimulation (superovulation), and DBA/2 34.2 oocytes

per female¹⁷³. Although the number of ovulated oocytes per donor was slightly reduced for both strains in the present work, the tendency of C57BL/6 mice to ovulate less oocytes than DBA/2 mice was confirmed. The fact that DBA/2 mice perform better under hormonal stimulation is surprising, because they ovulate less oocytes spontaneously after mating and also show smaller litter sizes.

Earlier studies performed IVF with and without laser perforation of the ZP to test, if a defect in the ZP blocks fertilization^{17,19}. Conventional IVF of 162 C57BL/6 derived fetuin-B deficient oocytes remained unsuccessful, whereas 51% of wildtype oocytes became fertilized (n=345; figure 10 I, L). In contrast, laser assisted perforation of the ZP followed by IVF (LA-IVF) was met with success (figure 10 M, N). Of 172 wildtype oocytes, 50% became fertilized and 35% of 261 fetuin-B deficient oocytes, respectively. Experiments done with DBA/2 oocytes showed comparable results. None of the 55 fetuin-B deficient oocytes were fertilized after conventional IVF (figure 10 L), while 87% of the 88 wildtype oocytes developed to two-cell embryos (figure 10 K). LA-IVF led to a decreased fertilization success of 47% in wildtype oocytes (figure 10 O, n=30), which could be due to laser-induced oocyte damages as well as fetuin-B deficient oocytes (figure 10 P, n=45). After ZP laser perforation, fetuin-B deficient DBA/2 oocytes were fertilized as well, showing 47% of two-cell embryos. Thus both fetuin-B deficient oocytes carrying the C57BL/6 and the DBA/2 genetic background can be fertilized after overcoming the ZP by laser perforation.

Because both mouse background strains, C57BL/6 and DBA/2, showed the same phenotype of fetuin-B deficiency, we concluded that infertility of *Fetub*^{-/-} mice is genetic background-independent. Therefore, all data that obtained with DBA/2 background mice thereafter are presented as supplemental material, while all results presented in the main text were obtained with C57BL/6 background mice.

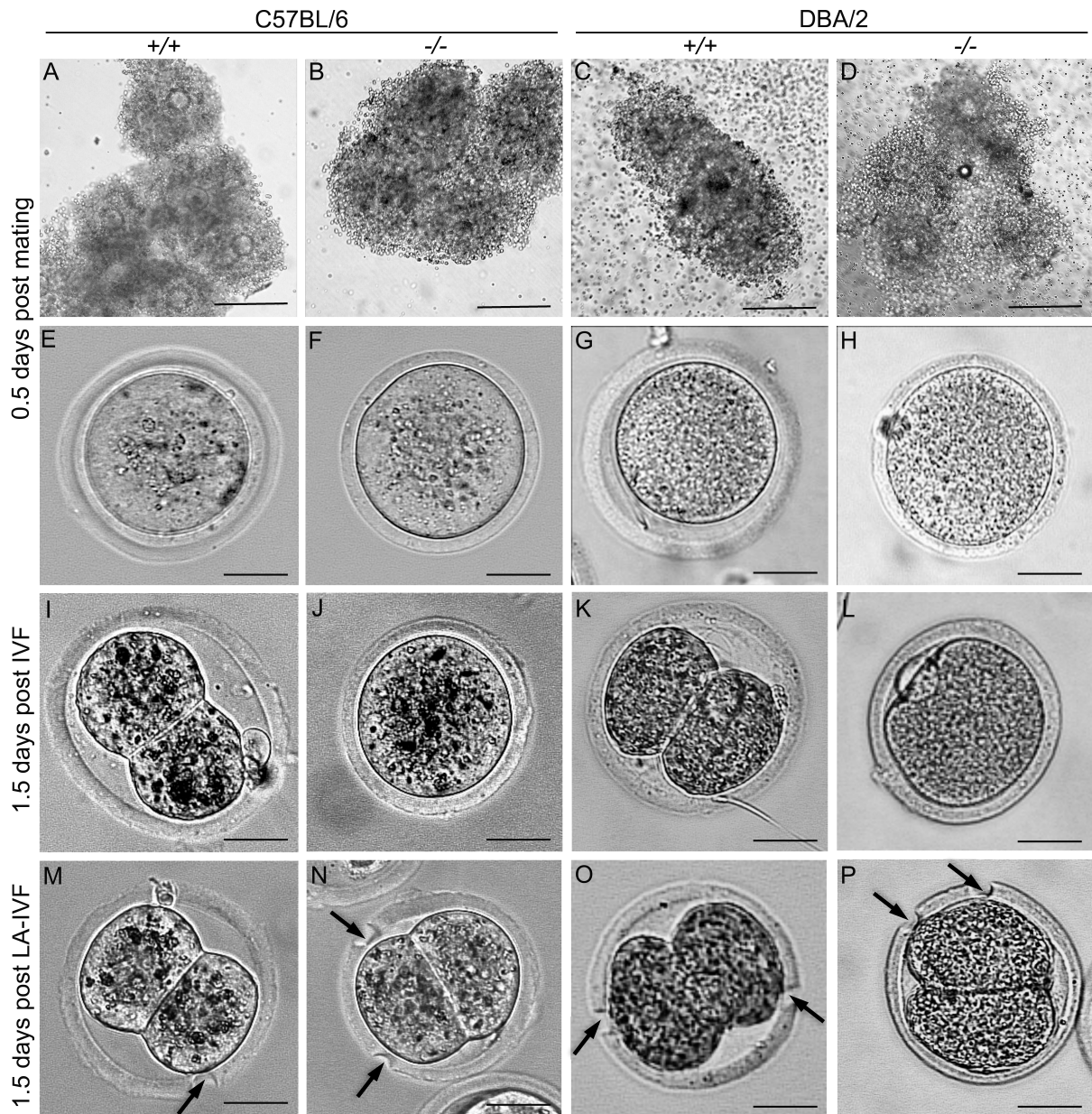


Figure 10. Fetuin-B deficient oocytes can be fertilized *in vitro* after overcoming the ZP by laser perforation. (A) Wildtype (+/+) cumulus-oocyte complex (COC) and (B) COC isolated eight hours after mating from a C57BL/6 fetuin-B deficient (-/-) mouse or (C, D) from DBA/2 mice, respectively. (E) Oocyte isolated from a C57BL/6 wildtype female showed an enlarged perivitelline space compared to (F) an oocyte isolated from *Fetub*^{-/-} female at day 0.5 after mating. (G, H) DBA/2 oocytes show the same results. Images of oocytes and two-cell embryos 1.5 days post-fertilization of (I, K) wildtype and (J, L) fetuin-B deficient oocytes recovered from C57BL/6 or DBA/2 mice following conventional IVF, or (M-P) laser-assisted IVF (LA-IVF). Arrows point to the laser lesions. Bars in A-D indicate 200 μ m, bars in E-P indicate 25 μ m (modified from ¹⁷).

Since fetuin-B deficient oocytes could be fertilized by LA-IVF we were interested to learn if these embryos would develop into healthy fetuses. Two-cell embryos, either derived from *Fetub*^{+/+} or *Fetub*^{-/-} oocytes, developed into fetuses when transferred to wildtype foster mothers as shown in figure 11. For the wildtype control one of two foster mothers produced a

total of three offspring. Identical one of two foster mothers that got the *Fetub*^{-/-} derived embryos produced a total of three offspring. Thus the fetal development of *Fetub*^{-/-} derived embryos was unaffected.

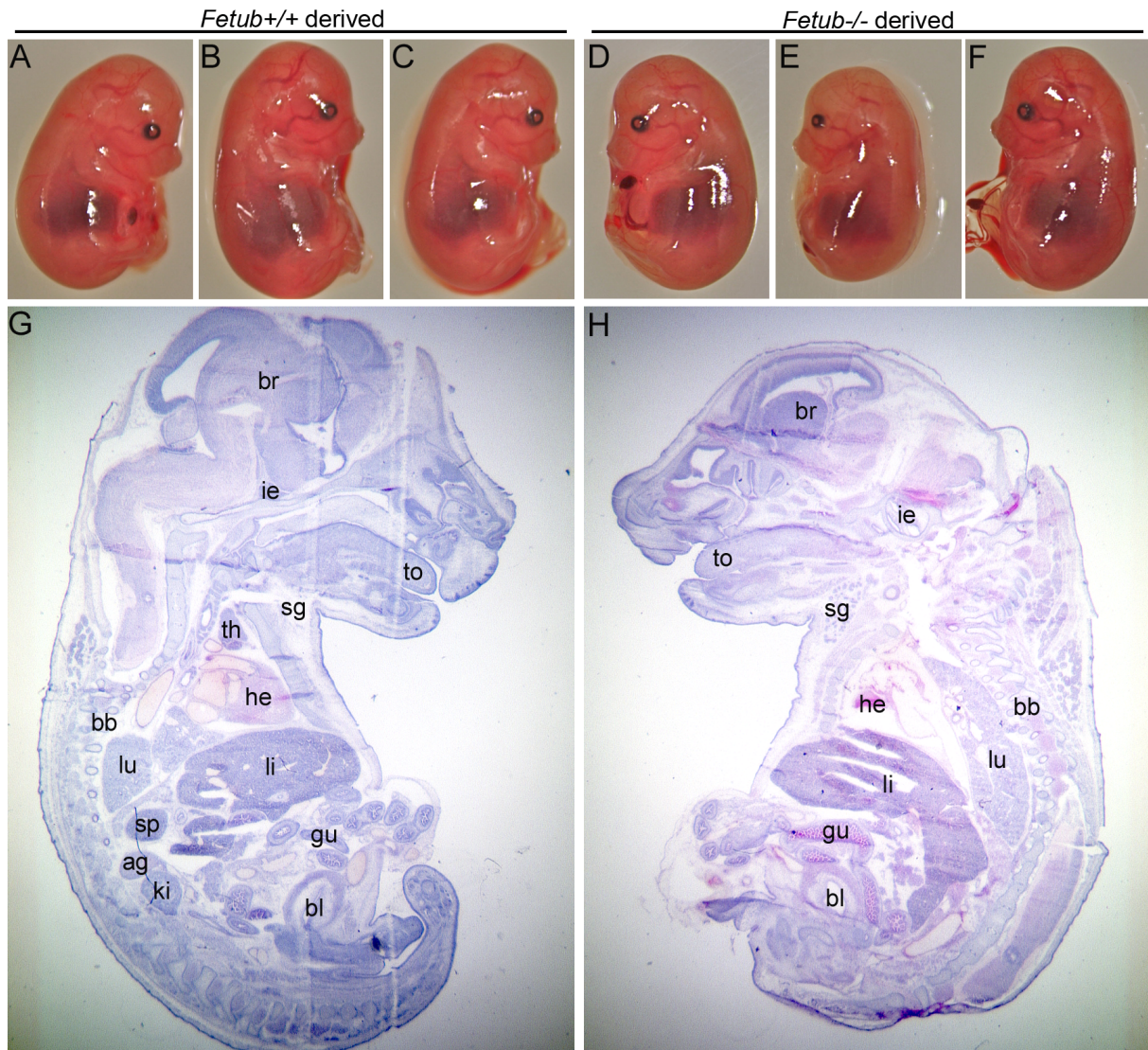


Figure 11. Fetuin-B deficient zygotes develop normal. (A - F) Photographs of fetuses dissected from wildtype foster mothers at day 16 following embryo transfer of LA-IVF fertilized oocytes. (G, H) Histological sections of fetuses after H&E staining showed all essential organs and no abnormalities. ag = adrenal gland, bb = backbone, bl = bladder, br = brain, gu = gut, he = heart, ki = kidney, li = liver, lu = lung, sg = salivary gland, sp = spleen, th = thymus, to = tongue (modified from ¹⁷).

To study the rearing potential of fetuin-B deficient females, two-cell embryos delivered by laser-assisted IVF using either fetuin-B deficient or wildtype oocytes were transferred into fetuin-B deficient females. All of three *Fetub*^{-/-} foster mothers that received *Fetub*^{-/-} embryos became pregnant and produced a total of seven offspring (2.3 pups per litter). From four *Fetub*^{-/-} foster mothers that received *Fetub*^{+/+} embryos three became pregnant and produced

a total of 14 offspring, while one mother had eaten her pups, so that the size of this litter could not be observed (7.0 pups per litter). These results show, that fetuin-B deficient embryos are able to develop into healthy young in a complete fetuin-B free environment.

To sum up we showed that half the fetuin-B serum concentration in *Fetub*^{+/-} mice is sufficient to maintain fertility. Female infertility of *Fetub*^{-/-} mice is caused by blocked fertilization. After overcoming the ZP barrier, fetuin-B deficient oocytes could be fertilized and developed into healthy offspring after transfer into *Fetub*^{-/-} foster mothers. Thus maternal fetuin-B is not essential for later stages of pregnancy, such as implantation and the maintenance of pregnancy. The infertility of fetuin-B deficient females is exclusively mediated by blocked fertilization.

3.2 Fetuin-B Deficient Oocytes Undergo Premature *Zona Pellucida* Hardening

Earlier work had demonstrated that commercial fetuin preparations can prevent ZP hardening^{148,152,154,155}. The authors could not discriminate between fetuin-A and fetuin-B at the time, because the existence of two distinct fetuin proteins was unknown until the year 2000. Considering that fetuin-A deficient mice have a severe phenotype of soft tissue calcification, yet are fully fertile^{7,8} we reasoned that the infertility of the *Fetub*^{-/-} mice was due to defective ZP maturation in the absence of fetuin-B. Indeed bovine fetuin preparations that had prevented ZP hardening *in vitro*, contained fetuin-B (figure 12). Human follicular fluid was also already shown to inhibit premature ZP hardening, and likewise scored positive for fetuin-B as well. Thus the demonstrated ZP hardening inhibition effected of bovine fetuin preparations was likely due to their fetuin-B content. Human fetuin-A, BSA and HSA showed no fetuin-B signal, consistent with the fact that these proteins are incapable of inhibiting ZP hardening¹⁵⁵. Therefore, we reasoned that the defective ZP observed in fetuin-B deficient oocytes was due to premature ZP hardening.

Furthermore, we asked how fetuin-B reached the oocytes despite the virtual absence of ovarian expression compared to liver expression². Western blotting detected fetuin-B in human follicular fluid in amounts similar to human serum suggesting transfer of fetuin-B from blood into follicular fluid (figure 12). Thus fetuin-B surrounds the oocyte during the development.

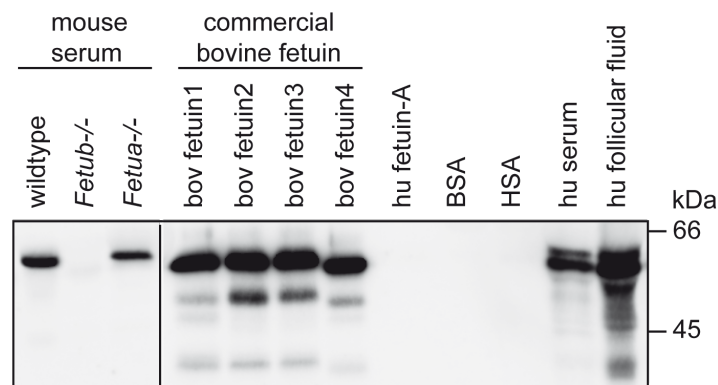


Figure 12. Commercial fetuin preparations with *zona pellucida* hardening inhibition activity contain fetuin-B. Human fetuin-B antibody, which shows cross-reactivity with murine and bovine fetuin-B, was used to probe for fetuin-B in sera of wildtype, *Fetub*^{-/-} and *Fetua*^{-/-} mice, as well as various commercial bovine fetuin preparations, Dade-Behring human plasma fetuin-A/Ahsg (hu fetuin-A), bovine serum albumin (BSA), human serum albumin (HSA), human serum and human follicular fluid. Molecular weight is indicated at the right (modified from¹⁷).

To study oocyte defects, we first analyzed general oocyte morphology. The diameter of fetuin-B deficient oocytes ($69.0 \pm 4.2 \mu\text{m}$, figure 13 left) was comparable to wildtype oocytes ($69.3 \pm 4.2 \mu\text{m}$) and also in line with published data¹⁷⁴. Descriptive data about the ZP thickness of individual unfertilized oocytes range from $4.3 - 8.1 \mu\text{m}$ ¹⁷⁵. Diameters of ZP had

large variation depending on the mouse background strain¹⁷⁶⁻¹⁷⁹. According to the literature C57BL/6 oocytes have a ZP thickness of $7.59 \pm 0.07 \mu\text{m}$, very close to what was measured here ($7.58 \pm 0.96 \mu\text{m}$, figure 13 right)¹⁷⁸. In comparison DBA/2 are meant to have a thinner ZP, which could however, not be confirmed ($7.70 \pm 0.70 \mu\text{m}$, supplemental figure S7)¹⁷⁹.

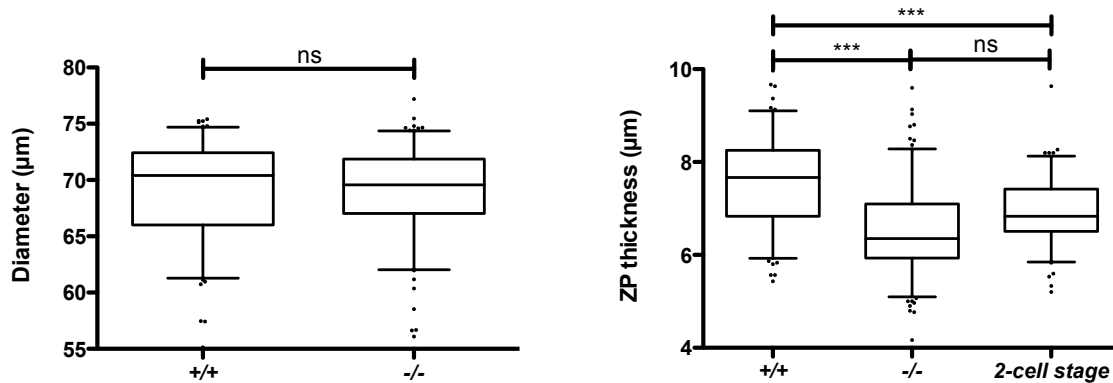


Figure 13. Zona pellucida of fetuin-B deficient oocytes is thinner. (left) Diameter of wildtype oocytes (+/+), $69.25 \pm 4.19 \mu\text{m}$, n = 137) and *Fetub*^{-/-} derived oocytes (-/-, $68.96 \pm 4.16 \mu\text{m}$, n = 196). (right) ZP thickness of wildtype oocytes ($7.58 \pm 0.96 \mu\text{m}$, n = 137), *Fetub*^{-/-} derived oocytes ($6.54 \pm 0.95 \mu\text{m}$, n = 196) and wildtype 2-cell stage embryos ($6.95 \pm 0.70 \mu\text{m}$, n = 108). Boxes represent the first to the third quartile, band inside shows the median. Every dot represents one oocyte as outliers. Whiskers indicate 5-95 percentile. Pairwise two-sided t test ns = not significant, ***p<0.001 (modified from¹⁷). Background strain was C57BL/6, data for DBA/2 mice are shown in supplemental figure S7.

After fertilization, ZP2 is cleaved resulting in structural ZP modifications. As a consequence ZP thickness decreases, which is readily visible in the present data (figure 13 right). ZP thickness of two-cell embryos ($6.95 \mu\text{m}$), which have a physiologically hardened ZP, was significantly reduced compared to unfertilized wildtype oocytes ($7.58 \mu\text{m}$), but was indistinguishable from fetuin-B deficient oocytes ($6.54 \mu\text{m}$). This indicated that fetuin-B deficient oocytes indeed show structural variations in their ZP and that this could be the reason for the observed fertilization block. In general ZP thickness correlates with fertilization success but not with ZP hardening by force^{177,180,181}. Thus we checked *Fetub*^{-/-} oocytes specific for ZP hardening.

ZP hardening is associated with increased resistance to proteolytic degradation¹¹². Thus we analyzed chymotrypsin-mediated ZP digestion in unfertilized fetuin-B deficient and wildtype oocytes, as well as two-cell embryos, which represent the physiologically hardened ZP phenotype. Figure 14 shows photographs of representative oocytes and two-cell embryos during proteolytic degradation of the ZP. Unfertilized wildtype oocytes showed clear signs of ZP degradation after less than one minute of chymotrypsin digestion (figure 14, upper row). The oocyte was free of visible ZP after a further five minutes. In *Fetub*^{-/-} derived oocytes

(figure 14, middle row) the ZP degradation started after about 16 minutes and was completed after ten additional minutes. The two-cell embryo (figure 14, bottom row), which represents the physiologically hardened ZP phenotype, showed first signs of ZP degradation after about 32 minutes and took about ten more minutes, comparable to the *Fetub*^{-/-}.

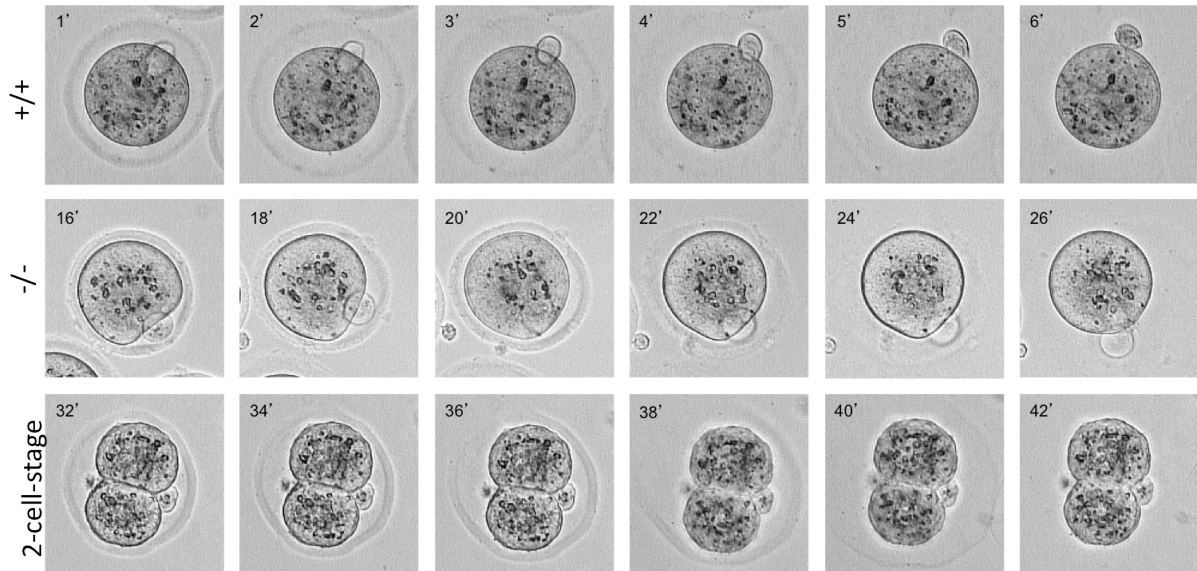


Figure 14. Zona pellucida of fetuin-B deficient oocytes is more resistant against enzymatic digestion. Microscopic pictures of a wildtype (+/+) and a fetuin-B deficient (-/-) oocyte as well as a two-cell embryo during proteolytic ZP degradation with chymotrypsin. Numbers in the left corners represent the time of chymotrypsin treatment in minutes.

We measured chymotrypsin-mediated ZP digestion time in unfertilized fetuin-B deficient and wildtype oocytes, as well as two-cell embryos (for each condition $n \geq 20$; 4 independent experiments). Figure 15 shows that t_{50} , the time required to digest the ZP in half of the oocytes in each matching series, was 5 times longer in fetuin-B deficient oocytes ($31.5 \text{ min} \pm 4.7 \text{ min}$) than in unfertilized wildtype oocytes ($6.4 \text{ min} \pm 0.9 \text{ min}$). Furthermore, the ZP digestion time of fetuin-B deficient oocytes was comparable to that of wildtype two-cell embryos ($38.5 \text{ min} \pm 6.0 \text{ min}$), indicating that the ZP structure of fetuin-B deficient oocytes resembled a hardened phenotype.

- Results -

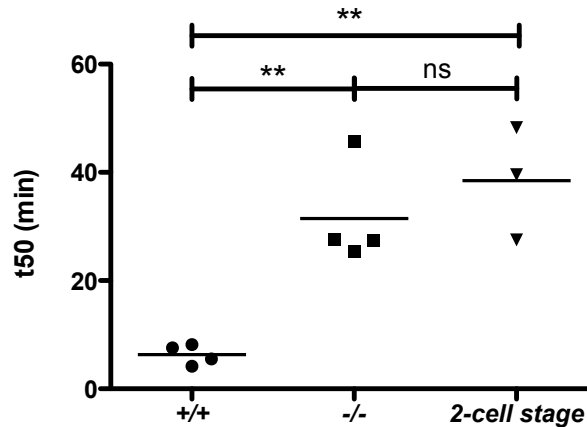


Figure 15. Zona pellucida digestion time is increase in fetuin-B deficient oocytes. ZP digestion times of wildtype oocytes (+/+), fetuin-B deficient oocytes (-/-) and wildtype 2-cell stage embryos. The ZP digestion time t50 equals the time required for 50% of the oocytes to become zona-free following α -chymotrypsin treatment. Every dot represents one assay performed with at least 20 oocytes harvested from one mouse. Pairwise two-sided t test ** $p < 0.01$, ns = not significant (modified from ¹⁷). Background strain was C57BL/6, data for DBA/2 mice are shown in supplemental figure S7.

Post-fertilization oocyte ZP hardening results in a block to further sperm binding. Figure 16 shows that oocytes obtained from superovulated *Fetub*^{-/-} mice (figure 16 B) indeed had strongly reduced sperm binding compared to wildtype oocytes (figure 16 A), even less than two-cell embryos (figure 16 C). Numbers of bound sperm are shown in the graph in figure 16 D. Unfertilized *Fetub*^{+/+} oocytes showed 52.9 ± 3.0 bounded sperm per oocyte (mean \pm SD; $n=103$), compared to 3.6 ± 0.6 bounded sperm at *Fetub*^{-/-} oocytes ($n=121$) and 10.3 ± 2.2 at two-cell embryos ($n=37$), respectively. Thus fetuin-B deficient oocytes showed a statistical significant reduction in sperm binding compared to wildtypes. This supports the view that oocytes from *Fetub*^{-/-} had undergone ZP hardening even without fertilization. Compared to two-cell embryos, which represent the physiological hardened phenotype, sperm binding to *Fetub*^{-/-} oocytes was also statistical significant decreased. Oocytes were isolated about 16 hours post-ovulation induction via hCG injection. With the assumption that spontaneous cortical granula release mainly occurs around ovulation, this would mean that ZP hardening in *Fetub*^{-/-} oocytes started 16 hours before sperm binding was tested. Two-cell embryos were obtained by IVF and used for sperm binding about 24 hours after fertilization. Thus two-cell embryos had more time to undergo ZP-hardening and one would expect that sperm binding should be lower compared to *Fetub*^{-/-} oocytes. Furthermore Burkart et al. showed that recombinant ovastacin takes *in vitro* about eight hours to completely cleave ZP2 of isolated ZPs ¹²². Thus after 16 hours for the *Fetub*^{-/-} oocytes and 24 hours for the two-cell embryos ZP2 should be completely cleaved. As a consequence time should not be the factor leading to different degrees of ZP hardening in two-cell stages and *Fetub*^{-/-} oocytes. As already

mentioned two-cell embryos were observed by IVF. Therefore COCs of wildtype females were isolated and sperm was directly added without previous removal of the cumulus cells. Thus we hypothesize that some fetuin-B was left in the environment during IVF, leading to a particular inhibition of ZP2 cleavage in the two-cell embryos and thus to a more drastic ZP hardening in *Fetub*^{-/-} oocytes.

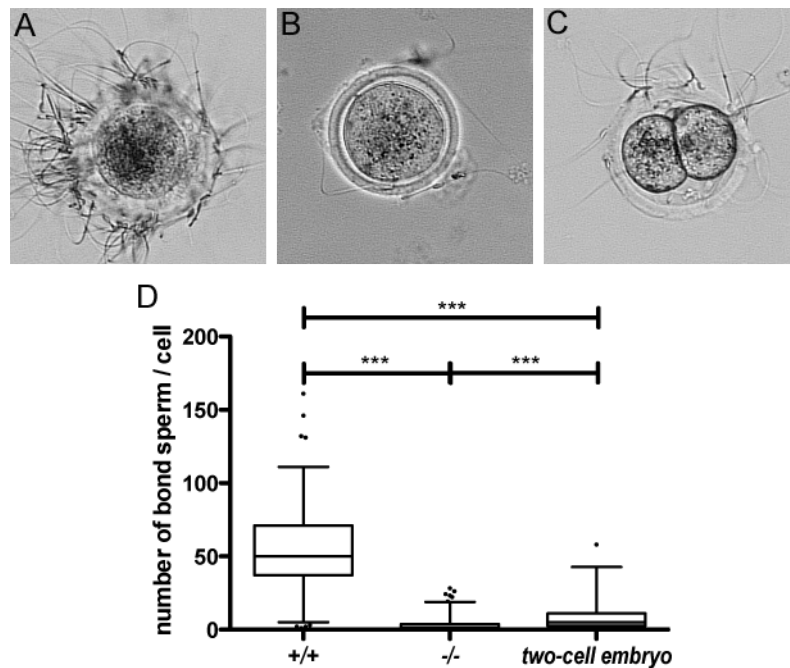


Figure 16. *In vitro* sperm binding is decreased at fetuin-B deficient oocytes compared to wildtype oocytes. (A) Microscopic picture of a representative wildtype oocyte with a high amount of attached sperm. (B) At the fetuin-B deficient oocyte the sperm binding was reduced and the amount of attached sperm was even less compared to (C) the two-cell embryo. (D) Box plot representing sperm binding quantification. Sperm binding was significantly decreased in fetuin-B deficient oocytes (-/-) compared to wildtype oocytes (+/+) and even less compared to two-cell embryos. Boxes represent the first to the third quartile, band inside shows the median. Every dot represents one oocyte as outliers. Whiskers indicate 5-95 percentile. Pairwise two-sided t test ns = not significant, *** $p < 0.001$ (modified from ¹⁷). Background strain was C57BL/6, data for DBA/2 mice are shown in supplemental figure S7.

Proteolytic cleavage of ZP2, a hallmark of ZP hardening, was analyzed using monoclonal antibody directed against ZP2 ^{111,182}. Western blots of extracts prepared from unfertilized wildtype oocytes showed a signal at 120 kDa that corresponds to uncleaved ZP2 protein (figure 17). Two-cell embryos showed an additional signal at 90 kDa that corresponds to the cleaved ZP2f protein as expected. It is known that partial ZP2 cleavage is sufficient to block sperm binding and fertilization, thus the incomplete ZP2 cleavage after fertilization was expected ¹⁴⁶. The incomplete ZP2 cleavage further confirmed results that were seen in sperm binding experiments and corroborates the hypothesis that the IVF received two-cell embryos

only showed partial ZP-hardening, eventually due to residual fetuin-B after COC isolation. As expected fetuin-B deficient oocytes showed a stronger signal at the molecular weight of ZP2f compared to two-cell embryos, as they also showed less sperm binding (figure 17). In *Fetub*^{-/-} oocytes derived from DBA/2 mice ZP2 in fact was completely cleaved, eventually indicating some strain specific differences in sensibility to premature ZP hardening (supplemental figure S7).

Spontaneous degranulation mainly occurs around ovulation. About one quarter of the cortical granules is released around this time period ⁴⁹. Thus one would expect that premature ZP hardening in *Fetub*^{-/-} mice becomes manifest at ovulation. For examination we either stimulated *Fetub*^{-/-} females with PMSG only, and isolated oocytes directly from the ovary (pre-ovulatory), or we further induced ovulations by hCG injection and isolated COCs from the oviduct (post-ovulatory). Indeed pre-ovulatory fetuin-B deficient oocytes only showed the uncleaved ZP2 protein, while in fetuin-B deficient oocytes the cleaved ZP2f protein band could be detected post-ovulatory (figure 17). This lead to the conclusion that premature ZP hardening in *Fetub*^{-/-} mice started at ovulation and was probably already progressed too far for successful fertilization before the sperm reach the oocyte.

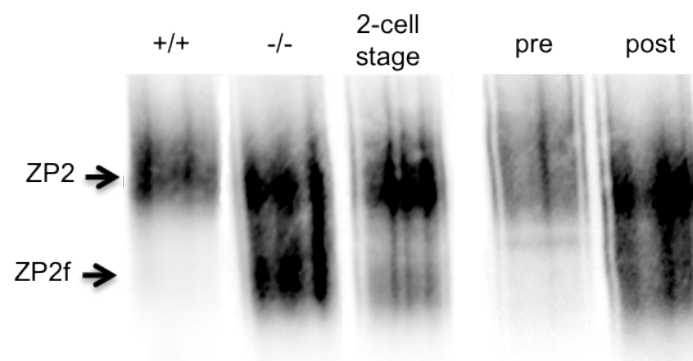


Figure 17. Fetuin-B deficient oocytes show premature ZP2 cleavage that persists after ovulation. Immune detection of ZP2 protein of wildtype (+/+) oocytes, fetuin-B deficient (-/-) oocytes and wildtype 2-cell embryos. Fetuin-B deficient oocytes were further isolated pre- and post-ovulatory (modified from ¹⁷). Background strain was C57BL/6, data for DBA/2 mice are shown in supplemental figure S7.

In summary, it can be stated that the ZP of fetuin-B deficient oocytes had hardened prematurely during ovulation and, accordingly, that infertility in *Fetub*^{-/-} females was due to premature ZP hardening, evaluated by measurements of ZP thickness, chymotrypsin digestion, sperm binding and ZP2 Western blot. In *Fetub*^{-/-} mice ZP hardening occurred at ovulation. Compared to two-cell wildtype embryos, *Fetub*^{-/-} oocytes even showed a higher degree of ZP hardening, indicating that ZP hardening in two-cell embryos might still be partially inhibited by COC-stored endogenous fetuin-B.

3.3 Fetuin-B Inhibits Ovastacin and Thus *Zona Pellucida* Hardening

This part of the thesis work was performed in collaboration with Ralf Weiskirchen and Julia Floehr, RWTH Aachen and Walter Stöcker, Johannes-Gutenberg-University Mainz and their co-workers who prepared recombinant fetuins and studied ovastacin inhibition, respectively.

We already showed that oocytes of *Fetub*^{-/-} undergo premature ZP hardening. Several factors are discussed to be involved in fertilization-triggered ZP hardening, while only the cortical granula protease ovastacin was shown to be critically involved in definitive ZP hardening by cleaving ZP2¹²². To draw a conclusion on the mechanism between fetuin-B and ZP hardening it was of great interest if recombinant mouse fetuin-B inhibits mouse ovastacin activity. To this end, we cloned mouse fetuin-A and fetuin-B into adenoviral expression vectors and purified His-tagged fusion proteins from virus infected cell supernatants. In addition, we expressed recombinant ovastacin in insect cells. Figure 18 shows that activated ovastacin was inhibited to background activity by recombinant fetuin-B (IC₅₀ 76.4 nM ± 3.35 nM), but not by recombinant fetuin-A. In the assay 990 nM pro-ovastacin was used, containing about 10% of activated ovastacin. Thus 76.4 nM recombinant fetuin-B were sufficient to decrease the activity of 99.0 nM activated ovastacin to the half, reflecting a molecular fetuin-B : ovastacin ratio of about 1:1.3. The concentrations of fetuin-B and ovastacin at the ZP are not known and can only be roughly estimated. It is known that about 100 pg protein are released into the perivitelline space after fertilization^{69,110}. Having regard to the data that one quarter of the cortical granula is already released at ovulation this would mean that about 33.3 pg of cortical granula protein is exocytosed spontaneously ($100 \text{ pg} / \frac{3}{4} * \frac{1}{4} = 33.3 \text{ pg}$). Unfortunately the amount of released ovastacin is not known. With the assumption that 33.3 pg ovastacin (50 kDa) is released into the perivitelline space with a volume of 82 pl (calculated from measurements of perivitelline space diameter of 137 mature wildtype oocytes with $9.3 \pm 0.40 \mu\text{m}$, for detailed calculation see supplemental figure S8), this would lead to a ovastacin concentration of 0.4 g/l ovastacin in the perivitelline space. Considering the molecular weight of ovastacin this would result in a concentration of 8.1 μM ovastacin in the perivitelline space. Fetuin-B has a molecular weight of 60 kDa and is thought to diffuse unhindered through the cumulus cell matrix as well as the ZP. With the knowledge that fetuin-B serum concentration in wildtype mice is about 0.275 g/l and with the assumption that it is the same in the perivitelline space this would lead to a concentration of 4.6 μM fetuin-B. Thus the molecular fetuin-B : ovastacin ratio at spontaneous cortical granula release would be about 1:1.8, similar as shown in the *in vitro* ovastacin inhibition assay. Thus we suggest that premature ZP hardening triggered by spontaneous cortical granula release of ovastacin should be entirely prevented by the micromolar concentrations of fetuin-B present in plasma and follicular fluid.

- Results -

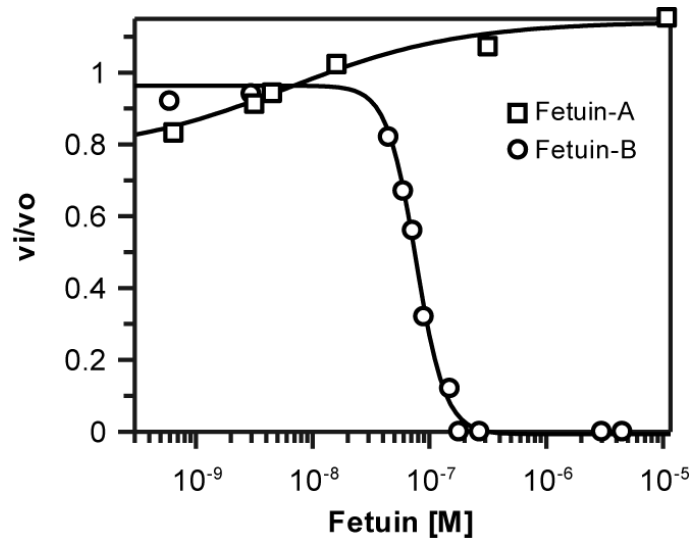


Figure 18. Recombinant ovastacin is inhibited by recombinant mouse fetuin-B (circles; concentration range: 0.6 nM - 4.5 μ M) with an IC_{50} of 76.4 nM \pm 3.4 nM. In contrast, recombinant murine fetuin-A did not inhibit ovastacin (squares; concentration range: 0.6 nM – 11.0 μ M) (modified from ¹⁷).

In conclusion, fetuin-B but not fetuin-A inhibited the ZP2 protease ovastacin. Taken together with the fact that bovine fetuin comprises fetuin-A and fetuin-B (paragraph 3.2, figure 12) we hypothesize that earlier shown inhibition of ZP hardening by bovine fetuin was mediated by fetuin-B and not by fetuin-A as predicted at that time.

3.4 Fetuin-B Increases Fertilization Success *in Vitro*

Commercial bovine fetuin preparations contain both fetuin-A and -B, and therefore can inhibit premature ZP hardening *in vitro* leading to an increased fertilization success^{148,154,155}. We showed that recombinant murine fetuin-B, but not recombinant murine fetuin-A inhibits the ZP2 protease ovastacin. Thus I asked if recombinant murine fetuin-B could inhibit premature ZP hardening during IVF treatment and thus increase fertilization success like it was shown earlier for mixed bovine fetuin preparations.

Fetuin-B was cloned into adenoviral expression vectors by Eddy van de Leur and Ralf Weiskirchen, RWTH Aachen. His-tagged fusion protein was purified from virus infected COS cell supernatants by Julia Floehr, RWTH Aachen. Recombinant murine fetuin-B (rmFetuB) was stored in PBS at concentrations of about 3.0 mg/ml. Schröder et al. showed best fertilization success with the use of 1.0 mg/ml bovine fetuin at IVF¹⁵⁵. Due to the lack of knowledge about the ratio of fetuin-A and fetuin-B in the bovine fetuin we decided to start with a concentration of 1.0 mg/ml rmFetuB in the IVF experiments. This would have led to a dilution of about 1:3 of the purified rmFetuB and thus to a high concentration of PBS in the IVF experiments. PBS is suspected to induce cortical granula release and thus spontaneous ZP hardening. To avoid PBS-induced ZP damages, we exchanged the buffer using centrifugal desalting devices. First results showed that the direct transfer from PBS to human tubal fluid (HTF) medium using the desalting devices caused precipitation of unidentified components. One likely explanation for precipitation was the formation of insoluble phosphate salts from PBS and HTF. Thus I performed a two-step buffer change, first exchanging the recombinant fetuin-B from PBS to ultrapure water and then to HTF medium. Each intermediary preparation was assayed for protein loss. A typical fetuin-B Western blot is shown in figure 19. Sequential dilutions of commercial rmFetuB were used for quantitation as before (figure 9, measurement of fetuin-B serum concentration). Both recombinant murine fetuin-B preparations (commercial and in-house expression) showed the same molecular weight of approximate 65 kDa. In house-produced rmFetuB had fragments at about 41 kDa, 43 kDa, 49 kDa and 50 kDa.

To transfer rmFetuB to HTF medium the column was first equilibrated four times with ultrapure water. After loading the purified protein (load) to the column and centrifugation the fetuin-B was transferred into ultrapure water (eluate 1). Afterwards the column was washed four times and thus equilibrated with HTF medium without BSA. RmFetuB in water (eluate 1) was loaded onto the same column and centrifuged to recover rmFetuB in HTF medium (eluate 2). As expected, the load as well as the eluates scored positive for fetuin-B (figure 19). Although the wash fractions (W1, W2) showed no fetuin-B signal, the signal in the eluates decreased in subsequent fractions, most likely due to dilution. Quantitation using ImageJ software showed a concentration reduction from 3.27 mg/ml (load) to 2.60 mg/ml

(eluate 1, E1) and further to 2.08 mg/ml (eluate 2, E2), which means that over all about 36 % of the protein was lost due during buffer exchange. Pipetting a small bulb at the column after sample loading might have increased recovery, but we decided against this procedure to avoid contamination of the IVF medium by overloading the column.

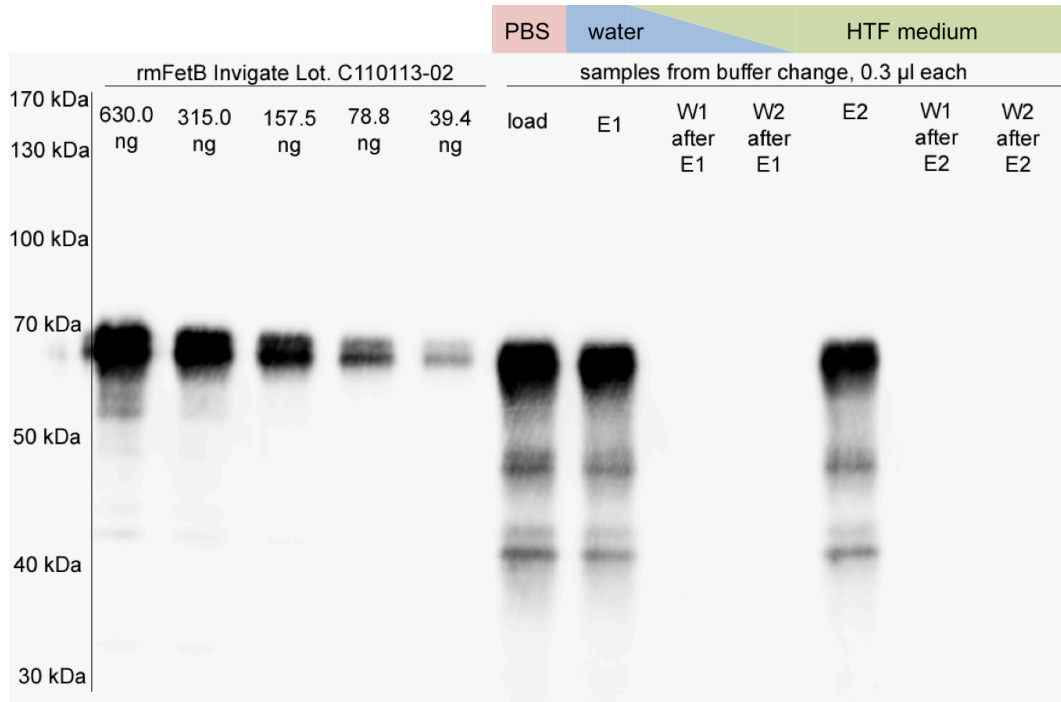


Figure 19. Evaluation of recombinant murine fetuin-B buffer transfer from PBS to HTF medium. Murine fetuin-B Western blot of rmFetueB buffer transfer procedure showed fetuin-B signal in load, first eluate (E1) and second eluate (E2), but not in the wash fractions (W1, W2).

Finally the eluate contained 2.08 mg/ml rmFetueB in HTF medium without BSA or antibiotics. To add BSA, rmFetueB in HTF medium without BSA and antibiotics was mixed with the same volume of HTF medium containing 2 X BSA and antibiotics (8 mg/ml BSA, 150 µg/ml penicillin, 100 µg/ml streptomycin). HTF medium with 1.04 mg/ml rmFetueB was either used directly or diluted to obtain HTF medium containing 0.5 mg/ml, 0.25 mg/ml, 0.125 mg/ml, 0.063 mg/ml, 0.031 mg/ml or 0.015 mg/ml fetuin-B.

The rmFetueB fortified HTF medium was used to study the impact of fetuin-B on fertilization success during IVF.

In the first experiment COCs of three wildtype females each were flushed directly into HTF medium without fetuin-B or into HTF medium supplemented with 1.0 mg/ml rmFetueB. Capacitated sperm was added immediately after COC isolation. The total procedure from sacrifice of the females to adding the sperm to COC took less than five minutes. The time line of a typical experiment is illustrated in figure 20. After four hours of fertilization the

oocytes were washed three times and placed into a fresh drop of either HTF medium without fetuin-B or HTF medium supplemented with 1.0 mg/ml rmFetuB. Another 20 hours later the number of two-cell embryos was counted to determine the fertilization success. Thereafter, half the embryos were transferred to M2 medium to support further development and the other half was analyzed for ZP hardening.

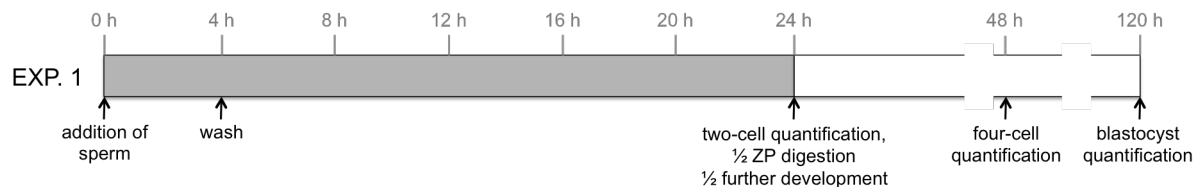


Figure 20. Time line of testing the impact of fetuin-B on fertilization and embryo development. COCs were isolated and sperm were immediately added. After four hours potential zygotes were wash. After 24 hours number of two-cell embryos was quantified. One half of the cells was used for ZP digestion with chymotrypsin while the other half was transferred to M2 medium to analyze further development. After 48 and 120 hours the amount of four-cell embryos and blastocysts was quantified, respectively. Gray section determines the presence of rmFetuB during incubation.

Independent of whether fetuin-B was contained in the medium or not, the embryos developed to the two-cell stage 24 hours post-fertilization (figure 21 A-D). Embryos that were fertilized in rmFetuB-containing HTF medium had larger numbers of sperm attached. This indicates that 1 mg/ml rmFetuB was sufficient to inhibit not only premature, but also fertilization-triggered ZP hardening. One would have expected that the inhibition of premature ZP hardening by fetuin-B should increase the proportion of two-cell embryos. Instead the fertilization success as well as the amount of fragmented, degraded embryos was comparable in both groups as shown in figure 21 E. With rmFetuB in the IVF medium, 71.2% developed into two-cell embryos, which was slightly less than without the supplementation of rmFetuB (77.1%). Fertilization success was nevertheless higher than in our previous work (50% fertilization success, see paragraph 3.1, figure 10), and also higher than in published data (66.2% fertilization success, see paragraph 1.4, table 2). ZP hardening is thought to prevent polyspermy. Pictures of two-cell embryos fertilized in a fetuin-B enriched environment indicated inhibition of ZP hardening. Thus one would have expected that the inhibition of fertilization-triggered ZP by fetuin-B should increase polyspermy and thus the percentage of degenerative embryos. Instead the amount of degenerative oocytes was comparable in both setups (figure 21 E). About 8.6% of oocytes degenerated in the absence of rmFetuB, and 5.1% degenerated with rmFetuB supplementation, respectively. To test two-cell embryos for ZP hardening the ZP was digested using chymotrypsin. Two-cell embryos that were fertilized in fetuin-B free medium showed a t50 of 32.1 min and were

comparable to earlier results (38.5 min for two-cell embryos and 31.5 min for *Fetub*^{-/-} oocytes, see paragraph 3.2, figure 14), indicating fertilization-triggered ZP hardening. Two-cell embryos that were fertilized in fetuin-B supplemented medium showed a t50 of 16.0 min, which was 2.5 times longer than t50 of unfertilized *Fetub*^{+/+} oocytes (6.4 min see paragraph 3.2, figure 14), but only half as long as two-cell embryos that were fertilized in fetuin-B free HTF medium. Thus it appeared as if rmFetuB did not completely inhibit fertilization-triggered ZP hardening.

Two-cell embryos, regardless of whether they were fertilized with or without fetuin-B, further developed into four-cell embryos 48 hours after fertilization (figure 21 F-I) , and further into blastocysts 120 hours after fertilization (figure 21 K, L). At the four-cell stage, both groups showed a decrease in percentage of healthy embryos compared to two-cell stages (figure 21 E, J). With the use of rmFetuB in the IVF medium, 67.6% developed to four-cell embryos and without the supplementation of rmFetuB 75.6%, respectively. The numbers further dropped until the blastocyst stage and were nearly identical for both groups (figure 21 O, 52.9% with rmFetuB, 52.5% without rmFetuB). Blastocysts in both groups started to hatch or already finished hatching leaving the empty ZP (figure 21 M, N).

Oocytes isolated from *Fetub*^{-/-} females could not be fertilized *in vitro* with supplementation of rmFetuB, showing that premature ZP hardening is irreversible.

The lack of a positive effect of fetuin-B on IVF fertilization success may be explained as follows. Firstly, the time between COC isolation and sperm adding was less than five minutes and thus likely to short to study ZP hardening. Second the extracellular matrix of the cumulus cells could store endogenous fetuin-B like already hypothesized in paragraph 3.2. To avoid confounding effects of endogenous fetuin-B during further experiments, I removed cumulus cells from oocytes by hyaluronidase digestion before using the oocytes for IVF assays.

- Results -

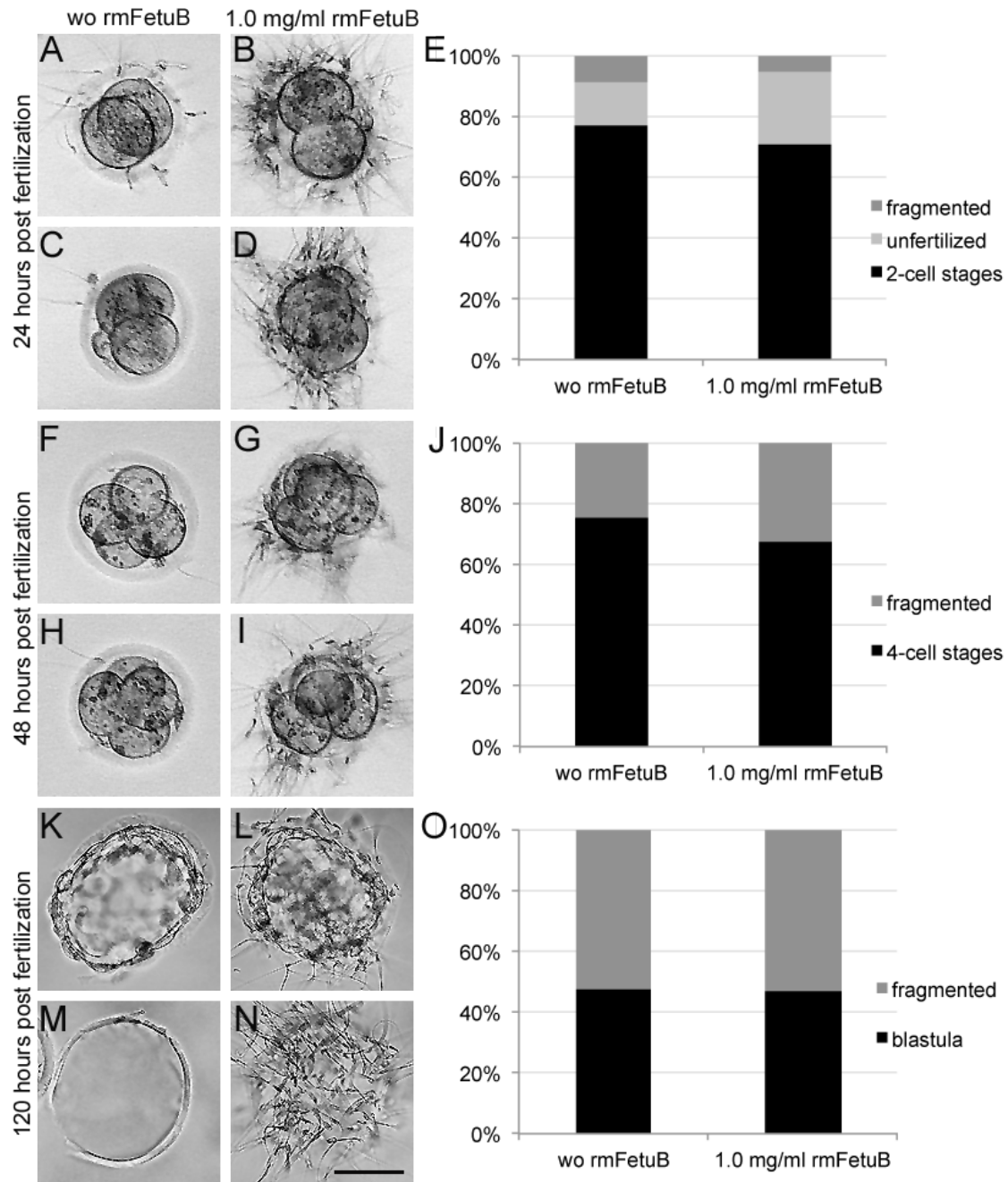


Figure 21. Recombinant murine fetuin-B did not influence embryo development. COC were either isolated in HTF medium without (wo) rmFetuB or supplemented with 1.0 mg/ml rmFetuB. (A-E) 24, (F-J) 48 and (K-O) 120 hours microscopic photos were taken and percentage of health embryos was quantified. Bar in picture N indicates 50 µm, all microscopic photographs were taken using the same magnification.

Next I analyzed the time point at which premature ZP hardening manifests during *in vitro* cultivation (IVC). Dodson et al. showed that ZP resistance to proteolytic digestion started to increase 40 hours after ovulation *in vivo*, while fertilization already decreases 15 minutes after IVC^{146,147}. Thus we studied ZP hardening for up to 36 hours of IVC. Time frame of the entire experiment is illustrated in figure 22. After isolation, COCs were digested with hyaluronidase and oocytes were washed three times in HTF medium, to get rid of the

cumulus cells and associated endogenous fetuin-B. Oocytes were pooled in one drop of HTF medium without any fetuin-B supplementation. At different time points a sample of 20-30 oocytes was used for ZP digestion to analyze ZP hardening.

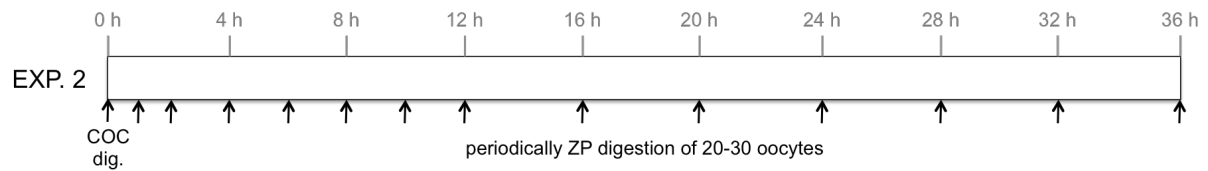


Figure 22. Timing diagram of analyzing ZP hardening after cumulus cell removal and IVC. COCs were isolated and cumulus cells were removed. After 0, 1, 2, 4, 6, 8, 10, 12, 16, 20, 24, 28, 32 and 36 hours of IVC (indicated by arrows) ZP hardening was examined by ZP digestion of 20-30 oocytes by chymotrypsin. The entire experiment was done without the use of rmFetuB.

Figure 23 shows that t_{50} , the time required to digest the ZP in half of the oocytes in each matching series, increased from 8.3 min \pm 0.9 min in oocytes that were immediately tested after isolation (0 hours of IVC) to 16.3 min \pm 2.0 min after one hour of IVC and further to 19.8 min \pm 0.1 min after two hours of IVC. Fetuin-B deficient oocytes were used as control, and had a t_{50} of 30.5 min (\pm 1.4 min). Results were comparable with earlier experiments (figure 15) with t_{50} of 31.5 min \pm 4.7 min in fetuin-B deficient oocytes and 6.4 min \pm 0.9 min in unfertilized wildtype oocytes, respectively. After two hours of IVC, the t_{50} remained constant, indicating that ZP hardening had completed. Hardened ZP of IVC oocytes nevertheless never reached the t_{50} values of fetuin-B deficient oocytes. This can be explained by the fact that the wildtype oocytes, used in this assay still were surrounded by endogenous fetuin-B at ovulation and until isolation. Thus a certain proportion of the released ovastacin likely was inhibited before isolation and cumulus cell removal, which is of course not the case in fetuin-B deficient mice. Nevertheless I observed increased ZP resistance against enzymatic digestion within one hour of fetuin-B free IVC and thus decided to pre-incubate the oocytes in HTF medium for one hour before sperm addition for the further experiments to trigger partial ZP hardening.

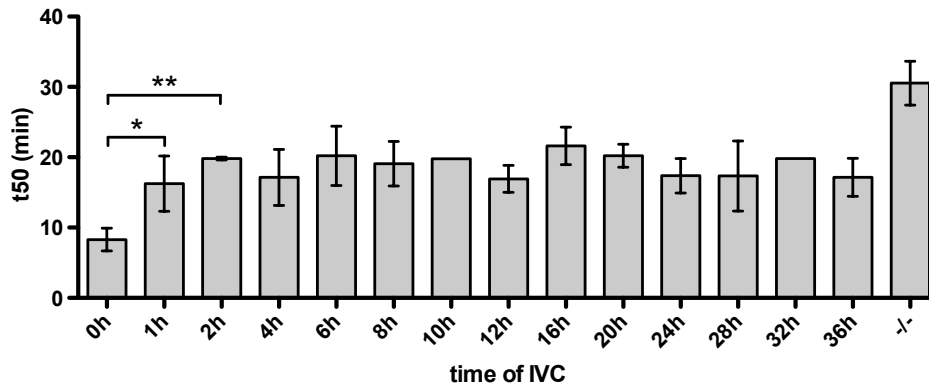


Figure 23. ZP hardening occurred after one hour of *in vitro* cultivation (IVC). ZP digestion times of wildtype oocytes undergoing different durations of IVC and fetuin-B deficient oocytes (-/-). The ZP digestion time t50 equals the time required for 50% of the oocytes to become zona-free following alpha-chymotrypsin treatment. Every column represents at least two assays performed with 20-30 oocytes each. Pairwise two-sided t test * p<0.05; ** p<0.01

I demonstrated that the use of fetuin-B at oocyte isolation without cumulus cell removal and immediate fertilization inhibited premature ZP hardening, but did not increase fertilization success. Furthermore the inhibition of fertilization-triggered ZP hardening did not lead to polyspermy. I also showed that premature ZP hardening manifests within one hour after oocyte isolation and removal of the cumulus cells.

Next, I analyzed if fetuin-B supplementation can inhibit premature ZP hardening during IVC. The time line of the entire experiment is illustrated in figure 24. After COC isolation and cumulus cell removal the oocytes were cultured *in vitro* for one hour to trigger partial ZP hardening in either HTF without rmFetuB or in HTF with rmFetuB. Four hours after the addition of sperm, zygotes were washed three times in HTF medium. To avoid the inhibition of fertilization-triggered ZP hardening, but also to minimize the amount of rmFetuB required, all oocytes were washed in HTF without rmFetuB. 24 hours after the addition of sperm the number of two-cell embryos was counted as well as the number of sperm bound per two-cell embryo. Post-fertilization ZP hardening was evaluated by ZP digestion of two cell embryos using chymotrypsin.

- Results -

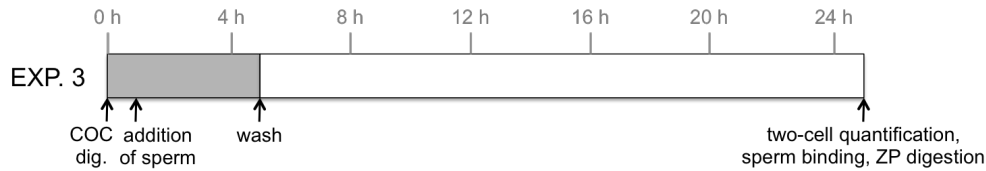


Figure 24. Timing diagram of testing the impact of fetuin-B after removal of the cumulus cells and one hour of IVC. COCs were isolated and cumulus cells were removed. After one hour of IVC sperm were added. After additional four hours potential zygotes were washed in fetuin-B free HTF medium. 24 hours post-fertilization the amount of two-cell embryos was quantified. To test ZP hardening bounded sperm per two-cell embryo were counted and ZP was digested by chymotrypsin. Gray section determines the presence of rmFetuB during incubation.

In the previous experiment I used HTF medium with 1.0 mg/ml rmFetuB, and I inhibited premature ZP hardening, but also fertilization-triggered ZP hardening. *Fetub*^{+/+} female mice showed serum concentrations of 161.4 ± 10.5 µg/ml fetuin-B (see paragraph 3.1 and figure 9). Half the serum fetuin-B level was sufficient to maintain fertility of *Fetub*^{+/-} females *in vivo*. To test the inhibition potential of fetuin-B *in vitro*, I used rmFetuB concentrations ranging from 0.015 mg/ml to 1 mg/ml. Oocytes were either isolated in fetuin-B free HTF medium or in HTF medium containing rmFetuB, and cumulus cells were removed. After one hour of IVC (to trigger premature ZP hardening) oocytes were fertilized by adding sperm into the medium. 24 hours post-fertilization the number of two-cell embryos was counted. The number of sperm attached per two-cell embryo and proteolytic resistance of ZP was determined to analyze for the persistence of fertilization-triggered ZP hardening.

The top panel of figure 25 shows the benefit of different concentrations of fetuin-B to IVF success. The middle and bottom panel of figure 25 illustrate fertilization-triggered ZP hardening mediated by attached sperm per two-cell embryo (middle), and t50 at ZP digestion (bottom). Light gray bars indicate mean serum fetuin-B level in *Fetub*^{+/-} mice and dark gray bar indicate mean serum fetuin-B level in *Fetub*^{+/+} mice. Even the lowest concentration of 0.015 mg/ml rmFetuB increased the amount of two-cell embryos. Oocytes that were isolated in fetuin-B free medium showed a fertilization success of 36.1%, while oocytes isolated in medium supplemented with 0.015 mg/ml to 0.1 mg/ml rmFetuB showed increased fertilization success of 61.4% and 74.5%. Thus without rmFetuB oocytes had probably undergone premature ZP hardening, while the use of fetuin-B during IVC and IVF inhibited premature ZP hardening and thus increased fertilization success.

In fetuin-B free HTF medium two-cell embryos showed a relatively low number of attached sperm (56.3 ± 30.5 sperm per two cell embryo) and a relatively high resistance to ZP digestion (t50 of 19.6 ± 3.4 min), indicating fertilization-triggered ZP hardening. The use of 0.015 mg/ml rmFetuB increased the number of attached sperm (121.3 ± 30.9 sperm per two-

cell embryo) and slightly decreased the t50 of ZP digestion to 18.0 ± 3.4 min. Supplementation of HTF medium with 0.03 mg/ml rmFetuB further increased the number of attached sperm (145.0 ± 39.9 sperm per two-cell embryo) and further decreased the t50 of ZP digestion to 15.8 ± 2.9 min. Further increase of fetuin-B concentration showed results comparable to 0.03 mg/ml rmFetuB. Thus 0.015 mg/ml rmFetuB only partially inhibited fertilization-triggered ZP hardening, while concentrations higher than 0.03 mg/ml inhibited fertilization-triggered ZP hardening completely. As already shown previously, the absence ZP hardening did not lead to polyspermy. The fact that fetuin-B supplementation protected against ZP hardening, even if fetuin-B was present only until four hours after fertilization indicates, that most ovastacin must have been released, but was immediately and efficiently inhibited in this relatively short time frame.

In summary these results indicate that in fetuin-B free medium oocytes underwent premature ZP hardening during IVC without surrounding cumulus cells, resulting in a decreased fertilization success. The two-cell embryos further underwent fertilization-triggered ZP hardening, leading to decreased sperm binding and increased resistance against proteolytic ZP digestion. Supplementing HTF with 0.015 mg/ml or more rmFetuB inhibited the premature ZP hardening, leading to an increased fertilization success. Concentrations of 0.03 mg/ml rmFetuB and higher completely inhibited fertilization-triggered ZP hardening, without increasing polyspermy.

- Results -

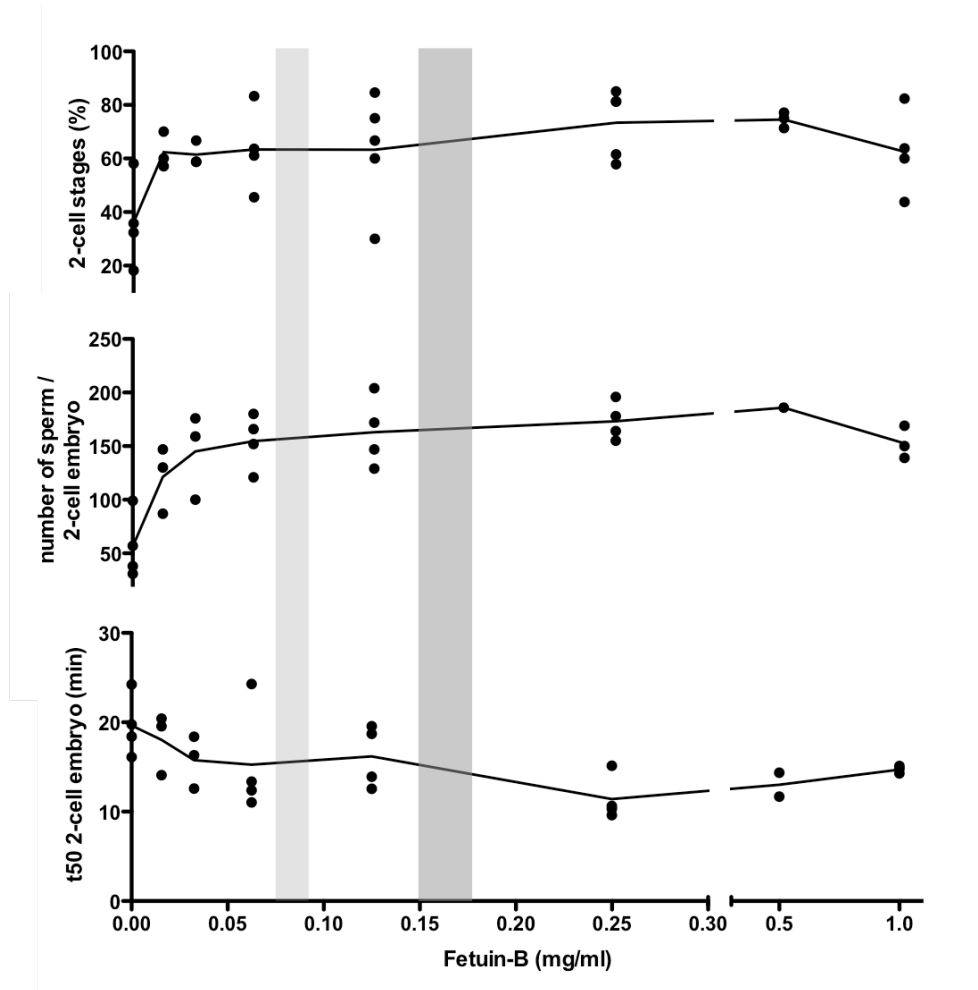


Figure 25. During *in vitro* cultivation recombinant murine fetuin-B inhibited ZP hardening and increased IVF success. Every dot represents one experimental setup performed with at least 30 oocytes. Light gray background indicates mean serum fetuin-B level in *Fetub*^{+/-} mice and dark gray background indicates mean serum fetuin-B level in *Fetub*^{+/+} mice.

I already stated that premature ZP hardening manifests within one hour after oocyte isolation and removal of the cumulus cells. Furthermore, rmFetuB inhibited premature ZP hardening and increased fertilization success.

In the following experiment I tested for how long rmFetuB is efficient to increase fertilization success. Because the inhibition of fertilization-triggered ZP hardening seemed not to have any negative effect, I used 0.05 mg/ml. Time lines describing the experimental setup are shown in figure 26. COCs were isolated in either fetuin-B free HTF medium, or HTF medium containing 0.05 mg/ml rmFetuB. Cumulus cells were removed and oocytes were washed three times and pooled. Furthermore I kept the cumulus cells in one condition using fetuin-B free medium to see, if they can substitute rmFetuB. Directly or after 1, 5, 9, or 13 hours a sample of 20-30 oocytes were taken and sperm were added. Four hours later, zygotes were washed in fetuin-B free HTF medium. 24 hours post-fertilization the number of two-cell

embryos was counted. Gray sections in figure 26 determine the presence of 0.05 mg/ml rmFetuB during IVC.

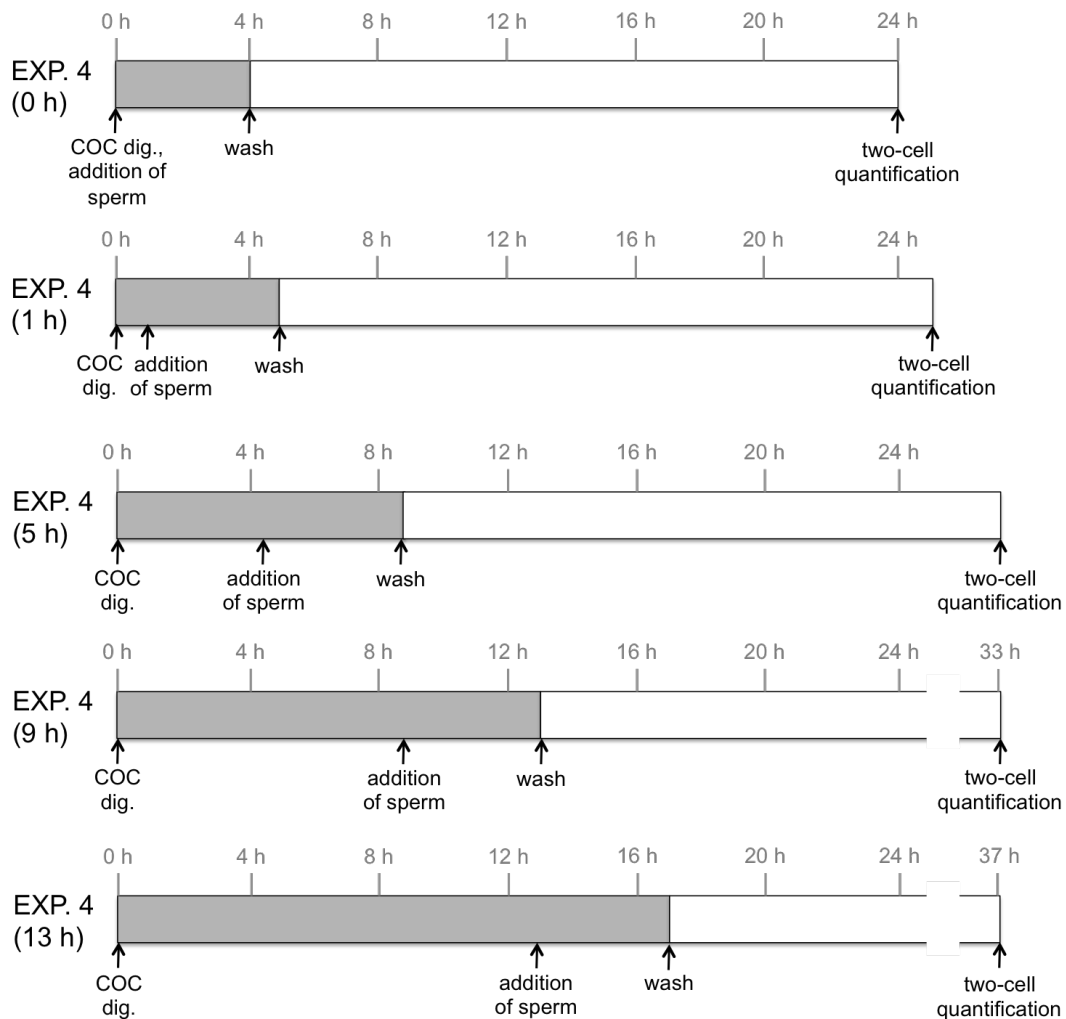


Figure 26. Exemplary illustration of four out of nine timing diagrams used for analyzing the possible timeframe for IVC with fetuin-B supplementation. COCs were isolated and cumulus cells were removed. Sperm were either added directly or after 1, 5, 9 or 13 hours. After additional four hours potential zygotes were washed in fetuin-B free HTF medium. 24 hours post-fertilization the amount of two-cell embryos was quantified. Gray section determines the presence of 0.05 mg/ml rmFetuB during incubation.

Figure 27 shows fertilization success after up to 13 hours of IVC following three different experimental protocols: 1) IVC after removal of the cumulus cells in HTF medium without fetuin-B 2) IVC after removal of the cumulus cells in HTF medium supplemented with 0.05 mg/ml rmFetuB, and 3) IVC in fetuin-B free HTF medium with cumulus cells present (to check for any effect of endogenous fetuin-B stored in the cumulus cell matrix). Figure 27 shows that 65.1% of oocytes were fertilized in the presence of rmFetuB. When isolated in

- Results -

fetuin-B free HTF medium, 74.9% of oocytes developed into two-cell stages, regardless of the presence of cumulus cells.

In experimental condition 1 (without cumulus cells and without fetuin-B supplementation) fertilization success dropped to 20.3% within one hour of IVC, and was further reduced if oocytes were cultured for an extended time interval before IVF.

In experimental condition 2 (without cumulus cells but with supplementation of 0.05 mg/ml to HTF medium), 44.1% of the oocytes were fertilized after one hour of IVC. Thus the fetuin-B supplementation doubled the fertilization success after one hour of IVC. IVF success and the development of two-cell stages was reduced to 25.0% at five hours of IVC, and dropped to 9,6 % after 13 hours of IVC. Compared to experimental condition 1 one can see, that the use of rmFetuB increased the fertilization success at all tested durations of IVC.

In experimental condition 3 (keeping the cumulus cells, but without fetuin-B supplementation) the fertilization success was 33.3%, after one hour of IVC and thus intermediary between the two alternative conditions. IVF success remained constant for up to five hours. After nine hours of IVC, only 13.0% of oocytes developed to two-cell embryos, and IVF success further decreased over time. Compared to experimental condition 1, retention of the cumulus cells and thus of endogenous fetuin-B increased fertilization success for up to five hours of IVC. Compared to experimental condition 2, supplementation of IVC medium with rmFetuB better suited to keep the oocytes fertilizable than was the retention of cumulus cells.

In conclusion, retention of cumulus cells during IVC increased IVF success for up to five hours. The supplementation of HTF medium with 0.05 mg/ml rmFetuB further increased IVF success for up to nine hours. Thus the inhibition of premature ZP hardening by cumulus cells could indeed be mediated by endogenous fetuin-B stored in the extracellular matrix of these cells.

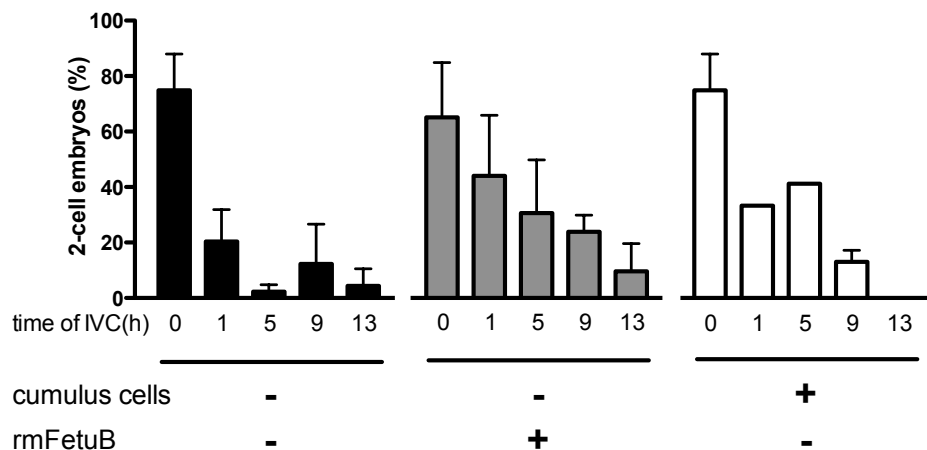


Figure 27. The use of recombinant murine fetuin-B during *in vitro* cultivation increased fertility for up to nine hours. IVF was either done in HTF medium without rmFetuB, in HTF medium containing 0.05 mg/ml rmFetuB or in HTF medium without rmFetuB but with retention of the cumulus cells. RmFetuB increased fertilization success for up to nine hours, while the retention of the cumulus cells increased the number of two-cell embryos for up to five hours.

In summary, rmFetuB did not increase fertilization success when sperm was added immediately after COC isolation. In contrast, rmFetuB strongly inhibited ZP hardening and increased IVF success when cumulus cells were removed, especially when oocytes were cultured before IVF for one hour or longer. Fetuin-B at 0.015 mg/ml inhibited premature ZP hardening, while 0.03 mg/ml fetuin-B also inhibited fertilization-triggered ZP hardening surprisingly not leading to polyspermy. Supplementation of HTF medium with rmFetuB increased fertilization success for up to 9 hours of IVC, while retention of the cumulus cells similarly kept oocytes fertilizable for 5 hours.

4. Discussion

4.1 Fetuin-B Deficient Female Mice are Infertile Due to an Early Block to Fertilization

Quantification of serum samples showed serum concentrations of $161.4 \pm 10.5 \mu\text{g/ml}$ fetuin-B in *Fetub*^{+/+} mice and $89.8 \pm 2.8 \mu\text{g/ml}$ in *Fetub*^{+/-} mice, respectively. Previous quantitative Western blots reported about $300 \mu\text{g/ml}$ serum fetuin-B in female wildtype mice ². This discrepancy is due to the use of different calibration proteins in various studies. Recombinant MBP-fetuin-B fusion protein had been used for calibration, but it was not detailed how the protein concentration of this reference was quantified. A similar study with ten *Fetub*^{+/+} adult female mice showed fetuin-B serum concentrations of $334 \pm 93 \mu\text{g/ml}$ ¹⁸. In this case, recombinant murine His-tagged fetuin-B was used to calibrate the quantitative Western blots. The concentration of purified His-tagged fetuin-B was determined by measurement of the absorbance at 280 nm (A_{280}) with bovine fetuin as the calibration standard. In contrast, wildtype females used in the present work only showed half the fetuin-B serum level judged against a commercial preparation of recombinant murine fetuin-B (rmFetuB, Invigate) employed as the calibration standard in quantitative Western blot. Invigate determined the protein concentration of their product by measuring the A_{280} figuring in a predicted extinction coefficient ϵ_{280} of 0.572 and a correction factor of 1.4 to for glycosylations. It should be noted that the amount estimated by Invigate is reduced by a factor of 2.1 if the protein is quantified using the commercial Pierce BCA protein quantification kit and the matching BSA calibration standard of 20-2000 $\mu\text{g/ml}$. Thus reported serum fetuin-B concentrations will vary depending on the calibration standard that was used. The estimation of absolute serum fetuin-B concentrations and indeed of correct amounts of fetuin-B will become possible once a pure fetuin-B preparation has been studied by quantitative amino acid analysis, and a correct ϵ_{280} has been determined from that preparation. Thus serum fetuin-B concentrations measured previously should be nominally 1.7 times higher than reported here, and the determination of the “true” amounts awaits confirmation by quantitative amino acid analysis. Correcting the serum levels by this factor of 1.7, the *Fetub*^{+/+} and *Fetub*^{+/-} females tested here show fetuin-B serum levels of $274.8 \pm 17.9 \mu\text{g/ml}$ and $152.7 \pm 4.8 \mu\text{g/ml}$, respectively which is compatible to the values of $300 \mu\text{g/ml}$ and $334 \mu\text{g/ml}$ reported above. Despite the discrepancies in absolute values, it was confirmed, that *Fetub*^{+/-} females have half the fetuin-B serum levels of *Fetub*^{+/+} females.

Female *Fetub*^{-/-} mice are completely infertile. *Fetub*^{+/-} females have half the serum fetuin-B level of wildtype animals and reproduce normal. Female infertility of *Fetub*^{-/-} mice was independent of the genetic background and was mediated by an early blockade in

fertilization. Fetuin-B deficient oocytes could be fertilized *in vitro* after overcoming the ZP barrier by laser perforation. After embryo transferring to foster mothers, the fetuses developed normal. *Fetub*^{-/-} foster mothers became pregnant, and delivered healthy offspring after embryo transfer. Thus the sole reason for infertility in *Fetub*^{-/-} females is an early blockade in fertilization indicating that fetuin-B is critically required before fertilization, but is dispensable during later stages of embryonic and fetal live.

More than 200 genetic mouse models are reported with reproductive defects^{162,183}. About 50 show complete female infertility, mostly due to sex hormone disturbance, developmental arrest or implantation defects. Fetuin-B adds to this group as a liver-derived non-hormonal plasma protein, which is essential for female fertility. In humans, infertility affects about 15% of couples worldwide who wish to have children, while both sexes affected to a similar degree. The main reasons for female infertility are ovulatory defects, malformations of the oviducts or endometriosis. Up to 25% of diagnoses have no apparent pathology, and are thus considered idiopathic. Since fetuin-B is well conserved in mammals, abnormalities in the *FETUB* gene could also lead to loss of function of the human fetuin-B protein and thus to female infertility. The genome project lists more than 4600 variations in the human fetuin-B gene, multiple splice variants and more than 330 sequence variants for *FETUB*, that change one or more bases, resulting in a different amino acid sequence but with preserved length (http://browser.1000genomes.org/Homo_sapiens/Gene/Variation_Gene/Table?db=core;g=ENSG00000090512;r=3:186353758-186370930). This unusually strong polymorphism argues against a gene conservation, which would be expected if fetuin-B was sensitive to mutations. Clearly, a loss of fetuin-B function would result in an evolutionary disadvantage and counterselection. Therefore the high number of mutations seems counterintuitive. Nevertheless, any or all of them might potentially affect the function of human fetuin-B protein. For lack of knowledge about the structure-function relationship, we do not know, if any of these variants are indeed functionally relevant. Thus the study of fetuin-B is not only an interesting topic of reproductive medicine, but also from an evolutionary point of view.

4.2 Fetuin-B Deficient Oocytes Undergo Premature *Zona Pellucida* Hardening

We showed that premature ZP hardening concurred with ovulation and blocked fertilization of fetuin-B deficient oocytes. Until now, premature ZP hardening was only known from *in vitro* oocyte culture and fertilization^{71,145}. Fetuin-B deficient mice are the first reported example of premature ZP hardening *in vivo*. Because spontaneous ZP hardening during *in vitro* culture is also reported in humans, alterations in the *FETUB* gene could also lead to premature ZP hardening *in vivo*⁷¹. One would predict, that IVF should fail in the absence of functional fetuin-B because of blocked oocyte-sperm binding. A study of Liu and Baker showed that

about 6% of failed IVF with low sperm-ZP interactions had normal sperm morphology, and thus could be due to defects of the ZP¹⁸⁴. Considering that about 15% of the couples worldwide are infertile and that up to 30% of IVF fail this would mean that 0.27 % (0.06 x 0.15 x 0.30) of the women worldwide eventually show ZP defects. This amount seems very low, but it has to be mentioned that the amount of women, showing premature ZP hardening would be expected to be very low until today, since females with a fetuin-B defect would not have been able to reproduce until ART and especially ICSI was investigated in the 1990th. In the next decades the amount of females carrying fetuin-B mutations could increase since the heredity will be promoted by the use of ARTs. Thus also the amount of infertile women will increase. For patients, who fail in IVF treatment, intracytoplasmic sperm injection (ICSI) is used nowadays to overcome the ZP barrier, both at higher costs and considerable loss of the number of implantable embryos¹⁸⁴. Addition of fetuin-B to oocytes at the earliest convenience might improve IVF success in humans with defects in the *FETUB* gene. The block of premature ZP hardening in these patients by medication with fetuin-B derivatives could even allow *in vivo* fertilization, avoiding previous hormonal stimulation and the associated risks.

Earlier reports showed, that FCS as well as bovine fetuin inhibit premature ZP hardening *in vitro*^{148,154,155}. First assumptions that fetuin-A was the factor inhibiting ZP hardening were not confirmed. We could show that both, FCS and bovine fetuin, contain fetuin-B. Thus fetuin-B rather than fetuin-A inhibited ZP hardening in earlier studies.

In all the shown experiments to check ZP hardening, two-cell embryos obtained by IVF were used as controls and surprisingly showed less ZP hardening compared to fetuin-B deficient oocytes. We hypothesized that this is due to endogenous fetuin-B that is stored at the extracellular matrix of the cumulus cells. Denecke et al. showed that fetuin-B expression is absent in mice ovaries but that fetuin-B is probably located in the extracellular matrix². This suggests the assumption that fetuin-B diffuses out of the blood into the follicular fluid at antrum formation like it was already proposed for other proteins^{157,185,186}. There it invades into the extracellular matrix of the cumulus cells whereby it reaches the oocyte. It was shown that the cumulus cell matrix is mainly composed of hyaluronic acid, but also composes serum maintained components, that are linked to the extracellular matrix by cumulus cell derived factors¹⁸⁷⁻¹⁹¹. As for the mode of action we suggest that fetuin-B of 55 - 60 kDa can freely diffuse through the ZP, which is permeable for molecules up to 150 kDa³⁹. Thus fetuin-B can readily antagonize the proteolytic action of prematurely released ZP2 protease ovastacin during oocyte maturation. Following ovulation and COC penetration the extracellular matrix is digested by sperm specific proteases to loose cumulus cells and thus make the oocyte accessible, also leading to a decrease of surrounding fetuin-B. Furthermore the developing embryo is transported through the oviduct to the uterus, which could add to the decrease in

surrounding fetuin-B concentration. Following fertilization and degranulation of the cortical granula, the amount of ZP2 protease ovastacin will overwhelm the inhibition capacity of fetuin-B, which is in steady state with plasma fetuin-B, but does not increase upon fertilization. As a consequence *in vivo* premature ZP hardening would be inhibited to maintain fertility, while fertilization-triggered ZP hardening would not be inhibited. At IVF the penetrating sperm remove cumulus cells as well, but in contrast to *in vivo* fertilization, the cumulus cells and their extracellular environment stay around the oocyte due to the limited space. Thus *in vitro* the dilution of fetuin-B would be less compared to the *in vivo* conditions. As a consequence premature ZP hardening would be inhibited *in vitro* only temporary. Fetuin-B diffuses out of the cumulus cell matrix with time, leading to fetuin-B dilution in the direct environment of the oocyte. Thus with progressive time the ZP hardens prematurely. After *in vitro* fertilization the amount of released ovastacin increases like *in vivo* while the surrounding fetuin-B is in steady state and does not decrease like *in vivo*, leading only to partial fertilization-triggered ZP hardening. At fetuin-B deficiency inhibition of premature ZP hardening is lost, leading to infertility.

4.3 Fetuin-B Inhibits Ovastacin and Thus *Zona Pellucida* Hardening

To elucidate the molecular mechanism of ZP hardening inhibition by fetuin-B, we turned to proteases, because fetuins belong to the cystatin superfamily, a group of thiol protease inhibitors¹. Early studies employing golden hamster oocytes showed that ZP hardening is triggered by the release of cortical granule material including proteases. Prompted by a recent report, which showed that the cortical granula metalloproteinase ovastacin cleaves ZP2, triggering definitive ZP hardening, we studied the molecular interaction of recombinant fetuin-B protein with ovastacin¹²². Indeed, recombinant fetuin-B inhibited recombinant ovastacin at concentrations fully compatible with the measured fetuin-B plasma and follicular fluid concentrations.

As already mentioned plasmin was also discussed to trigger ZP hardening, but the molecular mechanism behind these observations could not be clarified until today^{118,192}. Interestingly plasmin is known to activate metalloproteases. As ovastacin is classified as a metalloprotease and is expressed as a propeptide it could be possible, that plasmin activates ovastacin^{193,194}. Thus the noticed effect of plasmin to increase ZP hardening could be indirect⁵¹. Probably pro-ovastacin is released by the cortical granules and is activated in the perivitelline space by plasmin, eventually giving a new level of ZP hardening regulation^{195,196}. It was shown that oviductal fluid contains about 90 µg/ml plasminogen and thus surrounds the oocyte at least after ovulation¹¹⁸. Plasminogen was further detected at the oolemma and the ZP. Plasminogen activators are located at the oolemma as well and are further released

by the oocyte and the sperm after gamete interaction and fertilization^{118,119}. Thus low concentrations of active plasmin are already present during oocyte maturation and increases after fertilization¹¹⁸. Plasmin could then cleave pro-ovastacin leading to activation of ovastacin that cleaves ZP2 to induce ZP hardening. In humans plasminogen mutations correlate with subfertility, while mice deficient for either plasminogen or plasminogen activators are fertile^{120,121,197}. Thus the role of the plasminogen / plasminogen activator / plasmin seems to be species specific and eventually adds to the regulation of ZP hardening by ovastacin activation, but also seems to be compensable.

Fetuin are known to be potent protease inhibitors. Already in the 1970 Galembeck and colleagues described bovine fetuin as a trypsin inhibitor, not discriminating between fetuin-A and fetuin-B¹⁹⁸. Subsequent publications used the known trypsin inhibitor function of bovine fetuin to explain the inhibitory potency in ZP hardening^{152,154,155}. In these study they used purified bovine fetuin, that we now know can contain both fetuins. Human preparations enriched for fetuin-A do not have anti-proteolytic activity or inhibit ZP hardening^{152,199}. Furthermore results of experiments with recombinant fetuin-A lead to the suggestion that the trypsin specific anti-proteolytic activity associated with conventionally purified bovine fetuin may be due to a copurifying contaminant²⁰⁰. Other studies showed comparable results. Meprin α and β , two zinc metalloproteinases were also shown to be inhibited by purified human and bovine fetuin, while recombinant human fetuin-A only inhibited meprin β ²⁰¹. Thus the anti-proteolytic activity of purified bovine or human fetuin to several proteases, like trypsin and meprin β , could also be mediated by fetuin-B. Ongoing studies at the lab of professor Walter Stöcker (Mainz) with the use of recombinant murine fetuin-A and fetuin-B seem to confirm this assumption. Thus it is easily conceivable that fetuin-B has further functions beside the here shown inhibition of premature ZP hardening, even if the *Fetub*^{-/-} mice showed no obvious defect beside the female infertility.

4.4 Fetuin-B Increases Fertilization Success *in Vitro*

The supplementation of IVF medium with recombinant murine fetuin-B had no effect on fertilization success, when sperm was added immediately after COC isolation. After cumulus cell removal and one hour of *in vitro* cultivation rmFetuB inhibited ZP hardening and increased IVF success. Less than 0.015 mg/ml inhibited premature ZP hardening while 0.03 mg/ml further inhibited fertilization-triggered ZP hardening, surprisingly not leading to polyspermy. Supplementation of HTF medium with rmFetuB increased fertilization success for up to nine hours of *in vitro* cultivation, while retention of the cumulus cells showed similar results.

Earlier studies showed comparable results of FCS and bovine fetuin as described in the present work for rmFetuB. It is known that FCS and bovine fetuin comprise both, fetuin-A and fetuin-B, but unfortunately proportional distribution is not known. Thus results of the present work can only be compared with results of earlier studies to make a rough estimate about the amount of fetuin-B that is contained in FCS or purified bovine fetuin. With an amount of 10-20 mg/ml, fetuins are the most abundant constituent of FCS²⁰². Early studies used 5-20% FCS resulting in 0.5-4 mg/ml fetuin. These predicted concentrations were assumed by the fact that 20% FCS was effective as 3-5 mg/ml purified bovine fetuin in inhibiting ZP hardening¹⁵². Schröder and colleagues showed, that with the use of 1 mg/ml purified bovine fetuin, the inhibitory capacity is already reduced and using 0.1 mg/ml bovine fetuin the relative ZP hardening already doubles, compared to 5% FCS (depicting 0.5-1 mg/ml bovine fetuin)¹⁵⁵. Comparing the results of Schröder et al. and the data of the present work, 1 mg/ml bovine fetuin showed similar results to 0.015 mg/ml rmFetuB. Leaving out of account species specific variations of fetuin-B activity one could predict that bovine fetuin comprises about 1.5% of fetuin-B. As already mentioned before FCS, human serum or purified products of serum are general used in cell culture as a protein source, but with a risk of infections and LOT-to-LOT variations^{149,203}. Thus the long-term goal at *in vitro* cultivation and fertilization is the replacement of serum-derived additives by recombinant expressed proteins. To realize this intention 0.015 mg/ml rmFetuB could replace the inhibitory effect on ZP hardening of 1 mg/ml bovine fetuin or 5% FCS.

After fertilization ZP hardening is thought to block polyspermy. Controversial the use of fetuin-B during IVF procedure inhibited fertilization-triggered ZP hardening, but did not increase polyspermy. Thus fertilization-triggered changes at the membrane level seem to be efficient to inhibit polyspermy. Furthermore ZP hardening would not be necessary for an efficient polyspermy block, but eventually still for protecting the embryo until implantation. Ovastacin deficient mice (*Astf*^{-/-}) as well as mice that were mutated in the ZP2 cleavage site (*Zp2*^{mut/mut}) both lack ZP hardening^{97,122}. *Zp2*^{mut/mut} females show smaller litter sizes⁹⁷. After spontaneous mating and *in vivo* fertilization the number of one-cell embryos was comparable to wildtypes. There was no evidence of supernumerary sperm in the perivitelline space. Instead the ZP was thinner compared to wildtype oocytes and the amount of flushed blastocysts at day 3.5 post-fertilization was decreased. Thus, early embryonic loss probably due to premature ZP hatching appears as the major contributor to the subfertility observed in *Zp2*^{mut/mut} females. Ovastacin deficient mice show decreased fertility, but polyspermy was not shown, only predicted¹²². Thus subfertility of *Astf*^{-/-} females could also be mediated by early embryo loss like described for the *Zp2*^{mut/mut} mice. Our findings, that inhibition of fertilization-triggered ZP hardening by fetuin-B does not result in polyspermy, support the idea that an effective post-fertilization block to polyspermy is independent of ZP2 cleavage.

The present data show that retention of cumulus cells at IVF had similar effects on premature ZP hardening than the addition of fetuin-B to the IVF medium. As a consequence one could say that the fetuin-B supplementation of IVF medium would be redundant. But this is only true for IVF treatments that are done under optimal conditions, meaning active endogenous fetuin-B detained at the cumulus cell matrix and fertilization immediately after COC isolation. But also at these condition one would agree, that the use of fetuin-B was not counterproductive, since fetuin-B neither increased polyspermy nor decreased embryo development. In contrast under suboptimal conditions, meaning decreased fetuin-B activity or even completely loss of fetuin-B (simulated by cumulus cell removal) or increased duration until fertilization, the addition of fetuin-B to IVF medium can increase fertilization success. Thus even if fetuin-B supplementation might not improve fertilization success in all IVF cases, the use of fetuin-B in IVF medium makes sense until the need is not tested before each IVF treatment.

Beside the probably benefit of fetuin-B to human reproductive medicine, fetuin-B could also have an impact on mouse research, factory farming or IVF of other animals. As shown in the present work for C57BL/6 mice the supplementation of IVF medium with fetuin-B could be redundant, if IVF is done under optimal condition. But to visualize different processes in the oocyte, especially during fertilization, the cumulus cells often have to be removed. In this case the use of fetuin-B can improve results. Furthermore there are several mouse strains, which show decreased IVF success, caused by premature ZP hardening. For example the IVF success of the inbreed mouse strain 129S1/SvImJ is less than 25%¹⁷³. KE mice also perform low success at IVF and oocytes isolated from these mice showed higher resistance against proteolytic ZP digestion by chymotrypsin²⁰⁴. At the use of these mouse strains the supplementation of fetuin-B would event be more sensible, compared to C57BL/6 mice, used in this work.

In diary and meat industry IVF is used to achieve the ability to provide food for an ever-expanding world population²⁰⁵. The most productive animals are selected to be donors for IVF and less productive females are used as embryo recipient²⁰⁶. Thus the reproduction rate of profitable animals can be increased drastically. Furthermore sperm sorting by flow cytometry is used to influence offspring gender, for example to get more dairy cows²⁰⁷. In 2012 about 0.9 Mio embryos were transferred in cattle worldwide²⁰⁸. The use of IVF for other farm animals is less (23000 ovine; 15000 equine and 2500 porcine embryos worldwide in 2012), but is constantly growing, indicating the high commercial use of IVF in livestock farming. At assisted reproduction it was shown that fetuin prevents ZP hardening in horses²⁰⁹. In bovine IVF premature ZP hardening reduces fertilization success and the use of fetuin increased the amount of blastocysts^{204,210,211}. As a general consequence the use of

recombinant fetuin-B could increase IVF success in farm animals as well and thus should be of high commercial interest.

With growing global population the natural environment available for wild animals decreases and thus the number of endangered species increases. For endangered animals showing small populations, ARTs and especially IVF are the best way to produce a high number of offspring from selected donors. A good example of ART application in wild animals is the European mouflon. Ptak et al. demonstrated for the first time the potential of IVF to rescue an endangered species, the European mouflon, with substantial yields of oocytes, embryos and pregnancy, independent of age and breeding season ²¹². In other endangered species, for example non-human primates, oocyte *in vitro* maturation was improved by bovine fetuin, giving a new potential application for fetuin-B ¹⁵⁶. Embryos that are not used directly for transfer are often preserved by freezing, called cryopreservation. Cryopreserved embryos can be stored over decades and thus genetic diversity can be preserve ^{213,214}. Several specialized centers have been established that cryopreserve tissue from valuable, rare, and endangered species ^{215,216}. Reproductive tissue of highly diverse species already is preserved, for example the polar bear, chimpanzees, south American bush dogs, gorillas, Mexican wolves, Mongolian wild horses and orangutans. It was shown that cryopreservation of oocytes leads to spontaneous release of cortical granules and to ZP hardening ²¹⁷. Thus the improvement of cryopreservation and IVF, done with endangered animals, can be a further scope of application for fetuin-B to retain these species.

In humans embryos are cryopreserved after assisted reproduction for later implantation as well. In the last years furthermore oocyte cryopreservation has increased for several reasons ²¹⁸. Females diagnosed with cancer can save the oocytes against damages triggered by chemotherapy or radiotherapy. In some other cases females undergo ART, not considering embryo but oocyte freezing an option. In other cases of oocyte cryopreservation there are females who would like to preserve their future ability to have children, either because they do not yet have a partner, or for other personal or medical reasons. In these cases oocytes are cryopreserved for later use in ART. As it was already mentioned, oocyte cryopreservation leads to premature ZP hardening. Thus the use of fetuin-B during freezing procedure can inhibit ZP hardening and the oocytes can be fertilized by IVF after thawing ^{149,217,219}.

Coming back to the shown data, where endogenous cumulus cell retained fetuin-B showed similar results as supplemented recombinant fetuin-B, it is further important to mention that the experiments presented in this work were done with ovulated oocytes. It is known that the most spontaneous released cortical granules are exocytosed during germinal vesicle breakdown that starts before ovulation. Thus a certain proportion of premature released ovastacin was probably already inhibited by endogenous fetuin-B. To isolate several human oocytes females are typically hormonal stimulated for ovulation to induce oocytes maturation.

Afterwards the COCs are obtained by follicle puncture before ovulation and not as typically done for mice, where COCs are isolated out of the ampulla after ovulation. Thus it is possible that for human oocytes at IVF treatment the major amount of spontaneous cortical granula release happens *in vitro* and not *in vivo* like in mice. Thus the addition of recombinant fetuin-B to IVF medium would have a more obvious impact than shown in this work. For women with eventually *FETUB* defects the recent work shows that the oocytes should either be isolated before they undergo premature ZP hardening or the oocytes should be fertilized by overcoming the ZP as a barrier (for instance by laser assisted IVF or intracytoplasmic sperm injection ICSI). Thus the screening of infertile women for *FETUB* defects could help to decide which kind of ART would be the best. Further thinking it would be possible to spare these females the necessity of ART, if the premature ZP hardening could be inhibited probably by treatment with fetuin-B derivatives.

Conclusion and Future Aspects

Fetuin-B inhibits spuriously released ovastacin, either *in vivo* or *in vitro*, and thus maintains ZP permeability (figure 28). After fertilization, ovastacin concentration suddenly increases following degranulation of the cortical granula, overwhelming the inhibition capacity of fetuin-B, resulting in ZP2 cleavage and ultimately, ZP hardening. The fertilization-triggered polyspermy blockade seems to be independent of ZP hardening, while ZP hardening is important for protecting the pre-implantation embryo. In fetuin-B deficiency, either *in vivo* or *in vitro*, ZP hardens during maturation, which blocks fertilization. Thus fetuin-B represents an therapeutic target for fertilization biology and reproductive medicine.

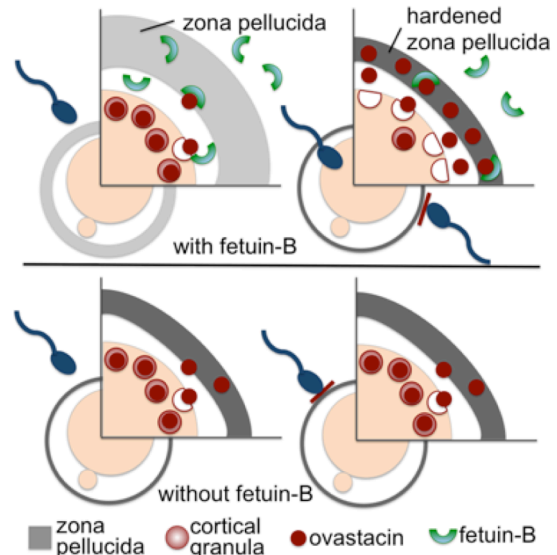


Figure 28. Illustration of the biological function of fetuin-B. (top) During oocyte maturation fetuin-B retains ZP permeability. (bottom) Fetuin-B deficiency leads to premature ZP hardening and female infertility.

Identifying functional defects in the human *FETUB* gene may explain hitherto “idiopathic” cases of female infertility. Supplementation of oocyte culture medium with recombinant fetuin-B could increase IVF success in several species by inhibiting premature ZP hardening. Fetuin-B may also obviate the damage inflicted to oocytes by established methods overcoming the ZP e.g. ICSI. In addition, fetuin-B may be used to inhibit fertilization-triggered ZP hardening to assist hatching without the embryo damage inflicted e.g. by ZP laser perforation or by partial ZP dissection. On a practical note, the regulation of female fertility through plasma fetuin-B may be exploited for a non-hormonal contraceptive therapy aiming at reducing serum fetuin-B below the critical values required for the inhibition of premature ZP hardening.

References

1. Lee, C., Bongcam-Rudloff, E., Sollner, C., Jahnen-Dechent, W. & Claesson-Welsh, L. Type 3 cystatins: fetuins, kininogen and histidine-rich glycoprotein. *Front. Biosci.* **14**, 2911–2922 (2009).
2. Denecke, B. *et al.* Tissue distribution and activity testing suggest a similar but not identical function of fetuin-B and fetuin-A. *Biochem. J.* **376**, 135–145 (2003).
3. Olivier, E. *et al.* A novel set of hepatic mRNAs preferentially expressed during an acute inflammation in rat represents mostly intracellular proteins. *Genomics* **57**, 352–364 (1999).
4. Olivier, E. *et al.* Fetuin-B, a second member of the fetuin family in mammals. *Biochem. J.* **350**, 589–597 (2000).
5. Altschul, S. F. *et al.* Protein database searches using compositionally adjusted substitution matrices. *FEBS J.* **272**, 5101–5109 (2005).
6. Altschul, S. F. *et al.* Gapped BLAST and PSI-BLAST: a new generation of protein database search programs. *Nucleic Acids Res.* **25**, 3389–3402 (1997).
7. Jahnen-Dechent, W. *et al.* Cloning and targeted deletion of the mouse fetuin gene. *J. Biol. Chem.* **272**, 31496–31503 (1997).
8. Schäfer, C. *et al.* The serum protein α 2-Heremans-Schmid glycoprotein/fetuin-A is a systemically acting inhibitor of ectopic calcification. *J. Clin. Invest.* **112**, 357–366 (2003).
9. Heiss, A. *et al.* Structural basis of calcification inhibition by alpha 2-HS glycoprotein/fetuin-A. Formation of colloidal calciprotein particles. *J. Biol. Chem.* **278**, 13333–13341 (2003).
10. Hsu, S. J., Nagase, H. & Balmain, A. Identification of Fetuin-B as a member of a cystatin-like gene family on mouse chromosome 16 with tumor suppressor activity. *Genome* **47**, 931–946 (2004).
11. Murakami, T. *et al.* The farnesoid X receptor induces fetuin-B gene expression in human hepatocytes. *Biochem. J.* **407**, 461–469 (2007).

12. Choi, J.-W., Liu, H., Mukherjee, R. & Yun, J. W. Downregulation of fetuin-B and zinc-alpha2-glycoprotein is linked to impaired fatty acid metabolism in liver cells. *Cell. Physiol. Biochem.* **30**, 295–306 (2012).
13. Choi, J.-W. *et al.* Plasma proteome analysis in diet-induced obesity-prone and obesity-resistant rats. *Proteomics* **10**, 4386–4400 (2010).
14. Sattlecker, M. *et al.* Alzheimer's disease biomarker discovery using SOMAscan multiplexed protein technology. *Alzheimers Dement.* **S1552-5260**, 00031–4 (2014).
15. Khan, S. R., Joshi, S., Wang, W. & Peck, A. B. Regulation of macromolecular modulators of urinary stone formation by reactive oxygen species: transcriptional study in an animal model of hyperoxaluria. *Am. J. Physiol. Renal. Physiol.* **306**, F1285–1295 (2014).
16. Choi, Y. *et al.* Microarray analyses of newborn mouse ovaries lacking Nobox. *Biol. Reprod.* **77**, 312–319 (2007).
17. Dietzel, E. *et al.* Fetuin-B, a liver-derived plasma protein is essential for fertilization. *Dev. Cell* **25**, 106–112 (2013).
18. Wessling, J. Gene deletion and functional analysis of fetuin-B. *Diss. RWTH Aachen* (2007).
19. Dietzel, E. The analysis of the female infertility of fetuin-B deficient mice. *Master thesis, RWTH Aachen* (2011).
20. Johnson, M. H. *Essential Reproduction*. 80–188 (2007).
21. Lawson, K. A. & Hage, W. J. Clonal analysis of the origin of primordial germ cells in the mouse. *Ciba Found Symp.* **182**, 68–91 (1994).
22. Gilbert, S. F. in *Dev. Biol.* 593–623 (Palgrave Macmillan, 2006).
23. Tingen, C., Kim, A. & Woodruff, T. K. The primordial pool of follicles and nest breakdown in mammalian ovaries. *Mol. Hum. Reprod.* **15**, 795–803 (2009).
24. Johnson, J. *et al.* Oocyte generation in adult mammalian ovaries by putative germ cells in bone marrow and peripheral blood. *Cell* **122**, 303–315 (2005).
25. Pinkerton, J. H., McKay, D. G., Adams, E. C. & Hertig, A. T. Development of the human ovary-a study using histochemical technics. *Obs. Gynecol.* **18**, 152–181 (1961).
26. Masui, Y. & Clarke, H. J. Oocyte maturation. *Int. Rev. Cytol.* **57**, 185–282 (1979).
27. McLaughlin, E. A. & Mclver, S. C. Awakening the oocyte: controlling primordial follicle development. *Reproduction* **137**, 1–11 (2009).

- References -

28. Eppig, J. J. Oocyte control of ovarian follicular development and function in mammals. *Reproduction* **122**, 829–838 (2001).
29. Skinner, M. K. Regulation of primordial follicle assembly and development. *Hum. Reprod. Updat.* **11**, 461–471 (2005).
30. Nilsson, E. E. & Skinner, M. K. Kit ligand and basic fibroblast growth factor interactions in the induction of ovarian primordial to primary follicle transition. *Mol. Cell. Endocrinol.* **214**, 19–25 (2004).
31. Nilsson, E. E., Kezele, P. & Skinner, M. K. Leukemia inhibitory factor (LIF) promotes the primordial to primary follicle transition in rat ovaries. *Mol. Cell. Endocrinol.* **188**, 65–73 (2002).
32. Nilsson, E. E. & Skinner, M. K. Bone morphogenetic protein-4 acts as an ovarian follicle survival factor and promotes primordial follicle development. *Biol. Reprod.* **69**, 1265–1272 (2003).
33. Lee, W. S., Otsuka, F., Moore, R. K. & Shimasaki, S. Effect of bone morphogenetic protein-7 on folliculogenesis and ovulation in the rat. *Biol. Reprod.* **65**, 994–999 (2001).
34. Jimenez-Movilla, M. & Dean, J. ZP2 and ZP3 cytoplasmic tails prevent premature interactions and ensure incorporation into the zona pellucida. *J. Cell Sci.* **124**, 940–950 (2010).
35. Durlinger, A. Regulation of ovarian function: the role of anti-Müllerian hormone. *Reproduction* **124**, 601–609 (2002).
36. Visser, J. A., de Jong, F. H., Laven, J. S. E. & Themmen, A. P. N. Anti-Müllerian hormone: a new marker for ovarian function. *Reproduction* **131**, 1–9 (2006).
37. Broer, S. L. *et al.* Anti-mullerian hormone predicts menopause: a long-term follow-up study in normoovulatory women. *J. Clin. Endocrinol. Metab.* **96**, 2532–2539 (2011).
38. Broer, S. L. *et al.* Added value of ovarian reserve testing on patient characteristics in the prediction of ovarian response and ongoing pregnancy: an individual patient data approach. *Hum. Reprod. Updat.* **19**, 26–36 (2013).
39. Legge, M. Oocyte and zygote zona pellucida permeability to macromolecules. *J. Exp. Zool.* **271**, 145–150 (1995).
40. Nagy, A., Gertsenstein, M., Vintersten, K. & Behringer, R. *Manipulating the mouse embryo: A laboratory manual.* (Cold Spring Harbor Laboratory, 2003).

- References -

41. McNatty, K. P. *et al.* Growth and paracrine factors regulating follicular formation and cellular function. *Mol. Cell. Endocrinol.* **163**, 11–20 (2000).
42. Li, R., Philips, D. M. & Mather, J. P. Activin promotes ovarian follicle development in vitro. *Endocrinology* **136**, 849–856 (1995).
43. Smitz, J., Cortvrindt, R., Hu, Y. & Vanderstichele, H. Effects of recombinant activin A on in vitro culture of mouse preantral follicles. *Mol. Reprod. Dev.* **50**, 294–304 (1998).
44. Xiao, S., Robertson, D. M. & Findlay, J. K. Effects of activin and follicle-stimulating hormone (FSH)-suppressing protein/follistatin on FSH receptors and differentiation of cultured rat granulosa cells. *Endocrinology* **131**, 1009–1016 (1992).
45. Knight, P. G. & Glister, C. TGF-beta superfamily members and ovarian follicle development. *Reproduction* **132**, 191–206 (2006).
46. Revelli, A. *et al.* Follicular fluid content and oocyte quality: from single biochemical markers to metabolomics. *Reprod. Biol. Endocrinol.* **7**, 40 (2009).
47. Magoffin, D. A. Ovarian theca cell. *Int. J. Biochem. Cell Biol.* **37**, 1344–1349 (2005).
48. Austin, C. R. Cortical granules in hamster eggs. *Exp. Cell Res.* **10**, 533–540 (1956).
49. Ducibella, T., Anderson, E., Albertini, D. F., Aalberg, J. & Rangarajan, S. Quantitative studies of changes in cortical granule number and distribution in the mouse oocyte during meiotic maturation. *Dev. Biol.* **130**, 184–197 (1988).
50. Zhang, L. *et al.* Plasminogen has a broad extrahepatic distribution. *Thromb. Haemost.* **87**, 493–501 (2002).
51. Huarte, J., Vassalli, J.-D., Belin, D. & Denny, S. Involvement of the plasminogen activator/plasmin proteolytic cascade in fertilization. *Dev. Biol.* **157**, 539–546 (1993).
52. Richards, J. S. *et al.* Novel signaling pathways that control ovarian follicular development, ovulation, and luteinization. *Recent Prog. Horm. Res.* **57**, 195–220 (2002).
53. Herath, C. B. *et al.* Regulation of follicle-stimulating hormone secretion by estradiol and dimeric inhibins in the infantile female rat. *Biol. Reprod.* **1633**, 1623–1633 (2001).
54. Knobil, E. & Neill, J. D. *The Physiology of Reproduction.* (1994).
55. Hawkins, S. M. & Matzuk, M. M. The menstrual cycle: basic biology. *Ann. NY Acad. Sci.* **1135**, 10–18 (2008).
56. Dym, M. Spermatogonial stem cells of the testis. *P. Natl Acad. Sci. USA* **91**, 11287–11289 (1994).

- References -

57. Newton, S. C., Blaschuk, O. W. & Millette, C. F. N-cadherin mediates Sertoli cell-spermatogenic cell adhesion. *Dev. Dyn.* **197**, 1–13 (1993).
58. Pratt, S. A., Scully, N. F. & Shur, B. D. Cell surface beta 1,4 galactosyltransferase on primary spermatocytes facilitates their initial adhesion to Sertoli cells in vitro. *Biol. Reprod.* **49**, 470–482 (1993).
59. Zhao, G. Q., Deng, K., Labosky, P. A., Liaw, L. & Hogan, B. L. The gene encoding bone morphogenetic protein 8B is required for the initiation and maintenance of spermatogenesis in the mouse. *Gene. Dev.* **10**, 1657–1669 (1996).
60. Dym, M. & Fawcett, D. W. Further observations on the numbers of spermatogonia, spermatocytes, and spermatids connected by intercellular bridges in the mammalian testis. *Biol. Reprod.* **4**, 195–214 (1971).
61. Braun, R. E., Behringer, R. R., Peschon, J. J., Brinster, R. L. & Palmiter, R. D. Genetically haploid spermatids are phenotypically diploid. *Nature* **337**, 373–376 (1989).
62. Mack, S., Bhattacharyya, A. K., Joyce, C., van der Ven, H. & Zaneveld, L. J. Acrosomal enzymes of human spermatozoa before and after in vitro capacitation. *Biol. Reprod.* **28**, 1032–1042 (1983).
63. Austin, C. R. *The mammalian egg*. (Blackwell Scientific Publications, 1961).
64. Bleil, J. D. & Wassarman, P. M. Structure and function of the zona pellucida: identification and characterization of the proteins of the mouse oocyte's zona pellucida. *Dev. Biol.* **76**, 185–202 (1980).
65. Lefièvre, L. *et al.* Four zona pellucida glycoproteins are expressed in the human. *Hum. Reprod.* **19**, 1580–1586 (2004).
66. Wassarman, P. M. Zona pellucida glycoproteins. *Annu. Rev. Biochem.* **57**, 415–442 (1988).
67. Epifano, O., Liang, L. F., Familiari, M., Moos, M. C. & Dean, J. Coordinate expression of the three zona pellucida genes during mouse oogenesis. *Development* **121**, 1947–1956 (1995).
68. Greve, J. M. & Wassarman, P. M. Mouse egg extracellular coat is a matrix of interconnected filaments possessing a structural repeat. *J. Mol. Biol.* **181**, 253–264 (1985).
69. Green, D. P. Three-dimensional structure of the zona pellucida. *Rev. Reprod.* **2**, 147–156 (1997).

70. Dietl, J. *The mammalian egg coat*. (Springer, 1989).
71. Schiewe, M. C., Araujo, E., Asch, R. H. & Balmaceda, J. P. Enzymatic characterization of zona pellucida hardening in human eggs and embryos. *J. Assist. Reprod. Genet.* **12**, 2–7 (1995).
72. Rankin, T. L., Talbot, P., Lee, E. & Dean, J. Abnormal zonae pellucidae in mice lacking ZP1 result in early embryonic loss. *Development* **126**, 3847–3855 (1999).
73. Männikkö, M. *et al.* Association between sequence variations in genes encoding human zona pellucida glycoproteins and fertilization failure in IVF. *Hum. Reprod.* **20**, 1578–1585 (2005).
74. Rankin, T. L. *et al.* Defective zonae pellucidae in Zp2-null mice disrupt folliculogenesis, fertility and development. *Development* **128**, 1119–1126 (2001).
75. Liu, C. *et al.* Targeted disruption of the mZP3 gene results in production of eggs lacking a zona pellucida and infertility in female mice. *Dev. Biol.* **93**, 5431–5436 (1996).
76. Conner, S. J., Lefièvre, L., Hughes, D. C. & Barratt, C. L. R. Cracking the egg: increased complexity in the zona pellucida. *Hum. Reprod.* **20**, 1148–1152 (2005).
77. Gilbert, S. F. in *Dev. Biol.* 175–209 (Palgrave Macmillan, 2006).
78. Hedrich, H. J. & Bullock, G. *The Laboratory Mouse - The handbook of experimental animals*. (Academic Press, 2004).
79. Quill, T. A. *et al.* Hyperactivated sperm motility driven by CatSper2 is required for fertilization. *P. Natl Acad. Sci. USA* **100**, 14869–14874 (2003).
80. Bahat, A. & Eisenbach, M. Sperm thermotaxis. *Mol. Cell. Endocrinol.* **252**, 115–119 (2006).
81. Cross, N. L. Role of cholesterol in sperm capacitation. *Biol. Reprod.* **59**, 7–11 (1998).
82. Visconti, P. E. *et al.* Capacitation of mouse spermatozoa. II. Protein tyrosine phosphorylation and capacitation are regulated by a cAMP-dependent pathway. *Development* **121**, 1139–1150 (1995).
83. Arnoult, C. *et al.* Control of the low voltage-activated calcium channel of mouse sperm by egg ZP3 and by membrane hyperpolarization during capacitation. *P. Natl Acad. Sci. USA* **96**, 6757–6762 (1999).
84. Cross, N. L. Reorganization of lipid rafts during capacitation of human sperm. *Biol. Reprod.* **71**, 1367–1373 (2004).

85. Lopez, L. C. *et al.* Receptor function of mouse sperm surface galactosyltransferase during fertilization. *J. Cell Biol.* **101**, 1501–1510 (1985).
86. Wang, Y., Storeng, R., Dale, P. O., Abyholm, T. & Tanbo, T. Effects of follicular fluid and steroid hormones on chemotaxis and motility of human spermatozoa in vitro. *Gynecol. Endocrinol.* **15**, 286–292 (2001).
87. Corselli, J. & Talbot, P. In vitro penetration of hamster oocyte-cumulus complexes using physiological numbers of sperm. *Dev. Biol.* **122**, 227–242 (1987).
88. Smith, T. T. The modulation of sperm function by the oviductal epithelium. *Biol. Reprod.* **58**, 1102–1104 (1998).
89. Suarez, S. S. The oviductal sperm reservoir in mammals: mechanisms of formation. *Biol. Reprod.* **58**, 1105–1107 (1998).
90. Töpfer-Petersen, E. *et al.* Function of the mammalian oviductal sperm reservoir. *J. Exp. Zool.* **292**, 210–215 (2002).
91. Lin, Y., Mahan, K., Lathrop, W. F., Myles, D. G. & Primakoff, P. A hyaluronidase activity of the sperm plasma membrane protein PH-20 enables sperm to penetrate the cumulus cell layer surrounding the egg. *J. Cell Biol.* **125**, 1157–1163 (1994).
92. Primakoff, P. & Myles, D. G. Penetration, adhesion, and fusion in mammalian sperm-egg interaction. *Science (80-.)*. **296**, 2183–2185 (2002).
93. Braden, A. W. H., Austin, C. R. & David, H. A. The reaction of the zona pellucida to sperm penetration. *Aust. J. Biol. Sci.* **7**, 391–410 (1954).
94. Visconti, P. E. & Florman, H. M. Mechanisms of sperm-egg interactions: between sugars and broken bonds. *Sci. Signal.* **3**, 1–3 (2010).
95. Florman, H. M. & Wassarman, P. M. O-linked oligosaccharides of mouse egg ZP3 account for its sperm receptor activity. *Cell* **41**, 313–324 (1985).
96. Florman, H. M. & Storey, B. T. Mouse gamete interactions: the zona pellucida is the site of the acrosome reaction leading to fertilization in vitro. *Dev. Biol.* **91**, 121–130 (1982).
97. Gahlay, G., Gauthier, L., Baibakov, B., Epifano, O. & Dean, J. Gamete recognition in mice depends on the cleavage status of an egg's zona pellucida protein. *Science (80-.)*. **329**, 216–219 (2010).
98. Baibakov, B., Boggs, N. A., Yauger, B., Baibakov, G. & Dean, J. Human sperm bind to the N-terminal domain of ZP2 in humanized zonae pellucidae in transgenic mice. *J. Cell Biol.* **197**, 897–905 (2012).

- References -

99. Avella, M. A., Xiong, B. & Dean, J. The molecular basis of gamete recognition in mice and humans. *Mol. Hum. Reprod.* **19**, 279–289 (2013).
100. Inoue, N., Satouh, Y., Ikawa, M., Okabe, M. & Yanagimachi, R. Acrosome-reacted mouse spermatozoa recovered from the perivitelline space can fertilize other eggs. *PNAS* **108**, 20008–20011 (2011).
101. Kaji, K. *et al.* The gamete fusion process is defective in eggs of Cd9-deficient mice. *Nat. Genet.* **24**, 279–282 (2000).
102. Miyado, K. *et al.* Requirement of CD9 on the egg plasma membrane for fertilization. *Science (80-)*. **287**, 321–324 (2000).
103. Cho, C. *et al.* Fertilization defects in sperm from mice lacking fertilin beta. *Science (80-)*. **281**, 1857–1859 (1998).
104. Kaji, K. & Kudo, A. The mechanism of sperm-oocyte fusion in mammals. *Reproduction* **127**, 423–429 (2004).
105. Jaffe, L. A. & Gould, M. in *Biol. Fertil.* (Metz, C. B. & Monroy, A.) 223–250 (Academic Press, 1985).
106. Jaffe, L. A., Sharp, A. P. & Wolf, D. P. Absence of an electrical polyspermy block in the mouse. *Dev. Biol.* **96**, 317–323 (1983).
107. Gardner, A. J. & Evans, J. P. Mammalian membrane block to polyspermy: new insights into how mammalian eggs prevent fertilisation by multiple sperm. *Reprod. Fertil. Dev.* **18**, 53–61 (2006).
108. Szollosi, D. Development of cortical granules and the cortical reaction in rat and hamster eggs. *Anat. Rec.* **159**, 431–446 (1967).
109. Barros, C. & Yanagimachi, R. Induction of zona reaction in golden hamster eggs by cortical granule material. *Nature* **233**, 268–269 (1971).
110. Moller, C. C. & Wassarman, P. M. Characterization of a proteinase that cleaves zona pellucida glycoprotein ZP2 following activation of mouse eggs. *Dev. Biol.* **132**, 103–112 (1989).
111. Bleil, J. D., Beall, C. F. & Wassarman, P. M. Mammalian sperm-egg interaction: fertilization of mouse eggs triggers modification of the major zona pellucida glycoprotein, ZP2. *Dev. Biol.* **86**, 189–197 (1981).
112. Inoue, M. & Wolf, D. P. Solubility properties of the murine zona pellucida. *Biol. Reprod.* **10**, 512–518 (1974).

113. Drobnis, E. Z., Andrew, J. B. & Katz, D. F. Biophysical properties of the zona pellucida measured by capillary suction: is zona hardening a mechanical phenomenon? *J. Exp. Zool.* **245**, 206–219 (1988).
114. Schmill, E. D. & Gulyas, B. J. Ovoperoxidase activity in ionophore treated mouse eggs . II . Evidence for the enzyme' s role in hardening the zona pellucida. *Gamete Res.* **3**, 279–290 (1980).
115. Miller, D. J., Gong, X., Decker, G. & Shur, B. D. Egg cortical granule N-acetylglucosaminidase is required for the mouse zona block to polyspermy. *J. Cell Biol.* **123**, 1431–1440 (1993).
116. Coy, P. *et al.* Oviduct-specific glycoprotein and heparin modulate sperm-zona pellucida interaction during fertilization and contribute to the control of polyspermy. *P. Natl Acad. Sci. USA* **105**, 15809–15814 (2008).
117. Rodeheffer, C. & Shur, B. D. Characterization of a novel ZP3-independent sperm-binding ligand that facilitates sperm adhesion to the egg coat. *Development* **131**, 503–512 (2004).
118. Mondéjar, I., Grullón, L. a, García-Vázquez, F. a, Romar, R. & Coy, P. Fertilization outcome could be regulated by binding of oviductal plasminogen to oocytes and by releasing of plasminogen activators during interplay between gametes. *Fertil. Steril.* **97**, 453–461 (2012).
119. Zhang, X., Rutledge, J., Khamsi, F. & Armstrong, D. T. Release of tissue-type plasminogen activator by activated rat eggs and its possible role in the zona reaction. *Mol. Reprod. Dev.* **32**, 28–32 (1992).
120. Bugge, T. H., Flick, M. J., Daugherty, C. C. & Degen, J. L. Plasminogen deficiency causes severe thrombosis but is compatible with development and reproduction. *Gene. Dev.* **9**, 794–807 (1995).
121. Carmeliet, P. *et al.* Physiological consequences of loss of plasminogen activator gene function in mice. *Nature* **368**, 419–424 (1994).
122. Burkart, A. D., Xiong, B., Baibakov, B., Jimenez-Movilla, M. & Dean, J. Ovastacin, a cortical granule protease, cleaves ZP2 in the zona pellucida to prevent polyspermy. *J. Cell Biol.* **197**, 37–44 (2012).
123. Jacobs, P. A. *et al.* The origin of human triploids. *Ann. Hum. Genet* **42**, 49–57 (1978).
124. Zaragoza, M. V *et al.* Parental origin and phenotype of triploidy in spontaneous abortions: predominance of diandry and association with the partial hydatidiform mole. *Am. J. Hum. Genet* **66**, 1807–1820 (2000).

- References -

125. Quesada, V., Sánchez, L. M., Alvarez, J. & López-Otín, C. Identification and characterization of human and mouse ovastacin: a novel metalloproteinase similar to hatching enzymes from arthropods, birds, amphibians, and fish. *J. Biol. Chem.* **279**, 26627–26634 (2004).
126. Agostoni, E. Preimplantation development of the mammalian embryo. *Ann Ist Super Sanita* **29**, 15–25 (1993).
127. Seshagiri, P. B., Sen Roy, S., Sireesha, G. & Rao, R. P. Cellular and molecular regulation of mammalian blastocyst hatching. *J. Reprod. Immunol.* **83**, 79–84 (2009).
128. Perona, R. M. & Wassarman, P. M. Mouse blastocysts hatch in vitro by using a trypsin-like proteinase associated with cells of mural trophoctoderm. *Dev. Biol.* **114**, 42–52 (1986).
129. O'Sullivan, C. M., Rancourt, S. L., Liu, S. Y. & Rancourt, D. E. A novel murine tryptase involved in blastocyst hatching and outgrowth. *Reproduction* **122**, 61–71 (2001).
130. O'Sullivan, C. M., Liu, S. Y., Rancourt, S. L. & Rancourt, D. E. Regulation of the strypsin-related proteinase ISP2 by progesterone in endometrial gland epithelium during implantation in mice. *Reproduction* **122**, 235–244 (2001).
131. O'Sullivan, C. M., Liu, S. Y., Karpinka, J. B. & Rancourt, D. E. Embryonic hatching enzyme strypsin/ISP1 is expressed with ISP2 in endometrial glands during implantation. *Mol. Reprod. Dev.* **62**, 328–334 (2002).
132. Blandau, R. J. Observations on implantation of the guinea pig ovum. *Anat. Rec.* **103**, 19–47 (1949).
133. Gonzales, D. S., Boatman, D. E. & Bavister, B. D. Kinematics of trophoctoderm projections and locomotion in the peri-implantation hamster blastocyst. *Dev. Dyn.* **205**, 435–444 (1996).
134. Gonzales, D. S. *et al.* Trophoctoderm projections: a potential means for locomotion, attachment and implantation of bovine, equine and human blastocysts. *Hum. Reprod.* **11**, 2739–2745 (1996).
135. Bergström, S. Shedding of the zona pellucida of the mouse blastocyst in normal pregnancy. *J. Reprod. Fertil.* **31**, 275–277 (1972).
136. Lopata, A. & Hay, D. L. The potential of early human embryos to form blastocysts, hatch from their zona and secrete HCG in culture. *Hum. Reprod.* **4**, 87–94 (1989).
137. Malter, H. E. & Cohen, J. Blastocyst formation and hatching in vitro following zona drilling of mouse and human embryos. *Gamete Res.* **24**, 67–80 (1989).

138. Feng, H. L., Hershlag, A., Scholl, G. M. & Cohen, M. A. A retrospective study comparing three different assisted hatching techniques. *Fertil. Steril.* **91**, 1323–1325 (2009).
139. Talansky, B. E. & Gordon, J. W. Cleavage characteristics of mouse embryos inseminated and cultured after zona pellucida drilling. *Gamete Res.* **21**, 277–287 (1988).
140. Committee, P. The role of assisted hatching in in vitro fertilization: a review of the literature. A Committee opinion. *Fertil. Steril.* **86**, S124–S126 (2006).
141. Schieve, L. A. *et al.* Does assisted hatching pose a risk for monozygotic twinning in pregnancies conceived through in vitro fertilization? *Fertil. Steril.* **74**, 288–294 (2000).
142. Edwards, R. G. Implantation, interception and contraception. *Hum. Reprod.* **9**, 985–995 (1994).
143. Melford, S. E., Taylor, A. H. & Konje, J. C. Of mice and (wo)men: factors influencing successful implantation including endocannabinoids. *Hum. Reprod. Updat.* **20**, 415–428 (2014).
144. Rousseau, P., Meda, P., Lecart, C., Haumont, S. & Ferin, J. Cortical granule release in human follicular oocytes. *Biol. Reprod.* **16**, 104–111 (1977).
145. Ducibella, T., Kurasawa, S., Rangarajan, S., Kopf, G. S. & Schultz, R. M. Precocious loss of cortical granules during mouse oocyte meiotic maturation and correlation with an egg-induced modification of the zona pellucida. *Dev. Biol.* **137**, 46–55 (1990).
146. Dodson, M. G., Minhas, B. S., Curtis, S. K., Palmer, T. V & Robertson, J. L. Spontaneous zona reaction in the mouse as a limiting factor for the time in which an oocyte may be fertilized. *J. Vitro. Fert. Embryo Transf.* **6**, 101–106 (1989).
147. Downs, S. M., Schroeder, A. C. & Eppig, J. J. Serum maintains the fertilizability of mouse oocytes matured in vitro by preventing hardening of the zona pellucida. *Gamete Res.* **15**, 115–122 (1986).
148. Kalab, P., Schultz, R. M. & Kopf, G. S. Modifications of the mouse zona pellucida during oocyte maturation: inhibitory effects of follicular fluid, fetuin, and alpha 2HS-glycoprotein. *Biol. Reprod.* **49**, 561–567 (1993).
149. Blake, D., Svalander, P., Jin, M., Silversand, C. & Hamberger, L. Protein supplementation of human IVF culture media. *J. Assist. Reprod. Genet.* **19**, 137–143 (2002).
150. Alberda, A. T., VanOs, H. C. & Zeilmaker, G. H. Hepatitis B virus-infectie bij Vrouwen behandeld met in-vitro fertilisatie. *Ned. Tijdschr. Voor Geneesk.* **133**, 20–25 (1989).

- References -

151. Otani, T. Earthquakes and prions [letter]. *Fertil. Steril.* **63**, 1137–1139 (1995).
152. George, M. A. & Johnson, M. H. Use of fetal bovine serum substitutes for the protection of the mouse zona pellucida against hardening during cryoprotectant addition. *Hum. Reprod.* **8**, 1898–1900 (1993).
153. De Felici, M. & Siracusa, G. “Spontaneous” hardening of the zona pellucida of mouse oocytes during in vitro culture. *Gamete Res.* **6**, 107–113 (1982).
154. Kalab, P., Kopf, G. S. & Schultz, R. M. Modifications of the mouse zona pellucida during oocyte maturation and egg activation: effects of newborn calf serum and fetuin. *Biol. Reprod.* **45**, 783–787 (1991).
155. Schröder, A. C. *et al.* Fetuin inhibits zona pellucida hardening and conversion of ZP2 to ZP2f during spontaneous mouse oocyte maturation in vitro in the absence of serum. *Biol. Reprod.* **43**, 891–897 (1990).
156. Xu, J. *et al.* Secondary follicle growth and oocyte maturation during encapsulated three-dimensional culture in rhesus monkeys: effects of gonadotrophins, oxygen and fetuin. *Hum. Reprod.* **26**, 1061–1072 (2011).
157. Bódis, J., Peti, A. M., Sulyok, E., Kovács, G. L. & Várnagy, A. Serum and follicular fluid fetuin-A in women undergoing in vitro fertilization. *Clin. Chem. Lab. Med.* 1–6 (2014).
158. Jahnen-Dechent, W., Heiss, A., Schäfer, C. & Ketteler, M. Fetuin-A regulation of calcified matrix metabolism. *Circ. Res.* **108**, 1494–1509 (2011).
159. Venter, J. C. *et al.* The sequence of the human genome. *Science (80-.)*. **291**, 1304–1351 (2001).
160. Waterston, R. H. *et al.* Initial sequencing and comparative analysis of the mouse genome. *Nature* **420**, 520–562 (2002).
161. Neill, J. D. *Physiology of Reproduction*. (Elsevier Inc., 2005).
162. Roy, A. & Matzuk, M. M. Deconstructing mammalian reproduction: using knockouts to define fertility pathways. *Reproduction* **131**, 207–219 (2006).
163. Murray, S. A. *et al.* Mouse gestation length is genetically determined. *PLoS One* **5**, e12418 (2010).
164. Jax3. Reproductive performance survey, females of 33 inbred strains of mice. MPD:Jax3. *Jackson Lab. Mouse Phenome Database web site*, The Jackson Labor (2014).

165. Jax5. Breeding performance survey, females of 35 commonly used strains of JAX Mice. MPD:Jax5. *Jackson Lab*. Mouse Phenome Database web site, The Jackson Labor (2014).
166. Yuan, R. *et al.* Genetic coregulation of age of female sexual maturation and lifespan through circulating IGF1 among inbred mouse strains. *PNAS* **109**, 8224–8229 (2012).
167. Laird, P. W. *et al.* Simplified mammalian DNA isolation procedure. *Nucleic Acids Res.* **19**, 4293 (1991).
168. Laemmli, U. K. Cleavage of structural proteins during the assembly of the head of bacteriophage T4. *Nature* **227**, 680–685 (1970).
169. Hogan, B., Beddington, R., Constantini, F. & Lacy, E. *Manipulating the mouse embryo. A laboratory manual*. (Cold Spring Harbor Laboratory Press, 1994).
170. Gulyas, B. J. & Yuan, L. C. Cortical reaction and zona hardening in mouse oocytes following exposure to ethanol. *J. Exp. Zool.* **233**, 269–276 (1985).
171. Rankin, T. L. *et al.* Fertility and taxon-specific sperm binding persist after replacement of mouse sperm receptors with human homologs. *Dev. Cell* **5**, 33–43 (2003).
172. Weiskirchen, R. *et al.* Comparative evaluation of gene delivery devices in primary cultures of rat hepatic stellate cells and rat myofibroblasts. *BMC Cell Biol.* **1**, 4 (2000).
173. Byers, S., Payson, S. & Taft, R. Performance of ten inbred mouse strains following assisted reproductive technologies (ARTs). *Theriogenology* **65**, 1716–1726 (2006).
174. Yanagimachi, R. in *Physiol. Reprod.* (Knobil, E. & Neil, J.) 189–317 (1994).
175. Wassarman, P. M. & Litscher, E. S. Mammalian fertilization: the egg's multifunctional zona pellucida. *Int. J. Dev. Biol.* **52**, 665–676 (2008).
176. Wassarman, P. M. Zona Pellucida Glycoproteins. *J. Biol. Chem.* **283**, 24285–24289 (2008).
177. Jennings, P. C., Merriman, J. a, Beckett, E. L., Hansbro, P. M. & Jones, K. T. Increased zona pellucida thickness and meiotic spindle disruption in oocytes from cigarette smoking mice. *Hum. Reprod.* **26**, 878–884 (2011).
178. Mai, Z., Lei, M., Yu, B., Du, H. & Liu, J. The effects of cigarette smoke extract on ovulation, oocyte morphology and ovarian gene expression in mice. *PLoS One* **9**, e95945 (2014).
179. Nayernia, K. *et al.* Proacrosin-deficient mice and zona pellucida modifications in an experimental model of multifactorial infertility. *Mol. Hum. Reprod.* **8**, 434–440 (2002).

- References -

180. Garside, W. T., Loret de Mola, J. R., Bucci, J. a, Tureck, R. W. & Heyner, S. Sequential analysis of zona thickness during in vitro culture of human zygotes: correlation with embryo quality, age, and implantation. *Mol. Reprod. Dev.* **47**, 99–104 (1997).
181. Gabrielsen, A., Bhatnager, P. R., Petersen, K. & Lindenberg, S. Influence of zona pellucida thickness of human embryos on clinical pregnancy outcome following in vitro fertilization treatment. *J. Assist. Reprod. Genet.* **17**, 323–328 (2000).
182. Rankin, T. L. *et al.* Fertility and taxon-specific sperm binding persist after replacement of mouse sperm receptors with human homologs. *Dev. Cell.* **5**, 33–43 (2003).
183. Matzuk, M. M. Revelations of ovarian follicle biology from gene knockout mice. *Mol. Cell. Endocrinol.* **163**, 61–66 (2000).
184. Liu, D. Y. & Baker, H. W. G. Disordered zona pellucida-induced acrosome reaction and failure of in vitro fertilization in patients with unexplained infertility. *Fertil. Steril.* **79**, 74–80 (2003).
185. Rom, E. *et al.* Follicular fluid contents as predictors of success of in-vitro fertilization-embryo transfer. *Hum. Reprod. Updat.* **2**, 505–510 (1987).
186. Spitzer, D., Murach, K. F., Lottspeich, F., Staudach, A. & Illmensee, K. Different protein patterns derived from follicular fluid of mature and immature human follicles. *Hum. Reprod.* **11**, 798–807 (1996).
187. Camaioni, A., Salustri, A., Yanagishita, M. & Hascall, V. C. Proteoglycans and proteins in the extracellular matrix of mouse cumulus cell-oocyte complexes. *Arch. Biochem. Biophys.* **325**, 190–198 (1996).
188. Camaioni, A., Hascall, V. C., Yanagishita, M. & Salustri, A. Effects of exogenous hyaluronic acid and serum on matrix organization and stability in the mouse cumulus cell-oocyte complex. *J. Biol. Chem.* **268**, 20473–20481 (1993).
189. Cherr, G. N., Yudin, A. I. & Katz, D. F. Organization of the hamster cumulus extracellular matrix: a hyaluronate-glycoprotein gel which modulates sperm access to the oocyte. *Dev. Growth Differ.* **32**, 353–365 (1990).
190. Chen, L., Mao, S. J. & Larsen, W. J. Identification of a factor in fetal bovine serum that stabilizes the cumulus extracellular matrix. A role for a member of the inter-alpha-trypsin inhibitor family. *J. Biol. Chem.* **267**, 12380–12386 (1992).
191. Chen, L., Zhang, H., Powers, R. W., Russell, P. T. & Larsen, W. J. Covalent linkage between proteins of the inter-alpha-inhibitor family and hyaluronic acid is mediated by a factor produced by granulosa cells. *J. Biol. Chem.* **271**, 19409–19414 (1996).

- References -

192. Coy, P. *et al.* Oocytes use the plasminogen-plasmin system to remove supernumerary spermatozoa. *Hum. Reprod.* 1–9 (2012). doi:10.1093/humrep/des146
193. Yiallourous, I. *et al.* Activation mechanism of pro-astacin: role of the pro-peptide, tryptic and autoproteolytic cleavage and importance of precise amino-terminal processing. *J. Mol. Biol.* **324**, 237–246 (2002).
194. Guevara, T. *et al.* Proenzyme structure and activation of astacin metallopeptidase. *J. Biol. Chem.* **285**, 13958–13965 (2010).
195. Hildebrand, A. Funktionelle und Strukturelle Charakterisierung des Ovastacins In Vivo und In Vitro. (2013).
196. Westphal, H. Ovastacin in der Hausmaus (*Mus musculus*). (2013).
197. Ebisch, I. M. W. *et al.* Possible role of the plasminogen activation system in human subfertility. *Fertil. Steril.* **87**, 619–626 (2007).
198. Galembeck, F. & Cann, J. R. Fetuin as a trypsin inhibitor. *Arch. Biochem. Biophys.* **164**, 326–331 (1974).
199. Brown, W. M., Saunders, N. R., Mollgran, K. & Dziegielewska, K. M. Fetuin - an old friend revisited. *Bioessays* **14**, 749–755 (1992).
200. Brown, W. M. *et al.* The nucleotide and deduced amino acid structures of sheep and pig fetuin. Common structural features of the mammalian fetuin family. *Eur. J. Biochem.* **205**, 321–331 (1992).
201. Hedrich, J. *et al.* Fetuin-A and cystatin C are endogenous inhibitors of human meprin metalloproteases. *Biochemistry* **49**, 8599–8607 (2010).
202. Pedersen, K. O. Fetuin, a new globulin isolated from serum. *Nature* **154**, 575 (1944).
203. Sagirkaya, H., Yagmur, M., Nur, Z. & Soylu, M. K. Replacement of fetal calf serum with synthetic serum substitute in the in vitro maturation medium: effects on maturation, fertilization and subsequent development of cattle oocytes in vitro. *Turk. J. Vet. Anim. Sci.* **28**, 779–784 (2004).
204. Kaleta, E. & Bieta. Sperm penetration in vitro into ovarian and tubal oocytes from mice of the inbred KE and C57 strains. *Gamete Res.* **2**, 99–104 (1979).
205. FAO's Animal Production and Health Division: Milk & Dairy Products. at <<http://www.fao.org/ag/againfo/themes/en/meat/background.html>>
206. Looney, C. R., Lindsey, B. R., Gonseth, C. L. & Johnson, D. L. Commercial aspects of oocyte retrieval and in vitro fertilization (IVF) for embryo production in problem cows. *Theriogenology* **41**, 67–72 (1994).

207. Sharpe, J. C. & Evans, K. M. Advances in flow cytometry for sperm sexing. *Theriogenology* **71**, 4–10 (2009).
208. Perry, G. *2012 statistics of embryo collection and transfer in domestic farm animals*. 23 (2013).
209. Dell'Aquila, M. E., De Felici, M., Massari, S., Maritato, F. & Minoia, P. Effects of fetuin on zona pellucida hardening and fertilizability of equine oocytes matured in vitro. *Biol. Reprod.* **61**, 533–540 (1999).
210. Romar, R., Coy, P., Gadea, J. & Rath, D. Effect of oviductal and cumulus cells on zona pellucida and cortical granules of porcine oocytes fertilized in vitro with epididymal spermatozoa. *Anim. Reprod. Sci.* **85**, 287–300 (2005).
211. Kanda, M., Miyazaki, T., Nakao, H. & Tsutsui, T. Development of in vitro fertilized feline embryos in a modified Earle's balanced salt solution: influence of protein supplements and culture dishes on fertilization success and blastocyst formation. *J. Vet. Med. Sci.* **60**, 423–431 (1998).
212. Ptak, G. *et al.* Preservation of the wild European mouflon: the first example of genetic management using a complete program of reproductive biotechnologies. *Biol. Reprod.* **66**, 796–801 (2002).
213. Comizzoli, P., Mermillod, P. & Mauget, R. Reproductive biotechnologies for endangered mammalian species. *Reprod. Nutr. Dev.* **40**, 493–504 (2000).
214. Andrabi, S. M. H. & Maxwell, W. M. C. A review on reproductive biotechnologies for conservation of endangered mammalian species. *Anim. Reprod. Sci.* **99**, 223–243 (2007).
215. Souza, J. M. G. De, Batista, R. I. T. P., Melo, L. M. & Freitas, V. J. D. F. Reproductive biotechnologies applied to the conservation of endangered ruminant - past , present and future. *Artig. revisao* 31–38 (2011).
216. Pizzi, F. *et al.* Conservation of endangered animals: from biotechnologies to digital preservation. *Nat. Sci.* **05**, 903–913 (2013).
217. Vincent, C., Pickering, S. J. & Johnson, M. H. The hardening effect of dimethylsulphoxide on the mouse zona pellucida requires the presence of an oocyte and is associated with a reduction in the number of cortical granules present. *J. Reprod. Fertil.* **89**, 253–259 (1990).
218. PCASRM-SART. Mature oocyte cryopreservation: a guideline. *Fertil. Steril.* **99**, 37–43 (2013).

- References -

219. Horvath, G. & Seidel, G. E. Use of fetuin before and during vitrification of bovine oocytes. *Reprod. Domest. Anim.* **43**, 333–338 (2008).

Abbreviations

ADAM	a disintegrin and metalloproteinase
<i>AHSG</i>	α 2-HS-glycoprotein gene, human fetuin-A gene
AHSG	α 2-HS-glycoprotein, human fetuin-A protein
AMH	anti-müllerian hormone
<i>Astl</i>	murine Ovastacin gene
<i>ASTL</i>	human Ovastacin gene
BMP4	bone morphogenetic protein-4
BMP7	bone morphogenetic protein-7
BMP8b	bone morphogenetic protein-8b
BMP15	bone morphogenetic protein-15
BSA	bovine serum albumin
cAMP	cyclic adenosine monophosphate
COC	cumulus-oocyte complex
CSF	cytostatic factor
DNA	deoxyribonucleic acid
ECL	electrogenerated chemiluminescence
EDTA	ethylenediaminetetraacetic acid
FCS	fetal calf serum
<i>FetuA</i>	murine fetuin-A gene
FetuA	fetuin-A protein
<i>Fetub</i>	murine fetuin-B gene
<i>FETUB</i>	human fetuin-B gene
FetuB	fetuin-B protein
FSH	follicle stimulating hormone
FXR	farnesoid X receptor
GDF9	growth and differentiation factor-9

- Abbreviations -

hCG	human chorionic gonadotropin
HK	high molecular weight kininogen
HRG	histidine rich glycoprotein
HRP	horseradish peroxidase
HSA	human serum albumin
HTF	human tubular fluid
ICM	inner cell mass
IVC	<i>in vitro</i> cultivation
IVF	<i>in vitro</i> fertilization
IU	international units
kb	kilobase
kDa	kilodalton
KNG	kininogen
LH	luteinizing hormone
LIF	leukemia inhibitory factor
LK	low molecular weight kininogen
MBCD	metyl-beta-cyclodextrin
MPF	maturation promoting factor
OGP	oviduct-specific glycoprotein
PAGE	polyacrylamide gel electrophoresis
PBS	phosphate buffered saline
PBST	phosphate buffered saline with 0.05% Tween20
PFA	paraformaldehyde
rmFetuB	recombinant murine fetuin-B
RNA	ribonucleic acid
SCF	stem cell factor
SDS	sodium dodecyl sulfate
TBST	TRIS buffered saline with 0.05% Tween20
TE	trophectoderm

- Abbreviations -

TEPs	trophectodermal projections
TGF- β	transforming growth factor β
TRIS	tris(hydroxymethyl)aminomethane
ZP	<i>zona pellucida</i>
<i>Zp1</i>	murine <i>zona pellucida</i> protein 1 gene
<i>ZP1</i>	human <i>zona pellucida</i> protein 1 gene
ZP1	<i>zona pellucida</i> protein 1
<i>Zp2</i>	murine <i>zona pellucida</i> protein 2 gene
<i>ZP2</i>	human <i>zona pellucida</i> protein 2 gene
ZP2	<i>zona pellucida</i> protein 2
<i>Zp3</i>	murine <i>zona pellucida</i> protein 3 gene
<i>ZP3</i>	human <i>zona pellucida</i> protein 3 gene
ZP3	<i>zona pellucida</i> protein 3
<i>Zp4</i>	murine <i>zona pellucida</i> protein 4 gene
<i>ZP4</i>	human <i>zona pellucida</i> protein 4 gene
ZP4	<i>zona pellucida</i> protein 4

List of Figures

- Figure 1. Multiple alignment of mouse (m) and human (h) fetuin-B (FetuB) and fetuin-A (FetuA)
- Figure 2. Schematic overview of the human type 3 cystatin superfamily
- Figure 3. Schematic overview of oogenesis and spermatogenesis
- Figure 4. Microscopic picture of a murine antral follicle
- Figure 5. Illustration of the mechanism between fertilization and polyspermy block
- Figure 6. Illustration of the absent polyspermy block under ovastacin deficiency
- Figure 7. Illustration of the mechanism between spontaneous cortical granula reaction and premature ZP hardening
- Figure 8. Illustration of the hypothesized function of fetuin-B
- Figure 9. Heterozygous (+/-) females show half the fetuin-B serum concentration of wildtype (+/+)
- Figure 10. Fetuin-B deficient oocytes can be fertilized *in vitro* after overcoming the ZP by laser perforation
- Figure 11. Fetuin-B deficient zygotes develop normal
- Figure 12. Commercial fetuin preparations with *zona pellucida* hardening inhibition activity contain fetuin-B
- Figure 13. *Zona pellucida* of fetuin-B deficient oocytes is thinner
- Figure 14. *Zona pellucida* of fetuin-B deficient oocytes is more resistant against enzymatic digestion
- Figure 15. *Zona pellucida* digestion time is increase in fetuin-B deficient oocytes
- Figure 16. *In vitro* sperm binding is decreased at fetuin-B deficient oocytes compared to wildtype oocytes
- Figure 17. Fetuin-B deficient oocytes show premature ZP2 cleavage that persists after ovulation
- Figure 18. Active recombinant ovastacin is inhibited by recombinant mouse fetuin-B

- List of Figures -

- Figure 19. Evaluation of recombinant murine fetuin-B transfer from PBS to HTF medium
- Figure 20. Timing diagram of experiment 1
- Figure 21. Recombinant murine fetuin-B did not influence embryo development
- Figure 22. Timing diagram of experiment 2
- Figure 23. ZP hardening occurred after one hour of *in vitro* cultivation (IVC)
- Figure 24. Timing diagram of experiment 3
- Figure 25. During *in vitro* cultivation recombinant murine fetuin-B inhibited ZP hardening and increased IVF success
- Figure 26. Exemplary illustration of four out of nine timing diagrams of experiment 4
- Figure 27. The use of recombinant murine fetuin-B during *in vitro* cultivation increased fertility for up to nine hours
- Figure 28. Illustration of the biological function of fetuin-B
-
- Figure S1. Alignment of murine and human Zp1 coding sequence
- Figure S2. Alignment of murine and human Zp2 coding sequence
- Figure S3. Alignment of murine and human Zp3 coding sequence
- Figure S4. Human Zp4 coding sequence
- Figure S5. Alignment of murine and human ovastacin coding sequence
- Figure S6. Fetuin-B deficient mice show ovulation rate comparable to wildtypes
- Figure S7. Premature *zona pellucida* hardening of fetuin-B deficient oocytes at DBA/2 background
- Figure S8. Calculation of the perivitelline space volume

List of Tables

Table 1.	Comparison of murine and human fetuin-B
Table 2.	Vital and reproductive statistics of C57BL/6J and DBA/2J mice.
Table 3.	Mastermix for fetuin-B genotyping
Table 4.	PCR program for fetuin-B genotyping
Table 5.	Chemical composition of human tubular fluid (HTF) medium
Table 6.	Chemical composition of TYH + MBCD (Methyl- β -cyclodextrin) medium
Table 7.	Breeding performance for C57BL/6 mice.
Table 8.	Breeding performance of DBA/2 mice.

Supplement

mZp1	PGFEYSYDCGVRGMQLLVFPRPNQTVQFKVLDEFGNRFEVNNCSICYHWVTSEAQEHHTVF	86
hZp1	PGLRHSYDCGIKGMQLLVFPRPCQTLRFKVVDEFGNRFDVNNCSICYHWVTSRPOEPAVF	94
mZp1	SADYKGCHVLEKDRFHLRVF IQAVLPNGRVDIAQDVTLICPKPDHTVTPDPYLAPFTTP	146
hZp1	SADYRGCHVLEKDRFHLRVFMEAVLPNGRVDVAQDATLICPKPDFSRITLDSOLAPFAMF	154
mZp1	EPFTPHAFALHPIPDHTLAGSGHTGLTTLIYPEQSFTHPTPAPPSTLGGPGAGSTVPHSQWG	206
hZp1	SVSTPQTLSTFLPTSGHTSQSGHAFPSPLDPEGHSSVHPTPALPSPGPGPTLATLAQPHWG	214
mZp1	TLEPWELTELDSVGTHLPQERCOVASGHIPCVMVNGSSKEACQOAGCCYDSTKEEPCYYGN	266
hZp1	TLEHWDVNRDVIETGTHLSQEQCOVASGHLPCIVRRRTSKEACQOAGCCYDNTREVPYYGN	274
mZp1	TVTLQCFKSGYFTLVMSQETALTHGVLLDNVHLAYAPNGCPTQKTSFAFVVFHPLTHCG	326
hZp1	TATVQCFRDGYFVLVVSQEMALTRITLANIHLAYAPTSCTPTQHTFAFVVFYFPLTHCG	334
mZp1	TATQVVGEOIYENQLVSDIDVOKGPOGSITRDSAERLHVRCIFNASDFLPIQASIFSPQ	386
hZp1	TTMQVAGDQIYENWLVSGIHIQKGPQGSITRDSITFQLHVRCVFNASDFLPIQASIFPPP	394
mZp1	PPAPVTQSGPLRLELRITDKTFSSYYQGS DYPLVRLLEPVYVEVRLQLQRTDPSLVLLL	446
hZp1	SPAPMTPGPLRLELRITAKDETSSYYGEDDYPVRLLEPVHVEVRLQLQRTDPNLVLLL	454
mZp1	HQCWATPTTSPFEQPOWPILSDGCPFKGDNYRTQVVAADKEALPFWSHYQRFTHTFMLL	506
hZp1	HQCWGAPSANPFQOPQWPILSDGCPFKGDSYRTQMVALDG--ATPFQSHYQRFVATTFALL	513
mZp1	DSSSQNALRGQVYFFCSASACHPLGSDTCSTTCDSGIARRRRSSGHHNITLRALDIVSSP	566
hZp1	DSGSQRALRGLVYLFCSSTACHTSGLTETCSTACSTGTTRQRRSSGHRNDTARPDIVSSP	573
mZp1	GAVGFEDAACLE-----PSGSSRNSSSRMLLLLATTLALAA-----GIFVGLIWAQKWLW	618
hZp1	GPVGFEDSYGOEPTLGPDSNGNSSLRPLLWAVLLLPAAVALVLGFGVVFVGLSQTWQKWLW	633
mZp1	EGIR 622	
hZp1	ESNR 637	

Figure S1. Alignment of murine (m) and human (h) Zp1 coding sequence, showing 68% identical and 77% similar amino acids. Species are noted on the left. Similar residues conserved in the two sequences are printed as white letters on black background. A minimum number of gaps, indicated by hyphens, has been introduced to maximize alignments. Alignments were produced using the web based alignment service BLAST (<http://blast.ncbi.nlm.nih.gov/Blast.cgi>) and default parameters (blastp algorithm, BLOSUM62 Matrix, Gap Cost existence:11 extension:1, conditional compositional score matrix adjustment).

- Supplement -

mZp2	MARWORKASVSSP----CGRSLYRFLSLFLTLVTSVNSVSLPQSENPAFPGLTICDKDEV	56
hZp2	MACRORGGSNPSGWFNAGWSTYRSISLFFALVTSGNISIDVSQLVNPAPFGTVTCDEREI	60
mZp2	RLEFSSRFDMEKWNPSSVVDTLGSEILNCTYALDLERFVLKFPYETCTIKVVGQYQVNTIRV	116
hZp2	TVEFPSSPGTKKWHASVVDPLGLDMPNCTYILDEPKLTLRATYDNCTRRVHGGHOMTIRV	120
mZp2	GDTTLDVRYKDDMYHFFCPAQAE--THEISEIVVCRRLISFSFPQLFSRLADENQNVS-	174
hZp2	MNNSAALRHGAVMYQFFCPAMQVEETQGLSASTTCQKDFMSFSLPRVFSGLADDSKGTGV	180
mZp2	EMGWIVKIGNGTRAHILPLKDAIVQGFNLLIDSKVTLHVPANATGIVHYVQESSYLYTV	234
hZp2	QMGWSIEVGDGARAKTTLPLPEAMKEGFSLLIDNHRMTFHVPFNATGVTTHYVQGNSHLYMV	240
mZp2	QLELLFSTTGQKIVFSSHAICAPDLSVACNATHMTLTIPEFPGKLESVDFGQWSIPEDQW	294
hZp2	SLKLTFTISPGQKIVFSSQAICAPD-PVTCNATHMTLTIPEFPGKLSVDFENQNDVSQL	299
mZp2	HANGIDKEATNGRLNFRKSLKTKPSEKCPFYQFYLSLKLTFYFGNMLSTVIDPECH	354
hZp2	HDNGIDLEATNGMKLHFSKTLKTKLSEKCLLHQFYLASLKLTFLLRPETVSMVIVPECL	359
mZp2	CESPVSI--DELCAODGFMDFEVYSHQTKPALNDTLLVGNSSCOPIFKVQSVGLARFHI	412
hZp2	CESPVSIVTGELCTODGFMDFEVYSYQTPALDLGTLRVGNSSCOPVFEAQSGLVRFHI	419
mZp2	PLNGCGTRQKFECDKVIYENEIHALWENPPSNIVFRNSEFRMTVRCYIIRDSMLLNAHVK	472
hZp2	PLNGCGTRYKFEEDKVVYENEIHALWTDFFPSKISRDSSEFRMTVKCSYSRNDMLNINVE	479
mZp2	GHPSPPEAFVKPGPLVLLVLQTYPDQSYQRPYRKDEYPLVRYLRQPIYMEVKVLSRNDPNIK	532
hZp2	SLTPPVASVKLGFFTLILQSYPDNSYQOPYGENEYPLVRFLRQPIYMEVRLNRDDPNIK	539
mZp2	LVLDDCWATSSQDPASAPQWQIVMDGCEYELDNRYRTTFHPAGSSAAHSGHYQRFDVKTFA	592
hZp2	LVLDDCWATSTMDDPSFPQWNVVVDGCAYDLDNRYQTTTFHPVSSVTHPDHYQRFDMKAF	599
mZp2	FVSEARGLSSLIYFHCSALICNQVSLDSPLCSVTCPASLRSKRE--ANKEDTMTVSLPGP	650
hZp2	FVSEAHVLSSLVYFHCSALICNRLSPDSPLCSVTCPVSSRRHRATGATEAEKMTVSLPGP	659
mZp2	ILLSDVSSSKGV-----DPSSSEITKDI-----IAKDIASKITLGA	686
hZp2	ILLSDSSFRGVGSSDLKASGSSGEKSRSETGEEVGSRGAMDTKGHKTAGDVGSKAVAA	719
mZp2	VAAVLGSAVILGFIQYLYKKRTIRFNH	713
hZp2	VAAFAGVVATLGFIVYLYEKRTVSNH	745

Figure S2. Alignment of murine (m) and human (h) Zp2 coding sequence, showing 58% identical and 72% similar amino acids. Species are noted on the left. Similar residues conserved in the two sequences are printed as white letters on black background. A minimum number of gaps, indicated by hyphens, has been introduced to maximize alignments. Alignments were produced using the web based alignment service BLAST (<http://blast.ncbi.nlm.nih.gov/Blast.cgi>) and default parameters (blastp algorithm, BLOSUM62 Matrix, Gap Cost existence:11 extension:1, conditional compositional score matrix adjustment).

- Supplement -

mZp3	MASSYFLFLCLLLCGGPELNCSTLWLLPGGTPTEVGSSSPVKVECLEAELVVTVSRDLF	60
hZp3	MELSYRLFICLLLWGSTELCYPOPLWLLQGCASHPETSVQPVLEVCQEATLMVMVSKDLF	60
mZp3	GTGKLVQPGDLTLGSEGCQPRVSVDT-DVVRFNAQLHECSSRVQMTKDALVYSTFLLHDP	119
hZp3	GTGKLRIRAADTLGPEACEPLVSMDEEDVVRFEVGLHECGNSMQVTDDALVYSTFLLHDP	120
mZp3	RPVSGLSILRTNRVEVPIECRYPROQNVSSHPIOPTWVPFRATVSSEEKLAFSLRLMEEN	179
hZp3	RPVGNLSIVRTNRAEIPIECRYPROQNVSSQAILPTWLPFRITVFSSEKLTFLSLRLMEEN	180
mZp3	WNTKESAPTFHLGEVAHLQAEVDTGSHLPLQLFVDHCVATPSLPDPNSSPYHFLVDFHG	239
hZp3	WNAEKRSPTFHLGDAHLQAEIHTGSHVPLRLFVDHCVATPTP--DONASPHYHFLVDFHG	238
mZp3	CLVDGLSESESAFQVPRRPELTLOFTVDVHFHFANSSRNNTLYITCHLKVAPANQIPDKLNK	299
hZp3	CLVDGLTDASAFKVPVRGPDLTLOFTVDVHFHFANSRNMIYITCHLKVTLAEQDPDELNK	298
mZp3	ACSFNKTSSQSWLPVEGDADICDCCSHGNCNSNSSSQFOIHGPRQWSKLVSRNRRHVTDDEA	359
hZp3	ACSFKPSNSWFPVEGPADICCCNKGDCTPSSHRRRPHVMSQWSRSASRNRHVTEEA	358
mZp3	DVTVGPLIFLGRKANDOTVEGWTASACTSVA-LGLGLATVAFLLAAIVLAVTRKCHSSSY	418
hZp3	DVTVGPLIFLDRRGDHEVEQWALPSDTSVVLGVGLAVVVSLLTAVILVLTRRCRTASH	418
mZp3	LVS	421
hZp3	PVS	421

Figure S3. Alignment of murine (m) and human (h) Zp3 coding sequence, showing 68% identical and 77% similar amino acids. Species are noted on the left. Similar residues conserved in the two sequences are printed as white letters on black background. A minimum number of gaps, indicated by hyphens, has been introduced to maximize alignments. Alignments were produced using the web based alignment service BLAST (<http://blast.ncbi.nlm.nih.gov/Blast.cgi>) and default parameters (blastp algorithm, BLOSUM62 Matrix, Gap Cost existence:11 extension:1, conditional compositional score matrix adjustment).

hZp4	MWLLRCVLLCVSLAVSGQHKEAPDYSSVLHCGPWSFQFAVNLNQEATSPPVLIAWDN
hZp4	QGLLHELQNDSDCGTWIRKGGSSVVLEATYSSCYVTEWDSHYIMPVGVGAGAAEHKVV
hZp4	TERKLLKCPMDLLARDAPDPTWCDSIPARDRLPCAPSPIISRGDCEGLGCCYSSEEVNSCY
hZp4	YGNTVTLLHCTREGHFSIAVSRNVTSPLLLLDSVRLALRNDACNPMATQAFVLFQFPFT
hZp4	SCGTTRQITGDRAVYENELVATRDVKNGSRGVSVTRDSIFRLHVSCSYSSNSLPIVQV
hZp4	FTLPPFPFETQPGPLTLELQIAKDKNYGSYYGVGDYPVVKLLRDPYVEVSILHRTDPYL
hZp4	GLLLQQCWATPSTDPLSQPQWPILVKGCPYIGDNYQTQLIPVQKALDLPPSHHQRFSSIF
hZp4	TFSFVNPTVEKQALRGPVHLHCSVSVCPAETPSCVVTCPDLSRRRNFDNSSQNTTASVS
hZp4	SKGPMILLQATKDPPEKLRVPVDSKVLWVAGLSGTLILGALLVSYLAVKKQKSCPDQMCQ

Figure S3. Human (h) Zp4 coding sequence. Since Zp4 is not translated in mice, no alignment was accessible.

- Supplement -

mAstI	MGSLWPWILTMLSLLGLSMGAPSSASRCSGVCSISVPEGF TPEGS PVFQDKDIPAINOGLI	63
hAstI	VGGLWPWVLGLLSLPGVILGAPLASSCAGACGTSFDPGLTPEGTQASGDKDIPAINOGLI	63
mAstI	SEETPESSFLVEGDIIRPSPFRLLSVTNNKWPKCVGGFVEIPFLLSRKYDEL SRRVIMDA	123
hAstI	LEETPESSFLIEGDIIRPSPFRLLSATSNNKWPMGSGGVVEVPFLLS SKYDEPSRQVILEA	123
mAstI	FAEFERF TCIRFVAYHGQRDFVSILPMA GCFSGVGRSGGMQVVSLAPTCLRKGRGIVLHE	183
hAstI	LAEFERS TCIRFVYIQDQRDFVSIIPMYGCFSGVGRSGGMQVVSLAPTCLQKGRGIVLHE	183
mAstI	LMHVLGFWHEHSRADRDRYIQVNWNEILPGFEINFIKSRSTNMLVPYDYSSVMHYGRFAF	243
hAstI	LMHVLGFWHEHTRADRDRYIRVNWNEILPGFEINFIKSQSSNMLTPYDYSSVMHYGRFAF	243
mAstI	SWRGOPTIIPLWTS SVHIGQRWNLSDITRVCRLYNCSRSVPSHGRGFEAQSDGSSLT	303
hAstI	SRRGLPTIIPLWAPS VHIGQRWNLSDITRVKLYGCSPSGPRPRGRGSHAHSTGRSPA	303
mAstI	PASISRLQRLLEALS EESGSSAPSGSRTGGQSI-AGLGNSQQGWEHPPOSTFVSGALARP	362
hAstI	PASLS-LQRLLEALS AESRSPDPSGS SAGGQVPAGPGE SPHGWE SPALKKLSAEPASARQ	362
mAstI	PQMLADASKSGPGAGADSLSEQFOLAQAPTVP LALFPEARDKPAPIQDAFERLAPLPGG	422
hAstI	PQTLASSPRSRPGAGAPGVAQEQSWLAGVSTKPTVPSSEAGIQVPVQGS----PALPGG	418
mAstI	CAPGSHIREVPRD	435
hAstI	CVPRNHFKGMSED	431

Figure S5. Alignment of murine (m) and human (h) ovastacin (AstI) coding sequence, showing 67% identical and 75% similar amino acids. Species are noted on the left. Similar residues conserved in the two sequences are printed as white letters on black background. A minimum number of gaps, indicated by hyphens, has been introduced to maximize alignments. Alignments were produced using the web based alignment service BLAST (<http://blast.ncbi.nlm.nih.gov/Blast.cgi>) and default parameters (blastp algorithm, BLOSUM62 Matrix, Gap Cost existence:11 extension:1, conditional compositional score matrix adjustment).

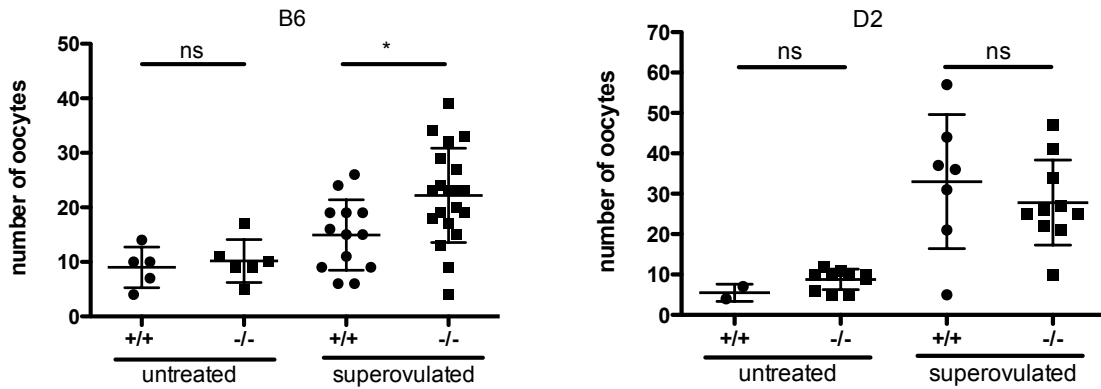


Figure S6. Fetuin-B deficient mice show ovulation rate comparable to wildtypes. (left) Number of ovulated oocytes after mating triggered ovulation and hormonal stimulation in C57BL/6 and (right) DBA/2 mice. Pairwise two-sided t test, ns = not significant, * $p < 0.05$

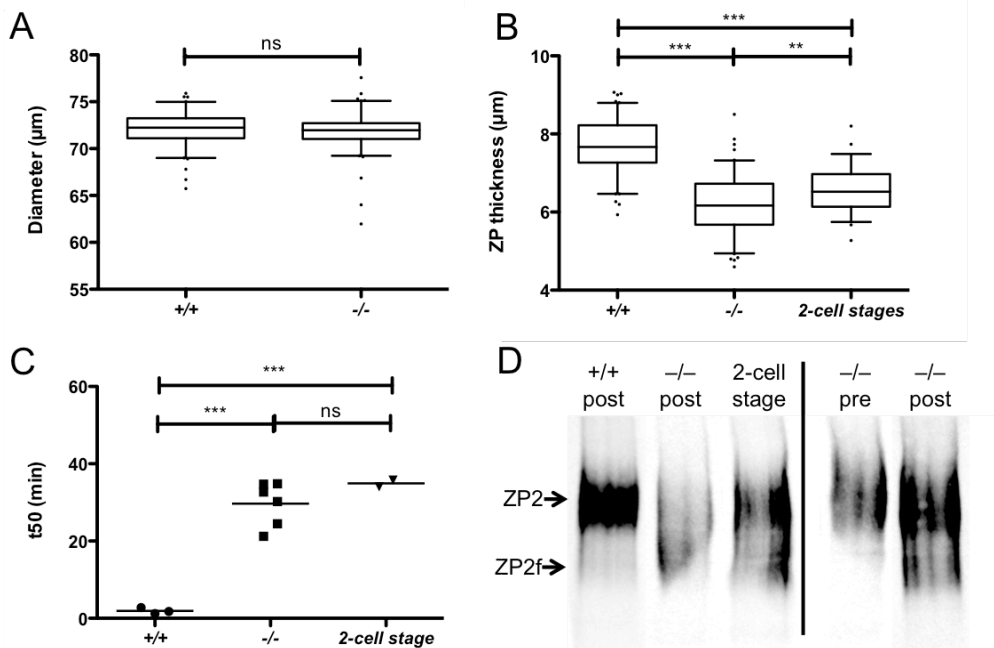
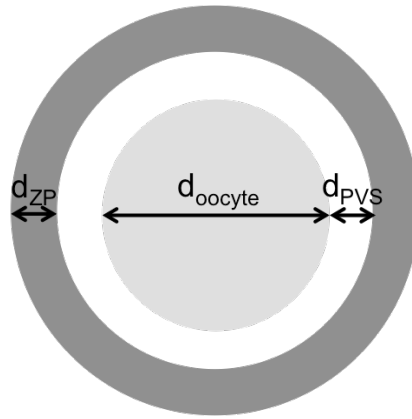


Figure S7. Premature zona pellucida (ZP) hardening of fetuin-B deficient oocytes at DBA/2 background. (A) Diameter of unfertilized wildtype (+/+) oocytes ($72.16 \pm 1.90 \mu\text{m}$, $n = 100$) and *Fetub*^{-/-} (-/-) derived oocytes ($71.83 \pm 2.01 \mu\text{m}$, $n = 100$). (B) ZP thickness of unfertilized wildtype oocytes ($7.70 \pm 0.70 \mu\text{m}$, $n = 100$), *Fetub*^{-/-} derived oocytes ($6.19 \pm 0.71 \mu\text{m}$, $n = 100$) and wildtype 2-cell stages ($6.57 \pm 0.58 \mu\text{m}$, $n = 54$). Boxes represents the first to the third quartile, band inside shows the median. Whiskers indicate 5-95 percentile. (C) ZP digestion time of wildtype oocytes, fetuin-B deficient oocytes and wildtype two-cell embryos (2-cell stage). The ZP digestion time was defined as the time required for 50% of the oocytes to become zona free (t50) following α -chymotrypsin treatment. Every dot represents one assay performed with at least 20 oocytes harvested from one mouse per genotype. (D) Immune detection of ZP2 protein of wildtype oocytes, fetuin-B deficient oocytes and wildtype 2-cell embryos. Fetuin-B deficient oocytes were further isolated pre- and post-ovulatory. Pairwise two-sided t test ** $p < 0,01$, *** $p < 0.001$, ns = not significant. The horizontal lines depicts (A, B) the mean \pm SD or (C) the mean (modified from).



$$V(PVS) = \frac{1}{6} \pi (d_{\text{oocyte}} + d_{\text{PVR}})^3 - \frac{1}{6} \pi (d_{\text{oocyte}})^3$$

Figure S8. Calculation of perivitelline space volume. Overview drawing of an oocyte illustrates the diameter of the oocyte (d_{oocyte}), the perivitelline space (d_{PVS}) and the zona pellucida (d_{ZP}). Oocyte diameter and diameter of the perivitelline space of 137 individual C57BL/6 wildtype oocytes were measured. Perivitelline space volume ($V(PVS)$) of each oocyte was calculated using the given formula. The mean $V(PVS)$ was used for further calculation in paragraph 3.3

Acknowledgement

I would like to thank all the people who supported me during this thesis.

First of all, I would like to acknowledge my supervisor Prof. Dr. Willi Jahnen-Dechent for this interesting project. I would like to thank for his trust he showed in my work and for his ongoing support. The participation at international workshops and conferences gave me the opportunity to train myself and to get in contact with other researchers.

Many thanks to Prof. Dr. Marc Spehr, not only for kindly co-refereeing this thesis, but also for his general interest in the topic and the stimulating discussions.

My thanks also go to several people who contributed to this thesis in different aspects:

Tanja Pfeffer (Institute for Animal Science, RWTH Aachen University), who was a indispensable help for the *in vitro* fertilizations and the embryo transfers;

Eddy Van de Leur and Ralf Weiskirchen (Institute for Molecular Pathobiochemistry, Experimental Gene Therapy and Clinical Chemistry, RWTH Aachen University), for expression of recombinant murine fetuin-A and -B;

All the people of Prof. Dr. Walter Stöckers group (Institute of Zoology, Cell and Matrix Biology, Johannes Gutenberg University Mainz), who were involved in ovastacin expression and fetuin-B / ovastacin kinetic experiments;

Dr. Jurrien Dean (National Institutes of Diabetes and Digestive and Kidney Diseases, Washington) for a gift of ZP2 antibody.

Special regards belong to my colleague and good friend Julia Floehr for her ongoing support and the perfect teamwork. I enjoyed the special time we spent together in the lab, at conferences and beyond this.

This work was supported by the DFG Graduate School Grant 1035 Biointerface and Merck-Serono Germany.

Finally, I would like to thank my family and friends for their support during my studies, especially my boyfriend Dirk for his help in all aspects of life.

Curriculum Vitae

Name: Eileen Dietzel
Address: Rolandstraße 2a, 52070 Aachen
Date of birth: 05. October 1984
Nationality: German
Phone: +49-241/8037416
E-Mail: eileen.dietzel@rwth-aachen.de

Academic career

since Oct. 2011 PhD thesis „The biological role of fetuin-B“, Helmholtz Institute for Biomedical Engineering (Prof. Dr. rer. nat. Jahnen-Dechent), RWTH Aachen University, Germany
Sep. 2011 Master examination
Apr.-Sep. 2011 Master thesis „The analysis of the female infertility in fetuin-b deficient mice“, Helmholtz Institute for Biomedical Engineering (Prof. Dr. rer. nat. Jahnen-Dechent), RWTH Aachen University, Germany
Sep. 2009 Bachelor examination
Apr.-Sep. 2009 Bachelor thesis „The analysis of the female infertility in fetuin-b deficient mice“, Helmholtz Institute for Biomedical Engineering (Prof. Dr. rer. nat. Jahnen-Dechent), RWTH Aachen University, Germany
Oct. 2006-Sep. 2011 Studies in biology, RWTH, Aachen, Germany

Work Experience

Jul. 2005-Aug. 2006 Full-time employee as biological-technical assistant (BTA), Centre of Biochemistry (PD Dr. Lechner), Ruprecht-Karls University, Heidelberg, Germany

Apprenticeship

Aug. 2001-Jul. 2005 Apprenticeship as BTA with higher education entrance qualification, Olsberg, Germany

Activities

May 2007-Sep. 2011 Student assistant, Helmholtz Institute for Biomedical Engineering (Prof. Dr. rer. nat. Jahnen-Dechent), RWTH Aachen University, Germany

Oct. 2009-Sep. 2011 Member of the student representatives in Biology and Biotechnology, RWTH Aachen University, Germany

Oct. 2011-Jun. 2014 Collegiate of the Research Training Group Biointerface (GK 1035) funded by the DFG (*Deutsche Forschungsgemeinschaft*)

since Apr. 2012 Member of the European Society of Human Reproduction and Embryology (ESHRE)

Publications

Dietzel, E., Wessling, J., Floehr, J., Schäfer, C., Ensslen, S., Denecke, B., Rösing, B., Neulen, J., Veitinger, T., Spehr, M., Tropartz, T., Tolba, R., Renné, T., Egert, A., Schorle, H., Gottenbusch, Y., Hildebrand, A., Yiallourous, I., Stöcker, W., Weiskirchen, R., and Jahnen-Dechent, W. (2013). Fetuin-B, a liver-derived plasma protein is essential for fertilization. *Dev. Cell* 25, 106–112.

Stöcker, W., Karmilin, K., Hildebrand, A., Westphal, H., Yiallourous, I., Weiskirchen, R., Dietzel, E., Floehr, J., and Jahnen-Dechent, W. (2014). Mammalian gamete fusion depends on the inhibition of ovastacin by fetuin-B. *Biol. Chem.* 395, 1195-1199

Participation at conferences / talks

Jul. 2011 Poster presentation at the Gordon Research Conference (GRC) for Fertilization and Activation of Development, Holderness, NH, USA; Dietzel et al. "Fetuin-B deficiency is associated with female infertility in mice."

- Curriculum Vitae -

- Jul. 2012 Poster presentation at the annual meeting of the European Society of Human Reproduction and Embryology (ESHRE), Istanbul; Dietzel et al. "The biological function of fetuin-B in female mice."
- Oct. 2012 Talk and poster presentation at the annual meeting of the *Deutsche Gesellschaft für Gynäkologie und Geburtshilfe (DGGG)*, Munich; Dietzel et al. "*Fetuin-B Defizienz ist assoziiert mit vorzeitiger Zona pellucida Härtung.*"
- Jul. 2013 Talk at the Gordon Research Seminar (GRS) and poster presentation at the Gordon Research Conference (GRC), Holderness, NH, USA; Dietzel et al. "Fetuin-B inhibits zona pellucida hardening."
- Nov. 2013 Talk at the molecular biology meeting of the *Deutsche Gesellschaft für Endokrinologie und Fortpflanzungsmedizin & Deutsche Gesellschaft für Reproduktionsmedizin (DGGEF & DGRM)*, Düsseldorf; Dietzel et al. "*Fetuin-B inhibiert die Zona pellucida Härtung.*"
- Aug. 2014 Talk at the Laboratory of Cellular and Developmental Biology, National Institutes of Health (NIH), Bethesda, MD, USA; Dietzel et al. "Fetuin-B increases in vitro fertilization success."
Talk and Poster presentation at the Gordon Research Conference (GRC) for Mammalian Reproduction, New London, NH, USA; Dietzel et al. "Fetuin-B increases in vitro fertilization success."
- Oct. 2014 Poster presentation at the annual meeting of the *Deutsche Gesellschaft für Gynäkologie und Geburtshilfe (DGGG)*, Munich; Dietzel et al. "*Fetuin-B inhibiert die frühzeitige Zona Pellucida Härtung und erhält so die Fertilität.*"
- Awards** Best talk at the molecular biology meeting of the *Deutsche Gesellschaft für Endokrinologie und Fortpflanzungsmedizin & Deutsche Gesellschaft für Reproduktionsmedizin (DGGEF & DGRM)*, 2013, Düsseldorf, honored with 500 €
- Scholarship** *Deutscher Akademischer Austausch Dienst (DAAD)* scholarship for an invited talk at the NIH, 2014

Further skills

Category-B course for animal experiments according to the Society of Laboratory Animal Science and the Federation of European Laboratory Animal Science Association, 2012 (40 hours)

Practical Seminar on cryopreservation of oocytes, sperm and embryos given by the *Gesellschaft für Versuchstierkunde* (GV-SOLAS), 2012 (6 hours)

Project management workshop given by Next Level Consulting, 2012 (28 hours)

Statutory Declaration

I, Eileen Dietzel, declare that I have authored this PhD thesis independently, that beside the marked parts I have done all the work completely or predominantly on my own, that I have not used other than the declared sources, and that I have explicitly marked all material, which has been quoted either literally or by content from the used sources.

Aachen, September 30, 2014

Signature _____